

# Schriftenreihe Umweltingenieurwesen

Agrar- und Umweltwissenschaftliche Fakultät

Band 109

Dissertation

*Michael Cramer*

## Dealing with heavily polluted storm-water-runoff from silo facilities

PROFESSUR

Wasserwirtschaft

Universität  
Rostock



Traditio et Innovatio

Universität  
Rostock



Traditio et Innovatio

ISBN 978-3-86009-530-0

[https://doi.org/10.18453/rosdok\\_id00003358](https://doi.org/10.18453/rosdok_id00003358)

Schriftenreihe

Bd.  
109

Umweltingenieurwesen ■ Wasserwirtschaft

**Schriftenreihe Umweltingenieurwesen**

Band 109

Dissertation

*Michael Cramer*

**Umgang mit stark verschmutztem  
Niederschlagswasser aus Siloanlagen**

Professur

**Wasserwirtschaft**

Agrar- und Umweltwissenschaftliche Fakultät

**Universität  
Rostock**



Traditio et Innovatio

Dissertation

## HERAUSGEBER

Prof. Dr.-Ing. habil. Jens Tränckner  
Universität Rostock  
Agrar- und Umweltwissenschaftliche Fakultät  
Professur Wasserwirtschaft  
18051 Rostock

## CIP-KURZTITELAUFNahme

Dissertation Michael Cramer  
Universität Rostock  
Agrar- und Umweltwissenschaftliche Fakultät  
Rostock, 2021

© Universität Rostock, Agrar- und Umweltwissenschaftliche Fakultät,  
18051 Rostock

## BEZUGSMÖGLICHKEITEN

Universität Rostock  
Universitätsbibliothek, Schriftentausch,  
18051 Rostock  
Tel.: 0381/498-8637, Fax: 0381/498-8632  
E-Mail: maria.schumacher@ub.uni-rostock.de

Universität Rostock  
Agrar- und Umweltwissenschaftliche Fakultät  
Professur Wasserwirtschaft  
Satower Straße 48, 18059 Rostock  
Tel.: 0381/498-3461, Fax: 0381/498-3462

ISBN 978-3-86009-530-0  
[https://doi.org/10.18453/rosdok\\_id00003358](https://doi.org/10.18453/rosdok_id00003358)

Universität Rostock  
Professur Wasserwirtschaft

## Foreword

Biogas plants are an essential pillar of the transformation to renewable energy supply. In Germany, more than 9000 biogas plants are operated. More than half of the produced energy is based on energy crops, which are commonly stored on site in large open silo facilities. This way, the high concentrated organic matter is exposed to the atmospheric conditions. Accordingly, stormwater runoff of the partly huge impervious areas can be highly polluted. This poses a severe threat to surface water bodies and groundwater if not managed appropriately.

Generally, this issue is identified, however so far hardly analysed in a structured way. Accordingly, there exists an obvious knowledge gap on wastewater composition of the different functional areas at a biogas plant and the subsequent options for a targeted stormwater treatment.

The work of Michael Cramer addresses both aspects. Based on a monitoring campaign on a characteristic biogas plants, he can classify the pollution potential of different functional areas and shows the impact of substrate composition, area operation and precipitation dynamics on stormwater composition. The larger part of the work is dedicated to the development of an appropriate treatment technology taking the specific operational conditions for agricultural stormwater into account. After assessing the biologic degradability, he developed in cooperation with an SME a trickling filter, which can be completely ponded to achieve denitrification and enhanced biological phosphorous removal (EBPR). The so-called SBR trickling filter might be also an interesting option for treating domestic wastewater with nutrient removal and low technological effort. Finally, Mr. Cramer investigates the decline of treatment performance of this technology under long starvation conditions, which can be expected in dry weather conditions. Applying two different methods (OUR measurement and pilote scale experiments) he detected a surprisingly low decay rate after very long starvation periods, leading to a proposed split of the common one-step decay kinetics in ASM models into two decay processes. So, the original research question, how to deal with heavily polluted stormwater on biogas plants, lead “en passant” to the development of a new treatment technology and scrutinizing a so far widely accepted model approach. This is applied science in its proper sense.

Summarising, the thesis is a valuable step towards a more sustainable stormwater management of highly polluted areas in agriculture. However, there is still a long way to go. Beside research and technological development, this requires common efforts of the responsible parties in agriculture and authorities.

Prof. Dr. Jens Tränckner

## Acknowledgements

Large parts of the work were developed in the project PROBENE BIO (FKZ 02WQ1361B) funded by the German federal ministry of education and research BMBF. We thank all partners in science and practice who provided valuable support.



Universität  
Rostock



Traditio et Innovatio

Aus der Professur für Wasserwirtschaft  
der Agrar- und Umweltwissenschaftlichen Fakultät

## Umgang mit stark verschmutztem Niederschlagswasser aus Siloanlagen

*„Von der Verschmutzungs-Quelle bis zur Behandlung am Beispiel einer Biogasanlage“*

---

### Dissertation

Zur Erlangung des akademischen Grades  
Doktor der Ingenieurwissenschaften (Dr.-Ing.)

an der Agrar- und Umweltwissenschaftlichen Fakultät  
der Universität Rostock

vorgelegt von M.Sc. Michael Cramer aus Rostock

Rostock, den 09.11.21



**Things are only impossible until they're not!**

*Captain Jean-Luc Picard, 2369*

Gutachter:

Prof. Dr. Jens Tränckner; Professur für Wasserwirtschaft, Universität  
Rostock

Prof. Dr. Marc Wichern; Lehrstuhl für Siedlungswasserwirtschaft,  
Universität Bochum

Prof. Dr. Christof Wetter; Fachbereich Energie, Gebäude, Umwelt,  
Fachhochschule Münster

**Jahr der Einreichung: 2021**

**Jahr der Verteidigung: 2021**

## Abstract

Due to the raw materials stored on site, stormwater from silo facilities has a high organic and nutrient load that must be treated before discharge to surface or groundwater. Due to the entirely different composition of this wastewater compared to urban runoff, completely new evaluation criteria and treatment systems must be developed for this. During the test period, strong fluctuations in the wastewater composition were observed. Measurements showed both very heavily polluted effluents with organic loads above  $12,000 \text{ mg}\cdot\text{L}^{-1}$  chemical oxygen demand (COD),  $\text{NH}_4\text{-N}$  contents above  $800 \text{ mg}\cdot\text{L}^{-1}$ , and  $\text{PO}_4\text{-P}$  contents of  $380 \text{ mg}\cdot\text{L}^{-1}$ , and effluents with COD concentrations above  $300 \text{ mg}\cdot\text{L}^{-1}$  and correspondingly low nutrient contents. The main sources of contamination are crumb losses from the wheel loader during transport, windswept dried substrates, and silage effluents resulting from lactic acid fermentation during storage. Frequent cleaning operations have a strong impact on reducing pollution and are strongly recommended. This shows that stormwater runoff from silage facilities is more comparable to domestic wastewater, but has the same dynamics as rainwater.

However, results showed that the stormwater has good biological treatability due to its high organic content, but also may contain a high amount of inert or poorly degradable COD, depending on the substrates stored on site. Facing all concerns, a proper process design based on a trickling filter operating in a sequencing-batch-reactor-mode was developed. Both, aerobic and anaerobic steps allow a good treatability regarding COD reduction, nitrification and denitrification as well as enhanced biological phosphorous removal. One main advantage is the ability to sustain long starvation periods with no inflow.

The aim of the research project was to define the technical basis for the treatment of stormwater runoff and to be able to offer the biogas plant operators a reliable stormwater treatment process that is suitable for approval.

## **Zusammenfassung**

Niederschlagswasser aus Siloanlagen hat aufgrund der vor Ort gelagerten Rohstoffe eine hohe Organik- und Nährstoffbelastung, die vor der Einleitung in Oberflächen- oder Grundwasser behandelt werden muss. Aufgrund der vollkommen anderen Zusammensetzung dieses Abwassers im Vergleich zu urbanen Abflüssen, müssen hierfür vollkommen neue Bewertungskriterien und Behandlungssysteme entwickelt werden. Während des Versuchszeitraums wurden starke Schwankungen in der Abwasserzusammensetzung beobachtet. Die Messungen zeigten sowohl sehr stark belastete Abwässer mit organischen Frachten über  $12.000 \text{ mg}\cdot\text{L}^{-1}$  an chemischen Sauerstoffbedarf (CSB),  $\text{NH}_4\text{-N}$ -Gehalten über  $800 \text{ mg}\cdot\text{L}^{-1}$  und  $\text{PO}_4\text{-P}$ -Gehalten von  $380 \text{ mg}\cdot\text{L}^{-1}$  als auch Abwässer mit CSB-Konzentrationen von nur  $300 \text{ mg}\cdot\text{L}^{-1}$  und entsprechend niedrigen Nährstoffgehalten. Hauptverursacher der Verunreinigungen sind die Krümelverluste des Radladers beim Transport, Windverwehungen von getrockneten Substraten und die durch eine Milchsäuregärung während der Lagerung entstehenden Silageabflüsse. Häufige Reinigungsvorgänge haben einen starken Einfluss auf die Reduzierung der Verschmutzung und werden dringend empfohlen. Dies zeigt, dass das Niederschlagswasser aus Siloanlagen eher mit häuslichem Abwasser vergleichbar ist, jedoch die gleiche Dynamik wie Regenwasser aufweist.

Ergebnisse zeigten, dass das Niederschlagswasser aufgrund seiner hohen organischen Inhaltsstoffe biologisch gut behandelbar ist, enthält aber auch unter Umständen einen hohen Anteil an inertem oder schwer abbaubarem CSB, abhängig von den vor Ort gelagerten Substraten. Unter Berücksichtigung aller Aspekte wurde ein geeignetes Verfahrenskonzept auf Basis eines Tropfkörpers entwickelt, der im Sequenz-Batch-Reaktor-Verfahren arbeitet. Sowohl die aerobe als auch die anaerobe Stufe ermöglichen eine gute Reinigungsleistung hinsichtlich CSB-Reduktion, Nitrifikation und Denitrifikation sowie eine verbesserte biologische Phosphorentfernung. Ein wesentlicher Vorteil ist die Fähigkeit, lange Hungerperioden ohne Zufluss zu überstehen.

Ziel des Forschungsprojektes war es, die technischen Grundlagen für die Behandlung von Regenwasserabflüssen zu definieren und den Biogasanlagenbetreibern ein zuverlässiges und genehmigungsfähiges Verfahren zur Regenwasserbehandlung von Siloanlagen anbieten zu können.

## Table of content

<b>1</b>	<b>INTRODUCTION.....</b>	<b>1</b>
1.1	WATER FLOWS ON SILO FACILITIES .....	1
1.2	STORMWATER SITUATION ON SILO FACILITIES .....	2
1.3	BASICS OF CONVENTIONAL NUTRIENT ELIMINATION WITH ACTIVATED SLUDGE .....	3
1.4	BIOFILM-SYSTEMS .....	5
1.5	MODELLING OF ORDINARY HETEROTROPHIC ORGANISM .....	6
1.6	STRUCTURE.....	8
<b>2</b>	<b>SURFACE CONTAMINATION OF IMPERVIOUS AREAS ON BIOGAS PLANTS AND CONCLUSIONS FOR AN IMPROVED STORMWATER MANAGEMENT .....</b>	<b>11</b>
2.1	INTRODUCTION .....	12
2.1.1	Motivation and Objectives.....	12
2.1.2	Condensed literature review .....	13
2.2	MATERIALS AND METHODS .....	16
2.2.1	Site description .....	16
2.2.2	Stormwater sampling.....	17
2.2.3	Surface contamination .....	18
2.2.4	Laboratory analysis .....	21
2.3	RESULTS .....	21
2.3.1	Stormwater runoff in detail.....	21
2.3.2	Characteristics of the solid substrate.....	22
2.3.3	Built-up process on the covered foil.....	23
2.3.4	Built-up process “dry-substrate” .....	23
2.3.5	Built-up process with wet substrate .....	25
2.3.6	Verification of cleaning method .....	29
2.4	DISCUSSION.....	30
2.5	CONCLUSION .....	31
2.6	ADDITIONAL THOUGHTS ABOUT SUBSTANCE FLOWS ON A SILO FACILITY .....	33
<b>3</b>	<b>DEGRADATION KINETICS AND COD FRACTIONING OF AGRICULTURAL WASTEWATERS FROM BIOGAS PLANTS APPLYING BIOFILM RESPIROMETRY .....</b>	<b>37</b>
3.1	INTRODUCTION .....	38
3.2	MATERIAL AND METHODS .....	40
3.2.1	Wastewater preparation .....	40
3.2.2	Analytical procedure.....	40
3.2.3	Mathematical model .....	42
3.3	RESULTS .....	46
3.3.1	Estimating kinetic constants and COD fractioning.....	46
3.3.2	Verifying the results of biofilm respirometry.....	51
3.3.3	Comparison of COD fractions from respiration with influent concentrations .....	53
3.4	DISCUSSION.....	53
3.5	CONCLUSION .....	55
3.6	COMPLEMENTARY THOUGHTS ABOUT DISCHARGE LIMITS BASED ON CONCENTRATIONS .....	56

<b>4</b>	<b>KINETIC OF DENITRIFICATION AND ENHANCED BIOLOGICAL PHOSPHOROUS REMOVAL (EBPR) OF A TRICKLING FILTER OPERATED IN A SEQUENCE-BATCH-REACTOR-MODE (SBR-TF).....</b>	<b>59</b>
4.1	INTRODUCTION .....	60
4.2	MATERIAL AND METHODS .....	62
4.2.1	Reactor design of SBR-TF system .....	62
4.2.2	Concept of SBR-TF with integrated DN and EBPR.....	63
4.2.3	Mathematical model .....	65
4.2.4	Analytical procedure.....	65
4.2.5	Wastewater properties .....	66
4.3	RESULTS .....	67
4.3.1	COD-removal efficiency.....	67
4.3.2	Nitrogen removal efficiency with nitrification and denitrification .....	68
4.3.3	Enhanced biological phosphorus removal EBPR.....	70
4.3.4	Degradation kinetics.....	71
4.4	DISCUSSION.....	74
4.5	CONCLUSION .....	75
4.6	CONTINUING THOUGHTS OF STORMWATER TREATMENT ON SILO FACILITIES .....	77
<b>5</b>	<b>DEVELOPMENT OF DECAY IN BIOFILMS UNDER STARVATION CONDITIONS – RETHINKING OF THE BIOMASS MODEL.....</b>	<b>79</b>
5.1	INTRODUCTION .....	80
5.2	MATERIAL AND METHODS .....	84
5.2.1	Design of Wastewater Treatment Plant.....	84
5.2.2	Analytical Procedure .....	86
5.2.3	Mathematical Model.....	88
5.3	RESULTS .....	89
5.3.1	Decay Rate During Starvation .....	89
5.3.2	Verification of the Low Decay Rate in Pilot Scale .....	91
5.4	CONCLUSIONS .....	96
<b>6</b>	<b>SUMMARY .....</b>	<b>100</b>
6.1	FINAL CONCLUSION.....	100
6.2	PERSPECTIVE .....	101
6.2.1	Implementation of a treatment system .....	101
6.2.2	Research and Development .....	102
	<b>REFERENCES.....</b>	<b>IX</b>

## Figures

FIG. 1:	WATER FLOWS ON AN EXEMPLARY SILO FACILITY .....	2
FIG. 2:	COD FRACTIONS FOR MODELLING ACTIVATED SLUDGE .....	7
FIG. 3:	STRUCTURE OF PUBLICATIONS .....	9
FIG. 4:	ENERGY MIX OF TOTAL ELECTRICAL GENERATION IN GERMANY 2017 ACCORDANCE TO FEDERAL STATISTICAL OFFICE .....	12
FIG. 5:	STORMWATER POLLUTION AT THE DISCHARGE POINT OF VARIOUS SILO WORKS (PARTLY WITH ADDITIONAL HUSBANDRY ACTIVITIES); DATA KINDLY PROVIDED BY THE "STAATLICHES AMT FÜR UMWELT UND NATUR MITTLERES MECKLENBURG" .....	13
FIG. 6:	INTEGRATION OF STORMWATER POLLUTION INTO LIFE CYCLE INVENTORY ANALYSIS.....	15
FIG. 7:	DRAINAGE SYSTEM AT THE MONITORED SILO .....	17
FIG. 8:	TYPICAL EXAMPLE THE HETEROGENEOUS CONTAMINATION OF A SILO AREA.....	18
FIG. 9:	CLEANING METHOD OF THE GRID SQUARE WITH A WET VACUUM CLEANER BEFORE, DURING AND AFTER CLEANING .....	19
FIG. 10:	SCHEMATIC DIAGRAM OF THE MONITORED SILO AREAS OF A SILO WITH SAMPLING METHOD 1..	19
FIG. 11:	SCHEMATIC DIAGRAM OF THE MONITORED SILO AREAS OF A SILO WITH SAMPLING METHOD 2..	20
FIG. 12:	STORMWATER POLLUTION OF SINGLE RAINFALL EVENTS IN DETAIL.....	22
FIG. 13:	BUILT-UP-PROCESS OF CHEMICAL OXYGEN DEMAND (COD) WITH CONTAMINANT OF THE "DRY-STORED-SUBSTRATE". AFTER EACH SAMPLING, THE AREA LOADING IS REDUCED TO NEARLY ZERO, HENCE, DUE TO FIXED SAMPLING POINTS, THE INTERVAL OF MEASURING INCREASES EACH DAY TO INCREASE THE DAYS OF ACCUMULATION .....	24
FIG. 14:	BUILT-UP-PROCESS OF CHEMICAL OXYGEN DEMAND (COD) WITH CONTAMINANT OF THE "WET-STORED-SUBSTRATE". AFTER EACH SAMPLING, THE AREA LOADING IS REDUCED TO NEARLY ZERO, HENCE, DUE TO FIXED SAMPLING POINTS, THE INTERVAL OF MEASURING INCREASES EACH DAY TO INCREASE THE DAYS OF ACCUMULATION .....	26
FIG. 15:	BUILT-UP-PROCESS OF CHEMICAL OXYGEN DEMAND (COD) WITH THE "WET-STORED-SUBSTRATE". THE SAMPLING POINTS VARY EACH DAY; HENCE, THE ACCUMULATION PROCESS IS PROGRESS EACH DAY ON THE NOT MEASURED POINTS.....	28
FIG. 16:	TOTAL AREA LOADING OF A SAMPLING POINT AFTER TWO CLEANING STEPS AND THREE DAYS OF ACCUMULATION .....	29
FIG. 17:	SUBSTANCE CONCENTRATIONS AND FLOWS THAT HAVE BEEN DIVIDED INTO DIFFERENT ZONES USING SWMM MODELLING .....	34
FIG. 18:	POSSIBLE DRAINAGE CONCEPTS FOR SILO FACILITIES .....	35
FIG. 19:	SCHEMA OF THE RESPIROMETRY MEASUREMENT OF THE OXYGEN UPTAKE RATE OUR.....	41
FIG. 20:	COD FRACTIONS OF INFLUENT WASTEWATERS AND ALTERATION AFTER BIODEGRADATION .....	42
FIG. 21:	PARAMETER DESCRIPTION FOR IDENTIFYING COD FRACTION WITH RESPIROMETRY .....	46
FIG. 22:	RESULTS OF THE OUR MEASUREMENT VIA RESPIRATION METHOD FOR CORN SILAGE (TOP LEFT), WHOLE CROP SILAGE (TOP RIGHT), SOLID MANURE (MIDDLE LEFT), DRY CHICKEN FACES (BOTTOM RIGHT), SILAGE EFFLUENT (BOTTOM LEFT) AND FERMENTATION RESIDUE (MIDDLE RIGHT); TWO REPLICATES .....	47

FIG. 23: RESULTS OF THE OUR MEASUREMENT VIA RESPIRATION METHOD FOR DOMESTIC WASTEWATER WITH A BIOFILM CARRIER SYSTEM (BS, LEFT) AND ACTIVATED SLUDGE (AS, RIGHT); TWO REPLICATES.....	52
FIG. 24: RESULTS OF THE COD FRACTIONING BY RESPIRATION MEASUREMENTS .....	53
FIG. 25: REACTOR DESIGN OF THE TRICKLING FILTER SYSTEM.....	63
FIG. 26: PRINCIPLE OF THE SBR TRICKLING FILTER PROCESS .....	64
FIG. 27: CHARACTERIZATION OF COD:N:P RATIO AS 100:N:P OF RAW WASTEWATER.....	66
FIG. 28: COD REMOVAL EFFICIENCY OF SBR-PILOT PLANT WITH BOTH SYNTHETIC AND REAL WASTEWATER.....	68
FIG. 29: RESULTS OF THE NITRIFICATION AND NITROGEN REMOVAL EFFICIENCY .....	69
FIG. 30: HIGH-RESOLVED MEASUREMENT OF A SBR CYCLE FOR VERIFYING AN EBPR.....	70
FIG. 31: RESULTS OF COD AND NO <sub>3</sub> DEGRADATION KINETICS .....	71
FIG. 32: CONCEPT OF STORMWATER TREATMENT SYSTEM.....	77
FIG. 33: CONTROL CONCEPT OF STORMWATER RETENTION BASIN .....	78
FIG. 34: PRINCIPLE OF THE ENDOGENOUS RESPIRATION MODEL. ....	81
FIG. 35: PRINCIPLE OF THE DEATH-REGENERATION MODEL.....	81
FIG. 36: CHEMICAL OXYGEN DEMAND (COD) FRACTIONS DURING BIOLOGICAL TREATMENT (CRAMER ET AL., 2019C). ....	83
FIG. 37: PRINCIPLE SCHEMA OF THE TRICKLING FILTER SYSTEM (CRAMER ET AL., 2019B). ....	85
FIG. 38: STEPS OF ONE SBR CYCLE (CRAMER ET AL., 2019B).....	86
FIG. 39: SCHEMA OF THE RESPIROMETRY MEASUREMENT OF THE OXYGEN UPTAKE RATE. ....	87
FIG. 40: ALTERNATION OF DECAY RATE DURING STARVATION OF BIOFILM CARRIER .....	90
FIG. 41: RESULTS OF ENDOGENOUS OUR AFTER SUBSTRATE FEEDING. ....	91
FIG. 42: RESULTS OF RESPIROMETRY MEASUREMENT IN A PILOT SCALE TRICKLING FILTER.....	92
FIG. 43: REACTIVITY OF MICROORGANISM AFTER STARVATION. ....	93
FIG. 44: EXTENDING OF THE DEATH-REGENERATION MODEL .....	95
FIG. 45: ADJUSTING OF THE ENDOGENOUS RESPIRATION MODEL .....	95
FIG. 46: DIFFUSION LIMITATION WITH RESPECT OF OXYGEN PENETRATION INTO THE BIOFILM. ....	99

## Tables

TABLE 1: REFERENCES REGARDING URBAN AND AGRICULTURAL BUILT-UP AND RUNOFF.....	16
TABLE 2: CHARACTERISTICS OF RRM OF THE SILOS.....	22
TABLE 3: RESULTS OF THE BUILT-UP OF CONTAMINANTS WITH THE “DRY-SUBSTRATE” .....	23
TABLE 4: RESULTS OF THE BUILT-UP OF CONTAMINANTS WITH THE “WET-SUBSTRATE”, FIRST MEASUREMENT .....	25
TABLE 5: RESULTS OF THE BUILT-UP OF CONTAMINANTS WITH THE “WET-SUBSTRATE”, SECOND MEASUREMENT .....	27
TABLE 6: PROPERTIES OF THE DISSOLVED SUBSTRATES; TWO REPLICATES.....	49
TABLE 7: RESULTS OF THE BIODEGRADATION EFFICIENCY AND KINETIC; TWO REPLICATES .....	50
TABLE 8: RESULTS OF THE COD FRACTIONING; TWO REPLICATES.....	51

TABLE 9: TRIPLE MEASUREMENTS OF DOMESTIC WASTEWATER USING HACH CUVETTE TESTS .....	66
TABLE 10: CHARACTERISTIC OF RAW WASTEWATER FROM THE BIOGAS PLANT .....	66
TABLE 11: RESULTS OF DEGRADATION KINETICS .....	73
TABLE 12: RESULTS OF P-RELEASE AND UPTAKE RATES DOCUMENTED IN LITERATURE.....	74

## LIST OF ABBREVIATIONS

Nomenclature	
A	surface area
ASM	activated sludge model
ASS	activated sludge system
b	decay rate
BF	biofilm
BOD	biological oxygen demand
BS	biofilm system
COD	chemical oxygen demand
DN	denitrification
DM	dry matter
DO	dissolved oxygen
EBPR	enhanced biological phosphorous removal
f	residue factor
$i_{N,BM}$	nitrogen content of biomass
$K_s$	saturation coefficient
k	rate constant
L	characteristic length
n	number of
N	oxygen demand for nitrification
N	nitrification
oDM	organic dry matter
OUR	oxygen uptake rate
PAO	phosphorous accumulating organism
PHA	poly-hydroxy-alkanoates
r	degradation rate
S	dissolved fraction
SBR	sequence-batch-reactor
SND	simultaneous nitrification and denitrification
SRT	sludge retention time
$\beta$	oxygen penetration factor
t	time
TF	trickling filter
TN	total nitrogen
TP	total phosphorous
TSS	total suspended solids
$t_{TS}$	sludge age
VSS	volatile suspended solids
X	particulate fraction
Y	yield coefficient
$\mu$	growth rate



---

**Indices**

---

0	initial
BM	biomass
deg	degraded
e	endogenous
eff	effluent
eli	elimination
ES	excess sludge
f	filtrated
H	heterotrophic organism
h	homogeneous
H+stor	degradation of heterotrophic organism and storage fraction
i	inert
i,BM	inert biomass residue
in	influent
max	maximum
N	nitrification
S	substrate
sp	specific
stor	storage
tot	total
U	unbiodegradable
US	ultra slow

---

## Theses

At silo facilities, organic energy-rich matter is openly stored. Through transportation losses and leaking silage effluent as a by-product of the lactic-acid-fermentation process, impervious and runoff-effective areas are heavily polluted. This organic pollution can easily be washed-off through stormwater. An untreated discharge of these runoffs would therefore have enormous effects on water bodies. With regard to the original definition of waste water in the Water Management Act, in which the energetic potential is not yet mentioned, rethinking waste water as waste to a product leads to greater sustainability as it reduces the carbon footprint. In this context “waste” (-water) in the native meaning depends upon the approach taken, as it has a highly energetical potential. For a holistic approach, water-management needs to be incorporated into an intelligent silo management which involves a separation of the different runoffs with respect to their energy level as well as regular sweeping cycles. However, these methods only partly help to prevent contamination of stormwater, yet an untreated discharge is still not preferable.

Biological degradation is an efficient and reliable way for wastewater treatment. Therefore, if biological treatment is preferred, the wastewater to be treated must be degraded until the impact on the water bodies is sufficiently low. Since the organic matter stored in silos is fed to biogas plants for anaerobic digestion, the wash-off from the surface of the silo is still easily treatable. Highly soluble substances like silage effluent have a higher ‘rapidly degradable fraction’, resulting in improved kinetics than substances that have undergone a digestion like manure. In contrast, the latter is more comparable to domestic wastewater.

Dealing with intermittent occurring stormwater runoff is not a straightforward task. Biofilm-systems with their sessile organisms as a simple and robust technology sustain long periods of starvation without losing much biological performance. Activated sludge systems adequately eliminate nutrients due to their good controllability. Thus, a smart combination of both systems provides a sufficient nutrient elimination and simultaneously sustain long starvation periods. The trickling-filter operated in a sequence-batch-reactor mode denitrifies nitrogen and offers conditions where phosphorous accumulating organisms can evolve.

Based on meteorological dynamics, dry weather periods can last for a long time. During this absence of stormwater, the organisms of a biological treatment plant suffer starvation. Though, biomass in trickling filter survive even long-time starvation. This raises the question what causes this surviving ability and if the commonly used activated sludge model (ASM) can adequately describe this effect. Long term activity experiments (in lab and pilot scale)

revealed that the current approach of the ASM with a simple first order decay rate overestimates the loss of active biomass under long starvation conditions. Introducing an additional biological fraction in the activated sludge in combination with a “base”-decay rate is able to describe the observed decay under starvation conditions more reliably.

## Acknowledgement

Each step of my thesis, of my life was filled with the support from people around me. Since I cannot name them all, I would like to name at least some of them.

I would like to acknowledge my supervisor and doctoral father, Professor Dr. Ing. Jens Tränckner. Without you and your technical expertise, this work would not be of the same quality as today. You coined me the most at the academic level. Thank you for all your work you put into advising me at all steps of this thesis and providing me with the right tools I needed to complete this thesis.

I would like to thank Ulrich Kotzbauer and all his company Rotaria with his valuable guidance and practical knowledge. You and your company provided me an exemplary prototype which has set the perfect conditions for research.

I would also like to acknowledge the whole colleague’s team of the institute Water Management of the University of Rostock. Thank you for supporting me with a helping hand, with brain storming or just with some interesting talks.

In addition, I would like to acknowledge my parents for helping me ever since I can remember. You made it possible for me to study and to find my own way. Finally, I would like to thank all my friends. You helped me to release the stress if everything went wrong and had always an open ear.

# 1 Introduction

## 1.1 WATER FLOWS ON SILO FACILITIES

Silo facilities are used to store highly energetic renewable raw materials (RRM) for livestock breeding and biogas plants. These RRM (often shredded maize and whole crop silage) are harvested in autumn and must be stored for an entire year, nearby the digester or animals. To ensure good food quality throughout the year, the raw matter must be sufficiently preserved. For this purpose, a lactic acid fermentation is performed by airtight storage. The raw material is heavily compacted at the silos and covered with a thick foil to exclude air and rain. Depending on substrate type and its moisture content (MC), lactic acid fermentation starts already at the silo (Moisio, 1994). This leads to the leakage of highly contaminated fluid of the cells (silage effluent) (Galanos et al., 1995). System inherent, the whole impervious area below a silo becomes wetted by the silage effluent and leaves a sticky, sugary surface behind. Therefore, two different types of wastewater accrue at silo facilities: 1) a rather low volume of concentrated silage effluent and 2) a large volume of contaminated stormwater during rainfall.

The silage effluent produced is characterized by low pH, high chemical oxygen demand (COD) and elevated nutrient concentrations (Deans and Svoboda, 1992; Gebrehanna et al., 2014). This highly contaminated wastewater cannot not be discharged untreated due to severe negative impacts on ambient water systems (Stekar 1998). With its high energetic content, it is worth to be treated at the digesters. However, the major hydraulic load is caused by stormwater-runoff from sealed surfaces of traffic and the parking zones, empty silo areas and foil covered silos, supplemented by runoff from roofs (which are not considered here). The pollution of this wash-off is influenced by many operational and meteorological factors and poorly understood so far.

For an economically and environmentally worthwhile silo management, these two substance flows have to be separately collected (Fig. 1). As long as a silo is uncut, they can be easily distinguished by different drainage shafts for silage effluent and stormwater runoff. To separate silage effluent from stormwater, the drained outflow of a silo can usually be shifted between digester (silage effluent) or stormwater-system. Drainage shafts for silage effluent have to be located under the stored raw matter, whereas the shafts for stormwater runoff can be located on the transportation areas so that the stormwater from the foil can drain to these. For this, the foils have to be adequately tensioned to avoid a drainage of stormwater

runoff from the foil into silage shafts and ensure a drainage only into stormwater shafts. Once the silo is opened, separation is no longer straightforward. A mixing of the two wastewaters seems unavoidable and the drainage line, so far discharging pure silage effluent towards the digester, is now collecting rainwater, too. Here, the question arises, if the increased amount of now diluted water can still be operated by the digester or if the drainage has to be switched from silage effluent to the storm water system with adverse effects on stormwater composition. If the drainage shall be discharged towards the digester, both the hydraulic transport system and the digester must be able to cope with the increased flow.

The first paper deals with the surface contamination of silo facilities and discusses an intelligent silo management, which aims to prevent contamination of stormwater while saving resources (see Fig. 3).

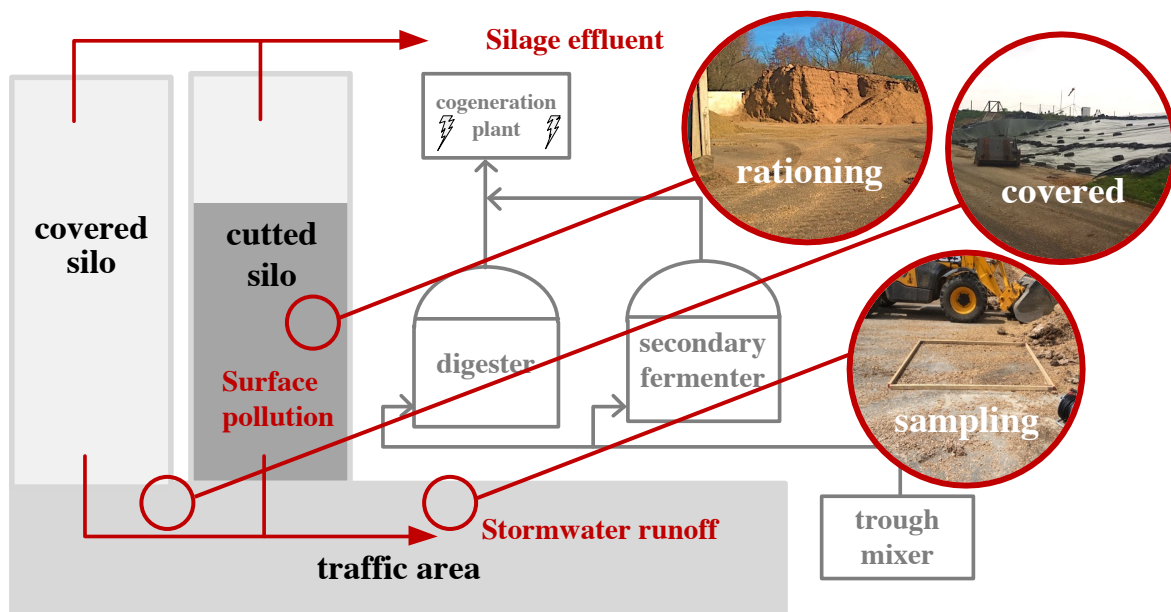


Fig. 1: Water flows on an exemplary silo facility

## 1.2 STORMWATER SITUATION ON SILO FACILITIES

The risk evaluation of stormwater runoff and basics of handling it is yet based on the regulatory standard DWA-A 102 in Germany (DWA-A-102-1, 2020). In this regulatory standard, the contamination of stormwater runoff is defined solely by the parameter 'filterable particles smaller 63  $\mu\text{m}$ ' [German: AFS63]. The idea behind this parameter is that the smaller the particles size, the higher the specific surface [ $\text{m}^2/\text{m}^3$ ] and the higher the specific surface, the higher the ability to adsorb heavy metals. From the perspective of authorities, heavy metals are difficult to measure without equipment, whereas particle size is

easy. However, this risk defining parameter fits well for stormwater runoff from urban surfaces like streets as the main pollution here are heavy metals (Acosta et al., 2014; Cheng et al., 2017; Wang et al., 2013).

Little is known about stormwater runoff from silo facilities. Contrary to sealed surfaces from urban areas like streets and parking lots, high-energy organic matter is stored on the surfaces and the stormwater load depends strongly on the solubility of the raw materials and their ability to mobilize them. Therefore, runoffs from silo areas are highly contaminated with COD, nitrogen (N) and phosphorus (P) (Holly and Larson, 2016; Larson and Safferman, 2009; Tränckner, 2018). In particular, if feces like chicken dry feces are stored on the silo, the N and P load of the runoff jumps higher. Both, the amount of dissolved and mobilized load depends on the intensity and duration of rainfall on the one side and on the specific stored substrate on the other.

According to the assessment by pollutant loads, stormwater runoff from silo facilities is rather comparable with domestic wastewater than typical stormwater as defined by DWA-A 102. Hence, the more proper fitting regulatory standard would be DWA-A 792 regarding manure-slurry-silage systems [German: JGS] as the runoffs from these areas usually contain silage effluent, slurry or fermentation residue (DWA-A-792, 2018). This set of rules lays down the basic principles for the design and construction of structures for the storage of silage effluent and slurry. In this context, stormwater runoff that has come into contact with manure or silage effluent is assessed as having the same hazard potential as manure or silage effluent and has to be handled accordingly.

The meteorological and operational dynamic complicates the prediction of stormwater pollution and as a consequence the planning of a reliable treatment plant under these specific circumstances. The treatment technology has to degrade highly COD loads as well as nutrient loads of N & P. None of the existing process technologies meet the requirements, as they have to deal with highly dynamic loads and intermittent inflow, i.e. in dry periods they have to sustain long starvation periods without substrate inflow.

### 1.3 BASICS OF CONVENTIONAL NUTRIENT ELIMINATION WITH ACTIVATED SLUDGE

Conventional nitrogen elimination is based on oxidation of ammonia during nitrification and a subsequent nitrate reduction with a denitrification to elementary nitrogen (Khunjar et al., 2014). Typically, the nitrification is the limiting step as the executing organisms are

autotrophic and therefore show a poor growth rate as the energy gain from ammonia oxidation is considerably smaller than from oxidation of organics. The nitrifiers are using ammonia as electron donor and oxygen as acceptor. The carbon source is dissolved  $\text{CO}_2$ . The nitrification process can be divided into oxidation of ammonia to nitrite performed by nitrosomonas and further to nitrate (Nielsen and McMahon, 2014). Contrary to initial suspicions, the dominating organism group performing nitrite oxidation is nitrospira and not nitrobacter (Juretschko et al., 1998). The stoichiometric relation is shown in eq. 1



The stoichiometry of ammonia oxidation reveals a specific oxygen demand of 4.6 g  $\text{O}_2$  per g  $\text{NH}_4\text{-N}$ . Also, for each mol of ammonia, two mol of acid ( $\text{H}^+$ ) is produced and therefore, acid capacity is consumed which leads to a pH decrease. A low pH inhibits the process. According to Wheaton (1994), the range of an optimal pH is between 6 and 9 (Wheaton et al., 1994). However, due to the finely dispersed sprinkling of wastewater in the trickling filter system,  $\text{CO}_2$  is stripped out and therefore, they tend to have a high pH, if sufficient organics are previously degraded.

During denitrification, oxygen is released and acid capacity produced (eq. 2). Here, the nitrate acts as electron acceptor. Stoichiometrically, for each mol of nitrogen, only one mol of acid capacity ( $\text{H}^+$ ) is produced. Hence, the net balance of nitrification and denitrification is negative ( $-1 \text{ mol H}^+$  per mol N) and the consumed acid capacity during nitrification can only partly be regained with the denitrification.



In addition to nitrogen removal, the phosphorous elimination plays a key role for subsequent wastewater discharge. The state of art for phosphorus removal in activated sludge systems (ASS) is performed with an enhanced biological phosphorus removal (EBPR) by applying alternating aerobic and anaerobic conditions. Both, denitrification and EBPR require mandatory the absence of oxygen. The development of a proper plant design that fulfills these requirements when dealing with stormwater runoff is discussed in detail in paper III.

#### 1.4 BIOFILM-SYSTEMS

Attached growth systems are robust and energy-efficient treatment technologies (Henrich and Marggraff, 2013; Metcalf and Eddy, 2014). Due to the ability of bacteria to form spores under degrading conditions, they can grow again under favorable conditions. Therefore, they have a certain capacity for both biological reactivation after long-term starvation and to handle shock-load conditions as sludge can easily adsorb COD at low sludge ages (Haider et al., 2003; Zhang et al., 2009). A generally accepted theory among biologist is the transformation of organism by entering into an exogenous dormant state under strictly endogenous conditions as a decisive survival strategy (Wik, 2003). Within a certain period of time they then can be reactivated from this dormant state or have to die if the time period is exceeded. At a first glance, these properties make trickling filter (TF) to an ideal solution for coping with highly contaminated intermittent stormwater-runoff. In a TF system, the wastewater to be treated is trickled with a rotating spreader over a fixed-bed. Due to this spreading, biomass starts to grow on the fixed-bed. Based on the chimney pulling effect, air is sucked through air holes at the bottom of the TF to the top. Hence, the surface of the fixed-bed is constantly in contact with fresh air, leading to oxygen diffusion into the grown sessile biomass. This fairly simple method is low in both capital and operating costs, as no additional aerator is required. The low control requirement is making it easy to operate even for unskilled workers. The advantages make this technology favorable for biogas operator as they are typically no wastewater experts.

In fact, the key constraint of this technology is the poor nutrient elimination and since the contamination is not limited to an organic load but to nutrients, it would only partially treat the stormwater. Based on marginal anaerobic zones (depending on the biofilm thickness) or periods, limited denitrification (DN) and no enhanced biological phosphorus removal (EBPR) can be expected.

Contrary to TF, ASS like sequence batch reactors (SBR) have the ability to integrate anaerobic zones or steps for an aimed nutrient elimination with DN and EBPR (Ekama and Wentzel, 1999). Alternating aerobic, anoxic and anaerobic condition lead to a significant active biomass conservation improvement (Torà et al., 2011; Yilmaz et al., 2007). Here again, a controlled reactivation of biomass is possible within days. Long-term starvation in ASS lead to a significant loss in biomass activity due damaged membranes under strictly aerobic conditions (Lopez et al., 2006). Another disadvantage of ASS is the energy demand for aeration and high controlling demand. As operator of biogas plant are usually not familiar



with wastewater treatment plants, is more simple and robust solution may be preferable. This is where trickling filters could come into play as they are simple and robust systems with less energy demand. However, due to nutrient discharge limits, TF have been displaced by ASS.

Faced with all these challenges, a combination of both systems seems to be the most appropriate solution. Paper III presents a possible process design for a trickling filter operating in a SBR mode to include anoxic and anaerobic steps in the process control. At this point, the technology has to be verified regarding 1) elimination efficiencies of COD and nutrients via EBPR, nitrification and denitrification and 2) the preservation of biological activity after long starvation periods.

### 1.5 MODELLING OF ORDINARY HETEROTROPHIC ORGANISM

Modelling microbial life has a long history and can be traced back to Monod (1949). Based on the Michaelis-Menten-theory for enzymes, he developed a theory to describe growth kinetics of microorganism using single substrates and laid the foundation of modelling activated sludge. According to Monod, the relation between biomass growth  $X_H$  and substrate utilization can be described with a constant, the yield coefficient  $Y$ , which is characteristic for each particular substrate (see Fig. 2). The substrate, expressed as chemical oxygen demand (COD), is converted by ordinary heterotrophic organism into  $X_H$  (=growth) during metabolism with the factor  $Y$  by oxygen consumption ( $O_2(1-Y_H)$ ). However, dissolved rapidly biodegradable substrate  $S_S$  can be directly utilized by heterotrophic organism, though, more complex substrates  $X_S$  (mostly particular) firstly have to be metabolized into  $S_S$  through hydrolyzation (Leslie Grady and Daigger, 1999). The yield coefficient can be used for estimation of sludge production and oxygen consumption, respectively. Paper II discusses the fractioning of COD from different wastewaters typically appearing on silo facilities in detail (Fig. 3).

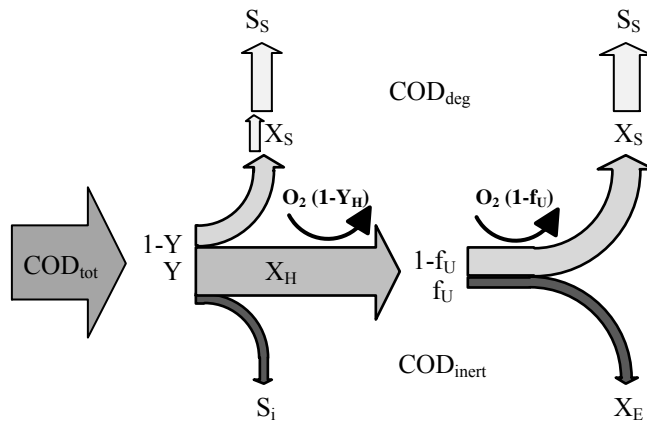


**Fig. 2: COD fractions for modelling activated sludge**

Herbert (1958) firstly introduced a decay rate to explain low yield coefficient at higher sludge retention time (SRT) (Herbert, 1958). He extended the so far common approach of a strictly anabolic substrate utilization with an endogenous metabolism to provide maintenance energy for the microorganisms. With this in mind, McKinney developed 1960 the endogenous residue model, on which the activated sludge model 3 (ASM3) is based on (McKinney, 1960). Under endogenous conditions, the starving organism can oxidize a fraction  $(1-f)$  of the active biomass  $X_H$  to provide maintenance energy. The remaining fraction  $f$  of active biomass is decayed into an endogenous residue  $X_E$ .

Derived from this model, Marais & Ekama (1976) and Dold et. Al (1980) integrated storage compounds and developed a model called death-regeneration model, which set the basis for the ASM1 and ASM2 (Dold et al., 1980; G.v.R. Marais and Ekama, 1976). During anaerobic conditions, they found an unexpected effect in microbial batch experiments under endogenous conditions. The decay still continued under anaerobic conditions and therefore, accumulated over time. With subsequent aerobic conditions, a significant increase in biological activity was observed. This could only mean, that decay is independent from oxygen consumption and biomass utilization. In this approach, a fraction of active biomass  $X_H$  is converted into a bioavailable fraction  $X_S$  through death and new biomass is “regenerated” by metabolism of these by-products from decayed organism under aerobic conditions using oxygen as electron acceptor (Dold et al., 1980; G. v. R. Marais and Ekama, 1976). However, also this decay rate was considered to be constant and yet independent from SRT and substrate supply (Van Haandel et al., 1998). Depending on the model used, the range of decay rate is between  $0.24 \text{ d}^{-1}$  (ASM1) and  $0.17 \text{ d}^{-1}$  (ASM3), which mathematically causes a significant loss in active biomass within days of starvation.

A constant decay rate does not seem to adequately reflect the reality and this mechanistic approach is neglecting the ability of physiological adaption of organism to certain conditions like long-term starvation, firstly proved by Friedrich et al. (2015). According to Friedrich, the bacteria can adapt to starvation conditions by reducing the required maintenance energy, which under endogenous conditions causes a decrease of the decay rate (Friedrich et al., 2015). This effect of adaption is described with two different decay rates, firstly,  $b_{\max}$  for unlimited substrate supply and secondly,  $b_e$  for starvation adapted organism. They found out that for low loaded systems, the decay rate is between both as the adaption already occurred. Hence, the current decay rate of organism is temporal and a function of the SRT. However, this adaption of decay rate to certain conditions is just a mathematical description of the observed effect of a reduced decrease of volatile suspended solid (VSS) in low loaded systems and did not lead to an improved process description of the ASM, yet. The question that arises here is, if this reflects the reality of microbial life and is the ASM in its current form sufficient or can the reason be found elsewhere? In fact, this approach requires knowledge of the SRT of the system, which is not known in trickling filter systems and can therefore not be transferred to these systems. Hence, an approach of continuous adaption of the biomass into the model is needed. A new approach of the ASM is discussed in paper IV (Fig. 3).

## 1.6 STRUCTURE

The thesis is based on 4 papers (Fig. 3). Each of them discusses specific topics from the areas mentioned above. Starting with the identification of the source and process accumulation of contamination appearing on silo facilities, paper II follows with the treatability of different wastewaters typically occurring at biogas plants. Based on these insights, paper III is presenting a possible treatment solution for stormwater runoff containing mainly organics and nutrients. In the last paper, the current approach regarding the decay rate is being questioned according to unexpected effects during long-term respiration batch-experiments.

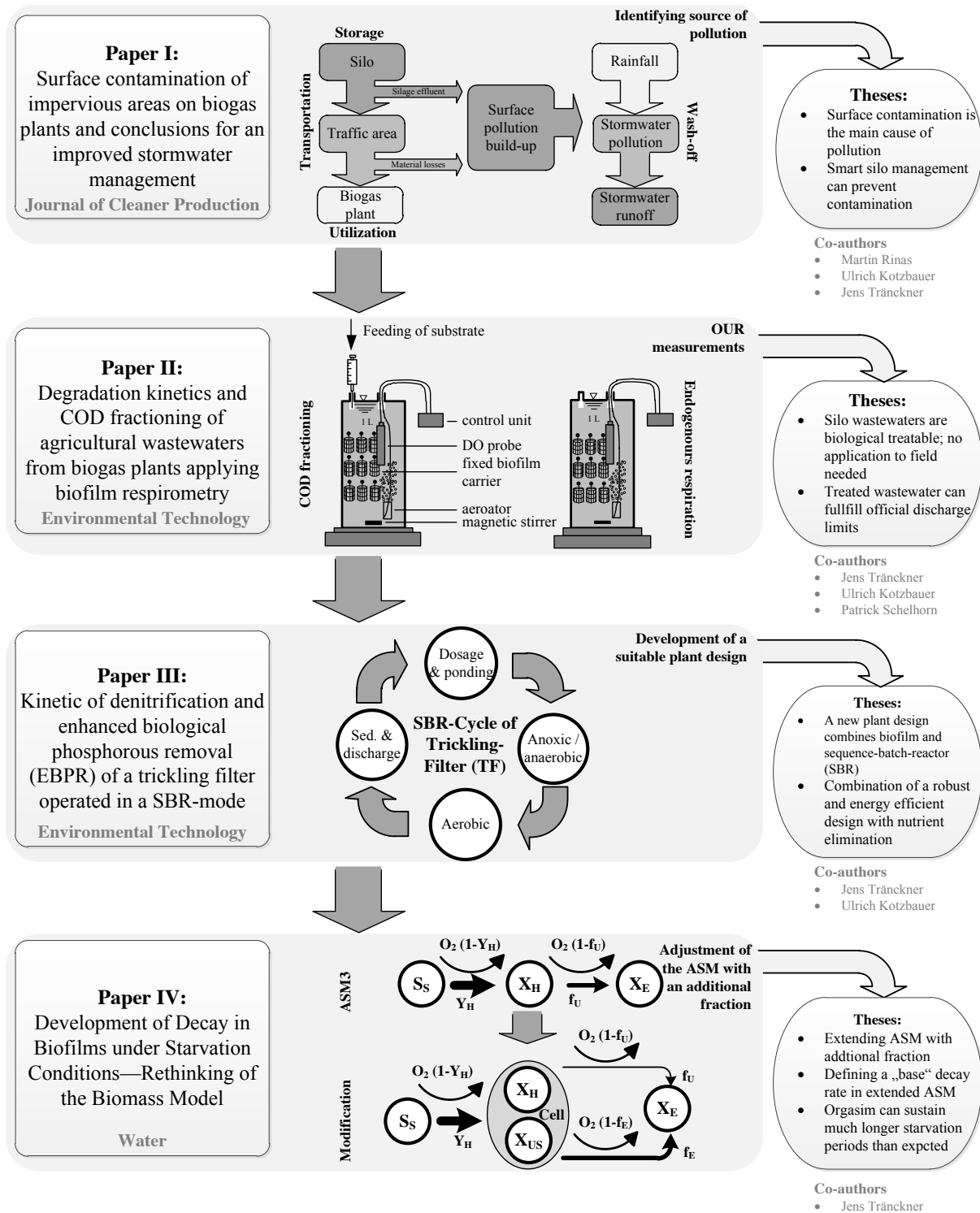


Fig. 3: Structure of publications

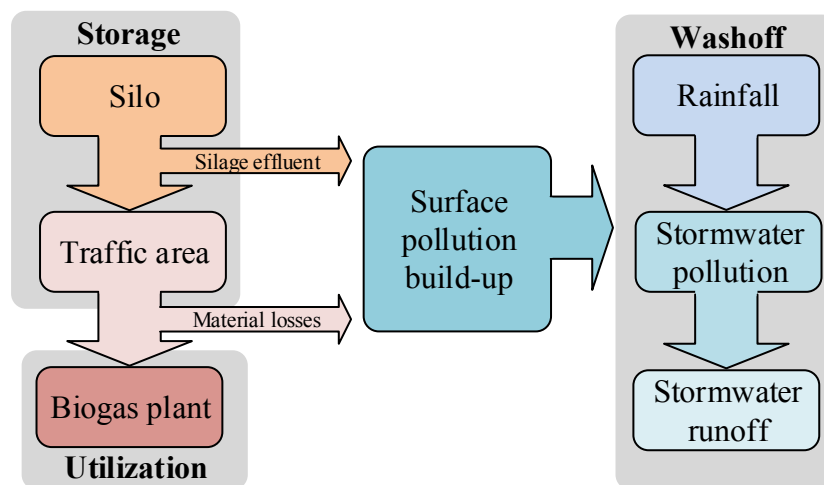


## 2 Surface contamination of impervious areas on biogas plants and conclusions for an improved stormwater management

This chapter is published in:

**Journal of Cleaner Production; Volume 217, 20.4.2019; 1-11**

<https://doi.org/10.1016/j.jclepro.2019.01.087>



Biogas plants are an important technology for the intended shift towards energy production from renewable resources. But the handling of biomass in open silo facilities can create heavily polluted stormwater with severe impacts on the environment if discharged directly. The purpose of this study on a biogas plant in North-East Germany is to i) identify the main pollution sources, ii) quantify the surface specific pollution potential and iii) derive consequences to mitigate the environmental impact of stormwater from biogas plants. Two main pollution sources were identified: i) silage effluent, mainly occurring on the silo surfaces and ii) substrate losses along the transport paths. The surface specific pollution potential of COD, N and P was measured for characteristic subareas applying wet vacuum cleaning. The accumulation of pollution on the cover foil was very low, whereas the range of daily accumulation on the actively operated surface varied between 8.3 and 41.7 g<sub>COD</sub>/(m<sup>2</sup>·d). The pollution built-up is a highly stochastic process influenced by many factors (handled substrate, operational practice, meteorological conditions). Daily sweeping can significantly reduce the pollution potential for stormwater but cannot avoid the requirement of treatment prior to a discharge into a surface water.

## 2.1 INTRODUCTION

### 2.1.1 MOTIVATION AND OBJECTIVES

The Paris Agreement climate proposal aims to limit the global warming to 1.5°C. This agreement yields in an upper limit of CO<sub>2</sub> equivalent emissions. Beside a substantial reduction of energy demand, this requires to replace fossil fuels with renewable energy like hydropower, wind power, solar power and biogas. In Germany, the current percentage of renewable energy is 32% of total power production with the goal of 80% to 95% until 2050 (

Fig. 4). Biogas plants are an important brick in the renewable energy supply as they can bridge short term variations in wind or solar power supply. Typically, biogas plants store the required biomass, mainly harvested in autumn, up to one year in large open silo facilities. From there, it is demand-oriented fed to the fermenters. Storage and operation of the high energy leads to significant surface and – in consequence – stormwater pollution. Still, these stormwater runoffs are often discharged to surface waters without any treatment with severe impact on the aquatic environment.

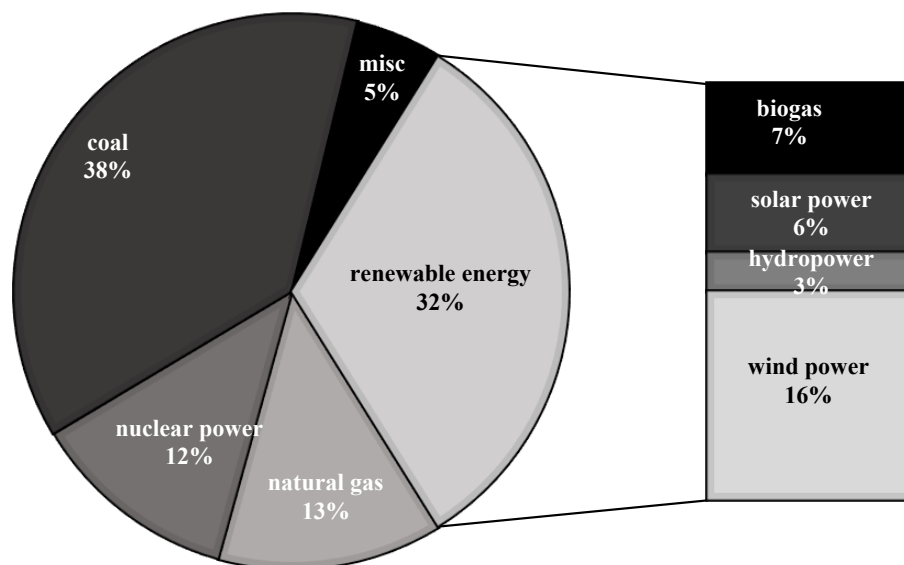


**Fig. 4: Energy mix of total electrical generation in Germany 2017 accordance to Federal Statistical Office**

Inter alia, this became evident when local environmental authorities in North-East Germany investigated potential sources of surface water pollution in the process of the European Water Framework Directive (WFD). In this context, stormwater discharge of 23 biogas plants and farming areas was measured by grab sampling (Fig. 5). The median of COD

(1,215 mg/L), total N (38 mg/L) and total P (13 mg/L) was in the range of domestic wastewater. Extreme values are partly by one to two orders of magnitude higher and in the range of pure silage effluent (Capodaglio and Callegari, 2016; McCarty et al., 2011).

It is evident, that the basically valuable contribution of biogas plants to fight climate change cannot be generated at the cost of the local and regional environment. Therefore, within a currently running project, strategies and technological approaches to mitigate the environmental impact of stormwater from biogas plants are developed. The aim of the present work and starting point for these developments is to:

- i) identify the pollution sources
- ii) quantify the resulting loads and concentrations in stormwater
- iii) search for source-oriented mitigation measures.

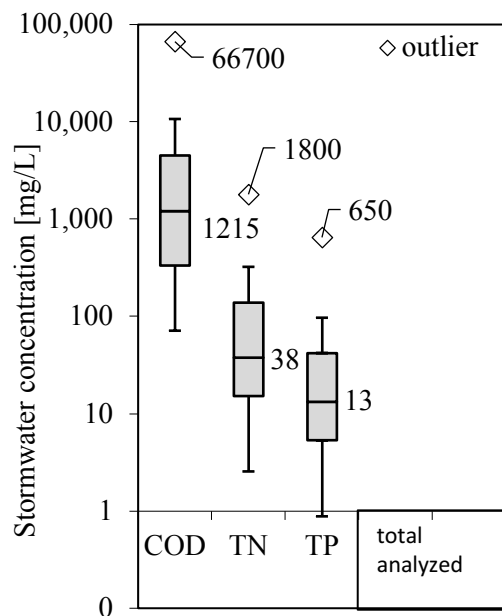


**Fig. 5: Stormwater pollution at the discharge point of various silo works (partly with additional husbandry activities); data kindly provided by the “Staatliches Amt für Umwelt und Natur Mittleres Mecklenburg”**

## 2.1.2 CONDENSED LITERATURE REVIEW

In contrast to impervious surface in agriculture, the built-up of pollutions regarding urban surfaces like roads and roofs are widely investigated (Acosta et al., 2014; Fedje, 2015; Goonetilleke et al., 2009; Murphy et al., 2015; Wicke et al., 2012). Here, the main sources of pollution are tire abrasion and fly ashes from combustion. Stormwater runoff from these



urban and industrial surfaces show high concentrations of heavy metals but relatively low concentrations of COD and nutrients compared with domestic wastewater (Barbosa et al., 2012; Cheng et al., 2017; Egodawatta et al., 2013; Herngren, 2005; Wang et al., 2013; Zhang et al., 2016, 2015). Though, on agricultural surface and silo facilities the conditions are completely different. The renewable raw materials (RRM) (often shredded corn) harvested in autumn is stored for a whole year in open spaces, nearby the digester. For this, the biomass is heavily compacted at the silos and covered with a thick foil to exclude air and rain. Depending on substrate type and its moisture content (MC), lactic acid fermentation starts already at the silo (Moisio, 1994). This leads to a leakage of highly contaminated fluid of the cells (silage effluent) (Galanos et al., 1995). System inherent, the whole impervious area below a silo becomes wetted by the silage effluent and will be ready for wash-off after opening a silo for operation. In contrary to urban runoff, this silage effluent runoff is heavily polluted with COD and nutrients like ammonium and phosphate (Faulkner et al., 2011; Holly et al., 2018). The COD of the silage effluent can exceed concentration of  $80,000 \text{ mg}\cdot\text{L}^{-1}$  (Gebrehanna et al., 2014). Different solutions exist to drain these effluents and valorize it in the fermenter and will be discussed later.

For several years, biogas plants have become subject of detailed life cycle analysis (LCA). Currently, LCA concentrate on global and local gas emissions from digestion itself (Fuchsz and Kohlheb, 2015; Huttunen et al., 2014; Ramírez-Arpide et al., 2018). Some studies include additionally emissions appearing during silaging (Lijó et al., 2014; Ravina and Genon, 2015). However, water and wastewater footprint are rarely regarded, yet. Very few studies regarding Life Cycle Inventory Analysis (LCIA) (Poeschl et al., 2012) and water footprint (Pacetti et al., 2015) are widening the systems scope to water demand. But no study is dealing with the wastewater problem arising directly on the site (Fig. 6). Also with regard to already published findings on stormwater pollution (Holly and Larson, 2016; Larson and Safferman, 2009) the environmental footprint of silo stormwater runoffs should be considered in future LCIA. With regard to targeted measures to improve ambient water quality it is important to understand the underlying processes and to develop efficient technologic solutions to mitigate environmental impact.

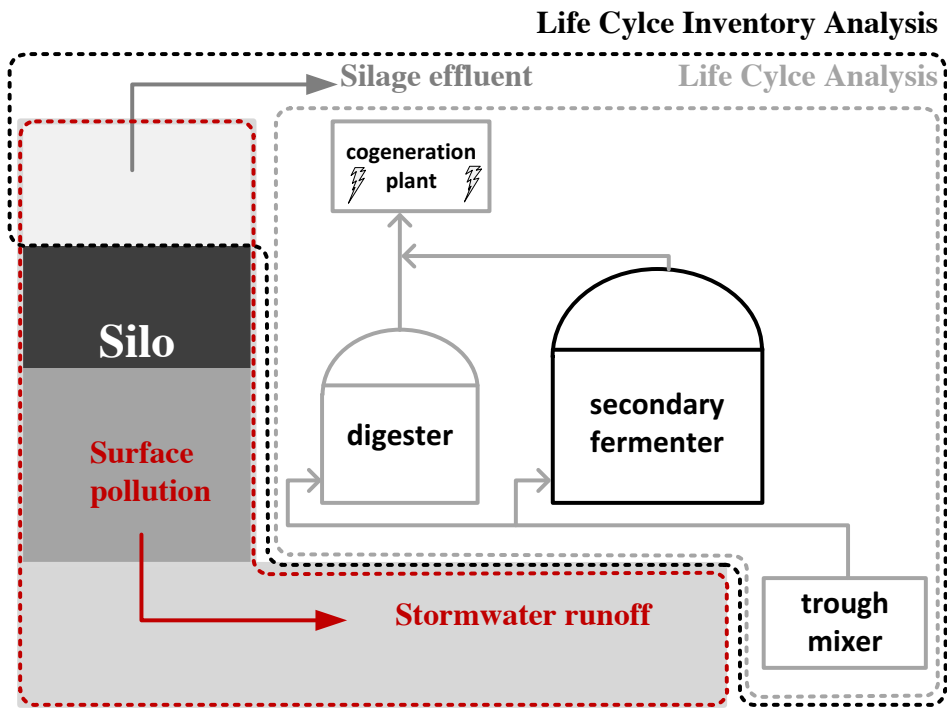


Fig. 6: Integration of stormwater pollution into Life Cycle Inventory Analysis

**Table 1: References regarding urban and agricultural built-up and runoff**

Reference	topic	study details
(Acosta et al., 2014)	Urban built-up	Risk assessment of street dust pollution
(Wicke et al., 2012)	Urban built-up	Pollution from asphalt
(Fedje, 2015)	Urban built-up	LCA from fly ashes
(Murphy et al., 2015)	Urban built-up and wash-off	Atmospheric pollution deposition and modelling runoff
(Goonetilleke et al., 2009)	Urban built-up and wash-off	Pollution concentrations of marine environmental
(Gebrehanna et al., 2014)	Silage effluent management	Cradle to grave cycle of silage effluent
(Holly and Larson, 2016)	Silage runoff and Treatment	Treatment of silage effluent with vegetated filter strips
(Holly et al., 2018)	Silage runoff	Properties and dynamic of silage effluent
(Faulkner et al., 2011)	Silage runoff	Nutrient removal with vegetative treatment areas
(Ramírez-Arpide et al., 2018)	Biogas production	LCA of anaerobic co-digestion
(Pacetti et al., 2015)	Biogas production	Water footprint and LCA of anaerobic digestion
(Lijó et al., 2014)	Biogas production	LCA of gas emissions from different feedstocks
(Huttunen et al., 2014)	Biogas production	Combining LCA with stakeholder interviews
(Poeschl et al., 2012)	Biogas production	LCIA of gas emissions and water pollutions, excluding stormwater from silo
(Ravina and Genon, 2015)	Biogas production	LCA of global and local gas emissions
(Fuchsz and Kohlheb, 2015)	Biogas production	LCA of gas emissions from digestion
(Barbosa et al., 2012)	Urban stormwater runoff	Sustainable management of urban stormwater
(Cheng et al., 2017)	Urban stormwater runoff	Stormwater pollution of first flush from asphalt
(Wang et al., 2013)	Urban stormwater runoff	Pollution concentrations from roofs and roads
(Larson and Safferman, 2009)	Agricultural stormwater runoff	Stormwater characterization from animal feed operations

This requires to investigate the stormwater pollution of silo surfaces in agriculture or on biogas plants in a source and process-oriented way. For this, the applied methods in urban areas are a valuable starting point.

## 2.2 MATERIALS AND METHODS

### 2.2.1 SITE DESCRIPTION

The accumulation of surface loading of COD and nutrient contaminants was monitored on a biogas plant, located in the north-east of Germany. The biogas plant has three different silo areas with a total size of 4,260 m<sup>2</sup>, which are filled once a year with RRM from the close farmland. A wheel loader transports twice a day the RRM to the feeding system.

The filled silos are covered with a thick foil. Stormwater from the foil flows depending on the hoven's morphology to the back (meadow) and front (traffic area) of the silo. The drainage system is characteristic for German biogas plants, built in the last decade. The bottom of a silo is constructed with a small slope towards a duct in front of the silo at the half width. The drainage system has two outflows: i) pumping station to the fermenter, ii) stormwater outflow. The flow towards one of these outflows can be manually directed with so called "system shafts". Drains below a closed silo are directed to the biogas plant to use silage effluent for biogas production. After opening the silos, this shaft can be switched to the rainwater system, draining towards a retention tank (see scheme Fig. 7).

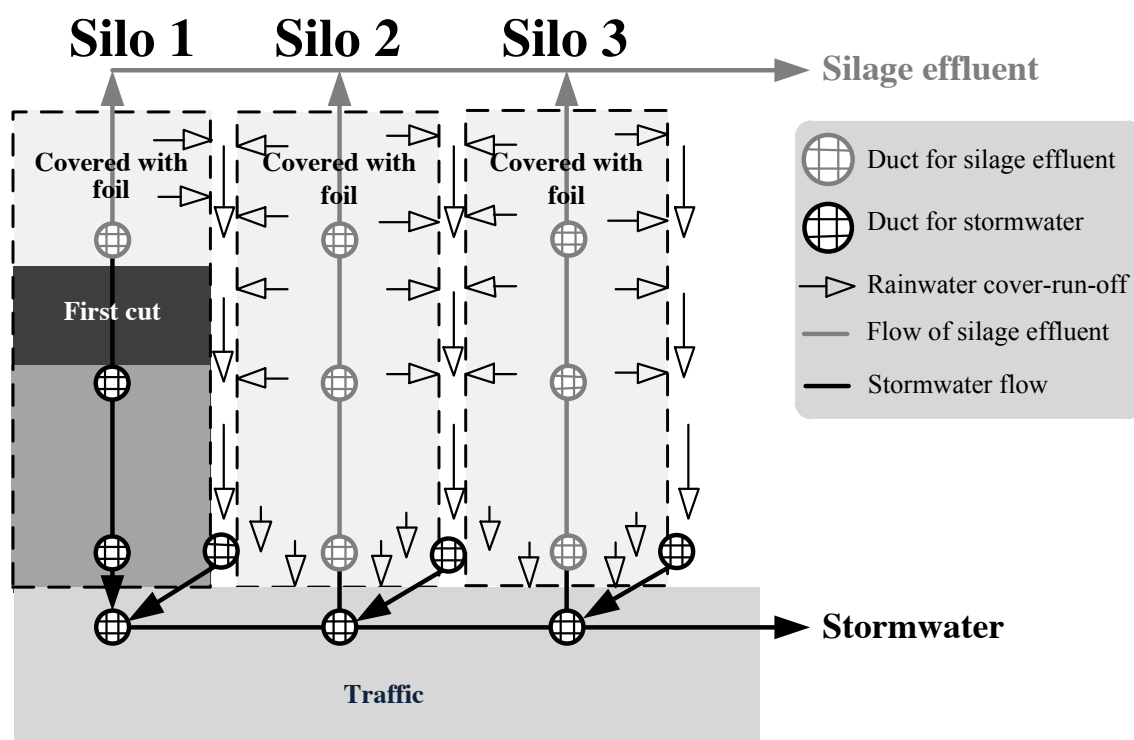


Fig. 7: Drainage system at the monitored silo

### 2.2.2 STORMWATER SAMPLING

To analyze the stormwater contaminants an automatic sampler (MAXX P6) was installed in the last manhole before the rainwater retention tank. Rain intensity was measured using an OTT pluviograph<sup>2</sup>. Sampling was automatically started when rain height exceeded 0.1 mm. with a sampling interval of 6 minutes and a bottle shift after 30 minutes. The samples were analyzed at the same day in the laboratory.

### 2.2.3 SURFACE CONTAMINATION

To quantify the surface contamination, the impervious area of the biogas plant was divided into 3 zones:

- Zone 1: silo foil
- Zone 2: moderate loaded silo (2a) and traffic area (2b)
- Zone 3: highly loaded first cut area



**Fig. 8: Typical example the heterogeneous contamination of a silo area**

The samples were taken in several campaigns between January and May 2017. The sampling method is based on the suggestions of Zhang and Krebs (2013) for characterizing the built-up process on road surfaces. The sampling points are located as shown in Fig. 10 and are marked out with a mobile 2x2 m square grid (Fig. 9, left). For each zone, two samples were taken: one in the middle and one in the fringe section, respectively. The sampling points were swept with a road sweeper prior to the first sample. For sampling, the area inside the grid square was completely wiped with a wet vacuum cleaner “Kärcher Professional Puzzi 10/1” (Fig. 9, middle & right). Both, the solid and the dissolved fraction of the collected wiping water were analyzed in the laboratory. In various preliminary test runs, a spray intensity of 600 mL/min and a cleaning velocity of 2.5 m<sup>2</sup>/min yielded the best balance between cleaning efficiency (> 99%) and logistical effort for sampling and analytics.



**Fig. 9: Cleaning method of the grid square with a wet vacuum cleaner before, during and after cleaning**

Because of the challenging operational conditions on a biogas plant, two different methods for assessing the daily contamination built-up were tested.

**1) Fixed Sampling points:** The sampling points are fixed but the sampling frequency increases with time of accumulation. So, for one day of accumulation, the measurement is accomplished on the same grid next day (on day 2) and for two days of accumulation after another two days (on day 4) after usual working shifts. The advantage of this method is, that the built-up of exactly one test area is measured. Its disadvantage is the long time for accomplishing a test series of several days (e.g. for a built-up of three days:  $1+2+3=6$  days). In a rather humid climate, this increases the risk that the intended measurement of dry weather built-up will be disturbed by intermediate rain events.

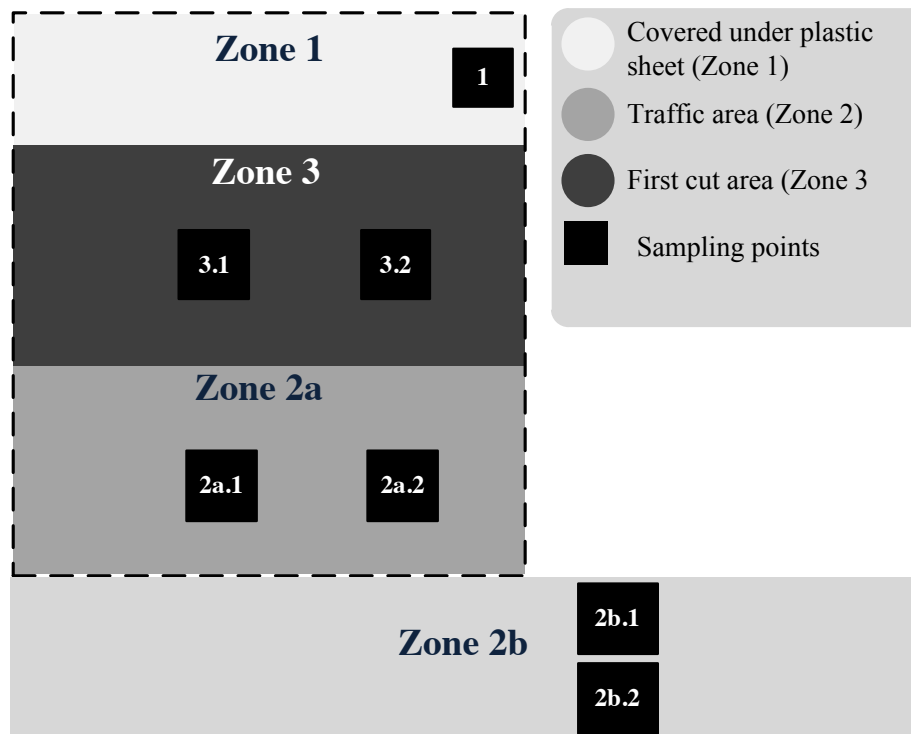


**Fig. 10: Schematic diagram of the monitored silo areas of a silo with sampling method 1**

**2) Varying sampling points:** Pre-assumption of this method is a homogeneous distribution of contaminants in each zone. Each zone is divided into 8 sampling points. Each sampling point is measured only once during the whole measuring campaign. To improve validity, two parallels are measured in each zone. On each measuring day, another sampling point is measured so that the sampling points vary each day. If one point is not cleaned yet, the accumulation process forges ahead until the day of cleaning. The sampling point (first and only) cleaned on day 3 is representative for 3 days of accumulation. Fig. 11 shows the procedure of measurement with the day of measuring of each sampling point. Advantage of this sampling procedure is the shorter total sampling period, reducing the risk of meteorological disturbances (namely rain during the sampling period). Its disadvantage is the potential impact of spatial heterogeneity of surface pollution.

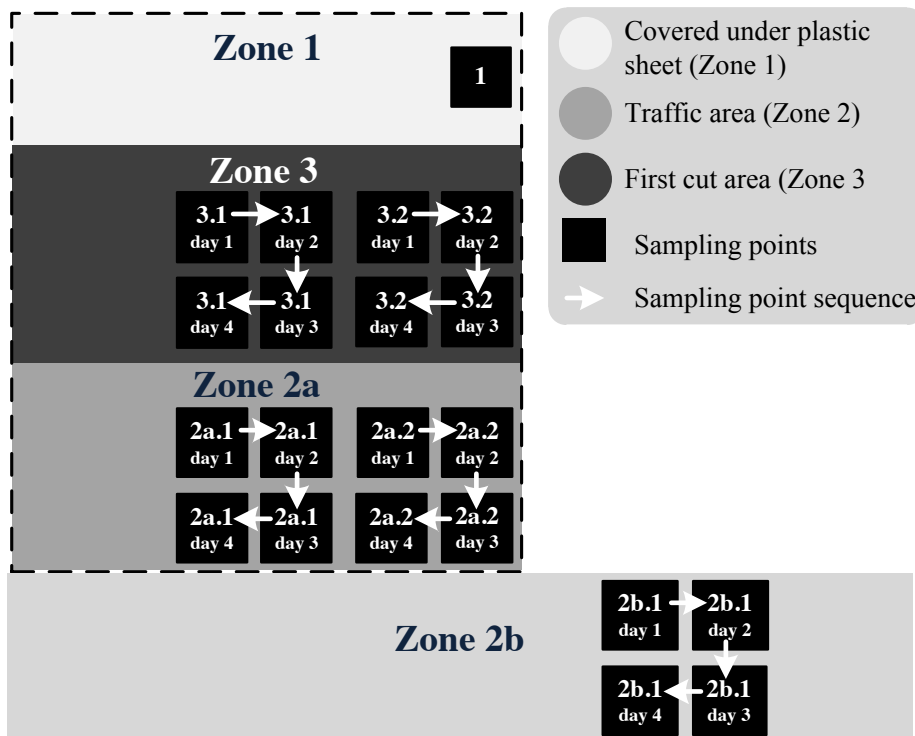


**Fig. 11:** Schematic diagram of the monitored silo areas of a silo with sampling method 2

The contaminants on the covered foil could not be measured with the vacuum cleaner. As surrogate, one square meter of the sheet was wiped with a sponge and which was subsequently cleaned with tap water. The tap water with the washed-out pollution was analyzed in the laboratory.

## 2.2.4 LABORATORY ANALYSIS

The dry and organic dry matter of the solids were analyzed at 105°C and 550°C, respectively. The chemical oxygen demand COD, total phosphorus TP and total nitrogen fraction TN of the liquor phase are measured with HACH-LANGE vessel tests LCK 014 for COD, LCK 350 for TP and LCK 338 for TN. The dried solids were ground in mortars and mixed with 30 mL distilled water to a homogenous suspension before measuring with Dr. Lange vessel tests. The total area loading  $B$  is calculated as follows:

$$B = \frac{c_{liquid} \cdot Q_{liquid} + \frac{m_{DS,total}}{m_{DS,analyzed}} (c_{susp} \cdot Q_{susp})}{A} \left[ \frac{g}{m^2} \right] \quad 1$$

where  $c_{liquid}$  and  $Q_{liquid}$  are the concentration of contaminants and volume of the liquid phase that is collected by the vacuum sweeper, whereas  $c_{susp}$  and  $Q_{susp}$  are the concentration and volume of the suspended solids in 30 mL distilled water,  $m_{DS,total}$  and  $m_{DS,analyzed}$  is the total collected and the grounded, analyzed amount of dried solids, respectively.  $A$  is the area of the grid square.

The daily built-up  $J$  is calculated by:

$$J = \frac{B}{d} \left[ \frac{g}{m^2 \cdot d} \right] \quad 2$$

where  $d$  is days of accumulation.

## 2.3 RESULTS

### 2.3.1 STORMWATER RUNOFF IN DETAIL

Fig. 12 shows the time series of flow and COD concentration of two exemplarily stormwater runoff events. At the time of monitoring these events, no cleaning procedure was integrated in the usual working shift. The COD-concentration raised up to 6'000 mg/L and in both events, the rain height/ rain intensity was not sufficient for a complete wash-off, leading to still elevated COD concentrations of about 2'000 mg/L at the end of the event. In total, about 12.0 kg and 17.4 kg COD were washed off. Taking domestic wastewater as comparison, this corresponds to daily loads of about 100 to 150 population equivalents.



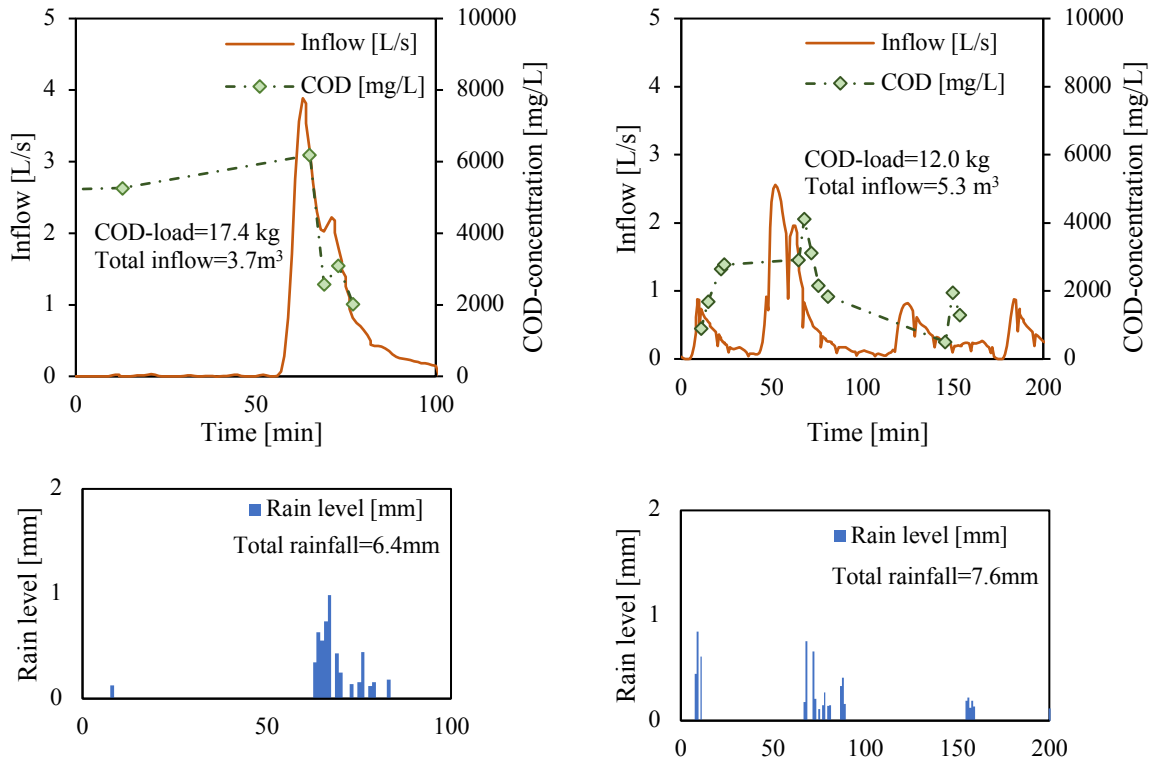


**Fig. 12:** Stormwater pollution of single rainfall events in detail

### 2.3.2 CHARACTERISTICS OF THE SOLID SUBSTRATE

In the investigated biogas plant, the same RRM (shredded corn) with rather different water content was stored in two silos. In the case of the defined “dry-stored-substrate”, the low water content in the cells inhibits the outflow of silage effluent. At this silo, nearly no sugary fluid of the cells and no sticky surface were monitored. These visual findings are supported by the considerably higher COD to oDM ratio compared to the “wet-stored substrate” (Table 2). At the silo with the “wet-stored-substrate” a clearly visible dark brown colored silage fluid seeped out of the shredded corn. The COD:N:P ratio of the solids at storage varies from 100:0.6:0.16 to 100:0.7:0.25.

**Table 2: Characteristics of RRM of the silos**

Substrate-type	DM at storage	oDM/DM at storage	COD/oD M	TN/oDM	TP/oDM
dry-stored	61.0 ± 0.3%	86.2 ± 5.5%	152 ± 18%	1.10 ± 0.34%	0.25 ± 0.08%
wet-stored	34.5 ± 8.1%	88.0 ± 9.3%	134 ± 16%	0.78 ± 0.33%	0.33 ± 0.07%

### 2.3.3 BUILT-UP PROCESS ON THE COVERED FOIL

On the covered foil, the surface contamination was with values of 0.1 to 0.4 g<sub>COD</sub>/m<sup>2</sup> rather low and no measurable accumulation within the time of measuring campaign was monitored. Accordingly, the further discussion focuses on the other zones due to this insignificant contamination.

### 2.3.4 BUILT-UP PROCESS “DRY-SUBSTRATE”

The sampling campaign for the built-up process with “dry-stored-substrate” was performed with sampling method 1 in May 2017 as silo 3 was cut (Fig. 10). The cleaning with the wet vacuum cleaner after sweeping the surface with the road sweeper marks day 0 of accumulation (Table 3).

Table 3 shows the results of the built-up-process of contaminants when the silo with the dry-stored-substrate is cut. The results listed in the table are mean values of the parallels. Apparent spikes (although these are not outliers in the narrow sense) are so far excluded in the calculation. The area loading strongly depends on the crump losses of the wheel loader. This fall-off results in a more or less random pattern of contamination, so it is not always clear to decide whether it is a spike to be excluded. In each case, a personal examination of the site is mandatory to interpret the measured data correctly and identify unrealistic spikes. As depicted in Fig. 13, an intensive rainfall caused a partly wash-off of contaminants between day 1 and 2 of accumulation, disturbing the measurement. These results are marked as spikes in Table 3. The COD:N:P ratio of the solids varies from 100:0.5:0.2 to 100:0.9:0.2.

**Table 3: Results of the built-up of contaminants with the “dry-substrate”**

Day of accumulation	Daily built-up [g/(m <sup>2</sup> ·d)]								
	Zone 3			Zone 2a			Zone 2b		
	COD	TN	TP	COD	TN	TP	COD	TN	TP
0	7.95	0.21	0.05	5.35	0.10	0.02	5.87	0.13	0.03
1	40.42	0.30	0.07	16.08	0.17	0.04	30.39	0.25	0.06
2	29.17	0.26	0.05	26.13	0.16	0.07	4.19*	0.07*	0.01*
3	55.49	0.44	0.10	69.51	0.52	0.12	25.13	0.22	0.05
Mean value	41.70	0.33	0.07	37.24	0.17	0.08	27.76	0.24	0.05

\*Spikes

After first differences in pollution built-up, zone 3 and 2a develop comparably with time after cleaning (Fig. 13). Within the time of accumulation, the RRM dried out on the surface to a

dry matter content of 82% (grab sample). Due to these dust-dry solids, apparent wind drifts lead to a progressing homogenization of the solid substrate.

At Fig. 13, the particulate and dissolved COD fraction are visualized with different axis scales. Using the same axis scale as the solid fraction COD of TSS and total COD above, it can be seen that the dissolved COD fraction is insignificantly low. The zoomed scale shows that neither a built-up nor a difference between the defined zones of the dissolved fraction was monitored. Obviously, contamination by silage liquor is rather low.

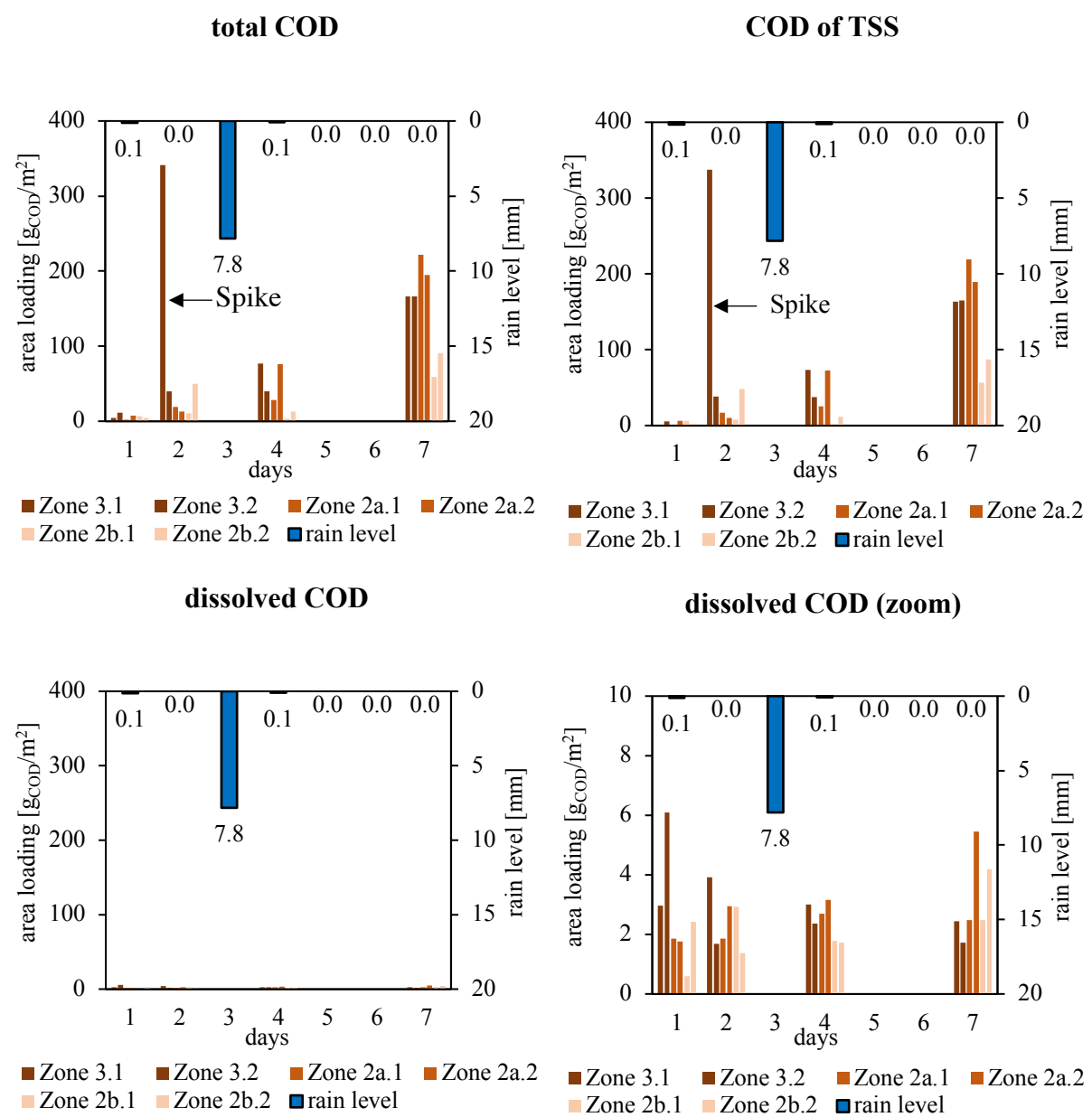


**Fig. 13:** Built-up-process of chemical oxygen demand (COD) with contaminant of the “dry-stored-substrate”. After each sampling, the area loading is reduced to nearly zero, hence, due to fixed sampling points, the interval of measuring increases each day to increase the days of accumulation

### 2.3.5 BUILT-UP PROCESS WITH WET SUBSTRATE

The measuring campaign for the built-up process with “wet-stored-substrate” was performed with sampling method 1 in February 2017 when silo 1 was operated (Fig. 10). The built-up of contaminants in the case of “wet-stored-substrate” distinctly differs to the “dry-stored-substrate”, as shown in Table 4. A clear differentiation between the zones 3 and 2 was visually observed on the spot, but a slight one between zone 2a and 2b. The substrate stuck more together on the fork of the wheel loader with the result that crump losses are reduced, especially in zone 2a (silo area, that is not the first cut zone) and at the traffic zone 2b. The sticky material was not prone to wind drifts. The last day of measuring, day 4 of accumulation, was strongly influenced by rain induced wash-off effects, which explains the low remaining contamination in zones 2a and 2b. The COD:N:P ratio of the solids is in the same range like as “dry-stored-substrate”. (100:0.6:0.1 to 100:0.8:0.2) However, the wash-off dynamics differs with the regarded parameters: nutrients seem to be washed off faster than COD and TSS.

**Table 4: Results of the built-up of contaminants with the “wet-substrate”, first measurement**

Day of accumulation	Daily built-up J [g/(m <sup>2</sup> ·d)]								
	Zone 3			Zone 2a			Zone 2b		
	COD	TN	TP	COD	TN	TP	COD	TN	TP
0	55.58	1.31	0.31	19.10	0.41	0.10	1.87	0.03	0.01
2	30.57	0.28	0.05	7.20	0.10	0.03	14.92	0.16	0.05
3	26.42	0.22	0.08	19.65	0.17	0.06	9.99	0.11	0.04
4	39.76	0.29	0.10	3.82*	0.03*	0.001*	13.63	0.07	0.03
<b>Mean value</b>	<b>32.25</b>	<b>0.26</b>	<b>0.08</b>	<b>15.32</b>	<b>0.14</b>	<b>0.05</b>	<b>12.84</b>	<b>0.11</b>	<b>0.04</b>

\*Spikes

In contrast to “dry stored substrate”, a high fraction of dissolved COD was measured on day 0, i.e. directly after sweeping (Fig. 14). In the first-cut-zone 3, the mean loading of 52 g/m<sup>2</sup> dissolved COD was higher than the subsequently measured total COD loading after several days of built-up. This contamination is caused by the silage effluent, permanently draining off the hoven and drying on the surface over a dry weather period of 2 week prior to the

measuring campaign. During the campaign, the outflow of silage sap continued, contaminating large parts of the silo surface. According to parallel grab samples the COD of the liquid varied between 50'000 to 100'000 mg/L. It is important to notice that mechanical street sweeping was not able to remove this pollution source, leading to a generally poor cleaning efficiency of the street sweeper on silos with wet-substrate and significant outflow of silage liquor. After removing the dissolved fraction by the wet sampling method, the built-up process is dominated by the built-up particulate matter (Fig. 14, bottom).

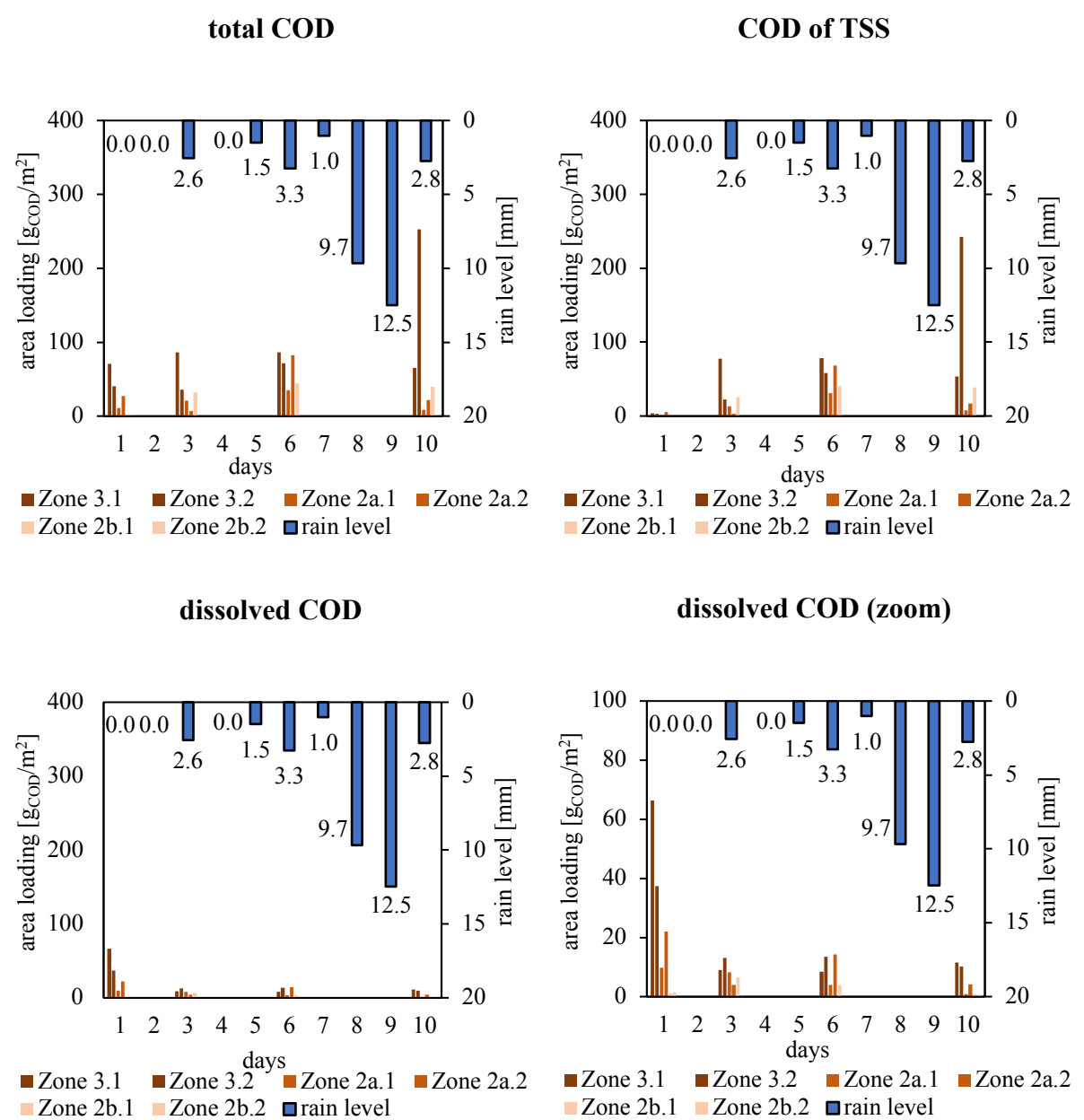


**Fig. 14:** Built-up-process of chemical oxygen demand (COD) with contaminant of the “wet-stored-substrate”. After each sampling, the area loading is reduced to nearly zero, hence, due to fixed sampling points, the interval of measuring increases each day to increase the days of accumulation

Because of the disturbing rain events, a second measurement of the built-up process of “wet-stored-substrate” was accomplished. To reduce the risk of meteorological disturbances, the samples were taken according to the second sampling method where the sampling points vary each day.

The results in Table 5 show a similar trend and built-up in the same range as during first measurement. A clear difference between the first cut zone 3 and zone 2 can be seen. In contrast to the first measurement, cold temperatures lead to an immobilization of substrate due to freezing of substrate on the surface. In consequence, the built-up of contaminants in zone 2a and the traffic zone 2b differs stronger. Additionally, the now changing sampling areas can increase the uncertainty, due to the random contamination pattern,

The area load on day 1 of accumulation hugely differs to the following days and is marked as a spike. Several reasons lead to this “bad day”. The cold temperatures around 0°C inhibited the drainage of silage effluent the days before and lead to a highly contaminated area. On day one, strong rainfall mobilized dissolved as well as solid fractions (Fig. 15). Furthermore, high substrate losses of the wheel loader could be noticed.

Despite all uncertainties and meteorological and operational impacts, both sampling methods proved to be applicable and showed similar results for the wet-stored-substrate.

**Table 5: Results of the built-up of contaminants with the “wet-substrate”, second measurement**

Day of accumulation	Daily built-up J [g/(m <sup>2</sup> ·d)]								
	Zone 3			Zone 2a			Zone 2b		
	COD	TN	TP	COD	TN	TP	COD	TN	TP
1	55.23*	0.31*	0.13*	36.67*	0.16*	0.07*	24.26*	0.07*	9E-04*
2	38.99	0.19	0.08	12.63	0.01	0.00	4.97	0.01	2E-04
3	35.77	0.16	0.07	11.48	0.03	0.01	3.39	0.03	7E-04
4	34.75	0.21	0.09	5.57	0.02	0.01	2.97	0.01	7E-04
Mean value	36.51	0.19	0.08	9.90	0.02	0.01	3.78	0.02	5E-04

\*Spikes

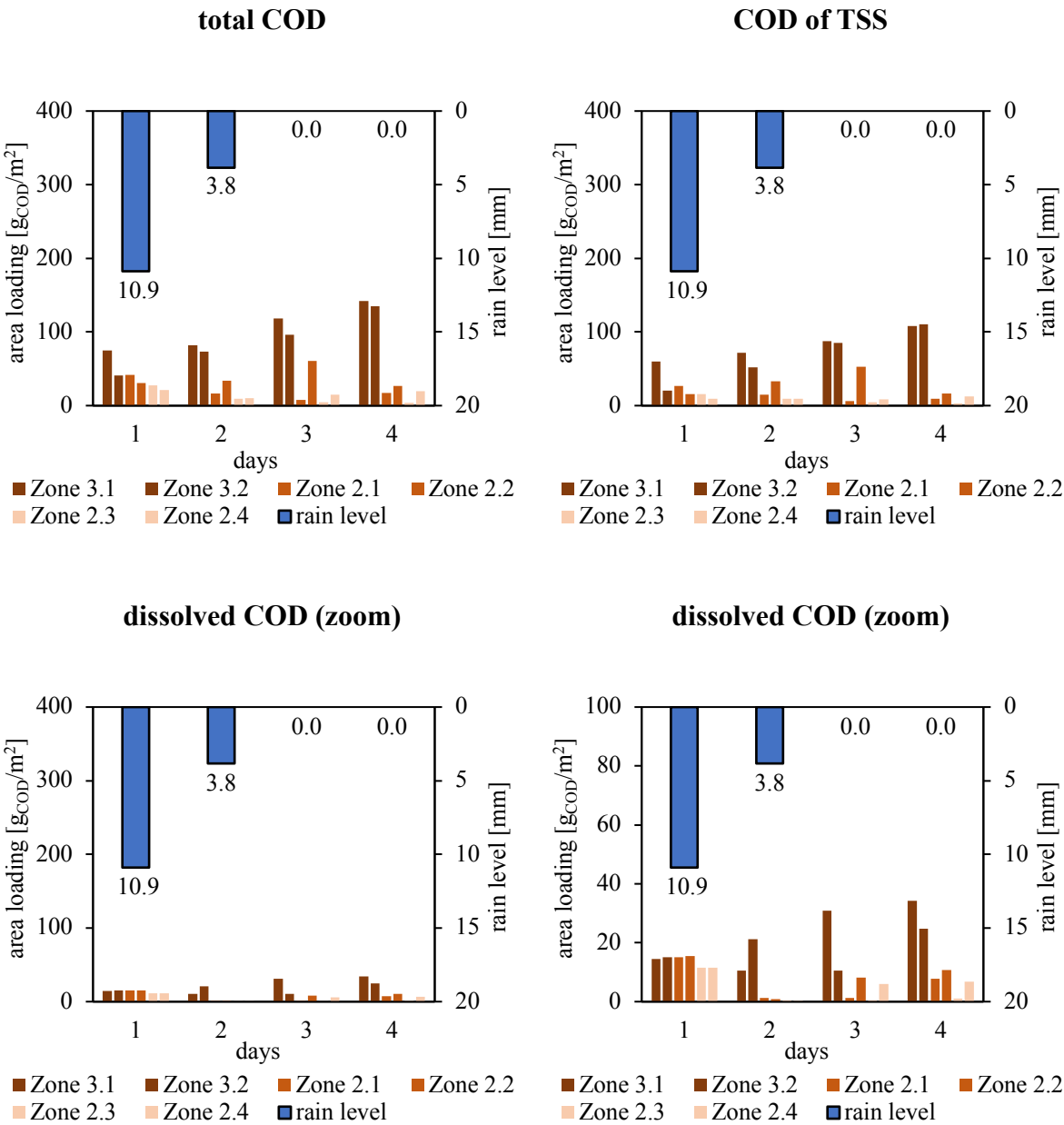


**Fig. 15:** Built-up-process of chemical oxygen demand (COD) with the “wet-stored-substrate”. The sampling points vary each day; hence, the accumulation process is progress each day on the not measured points.

### 2.3.6 VERIFICATION OF CLEANING METHOD

After sweeping the grid square and collecting the solids, the area is nearly free from total suspended solids (TSS) due to a smooth asphalt surface (Fig. 9). To check the cleaning efficiency, the cleaning procedure was performed twice after three days of accumulation. In the first run 163.8 g/m<sup>2</sup> particulate COD, in the second run nearly 0 g/m<sup>2</sup>. For the dissolved COD surface pollution decreased from 2.4 to 0.7 g<sub>COD</sub>/m<sup>2</sup> (Fig. 16). Even though the liquid COD is less reduced, the total cleaning efficiency is >99% so that the cleaning procedure is considered as valid method for this sampling campaign.

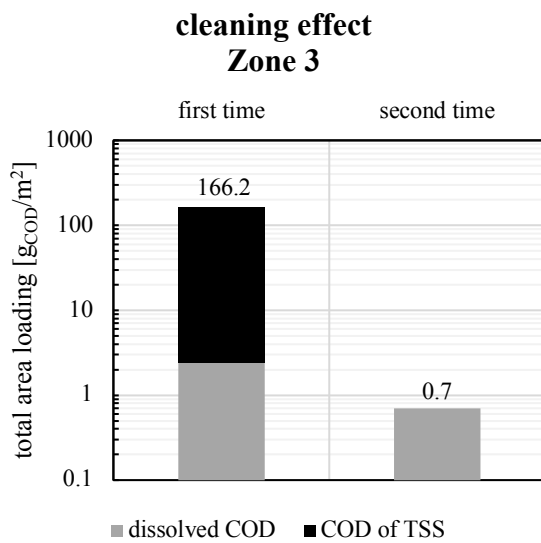


**Fig. 16:** Total area loading of a sampling point after two cleaning steps and three days of accumulation



## 2.4 DISCUSSION

The above compiled results lead to operational and constructive discussion points to achieve a more sustainable stormwater management.

**Drainage System:** At the silo facility, two different types of wastewater accrue: 1) a rather low volume of concentrated silage effluent and 2) a large volume of contaminated stormwater due to wash-off effects from the sealed surfaces. The silage effluent is characterized by low pH, high chemical oxygen demand (COD) and elevated nutrient concentrations (Deans and Svoboda, 1992; Gebrehanna et al., 2014).

For an economically and environmentally worthwhile silo management, the substance flows need to be separated. With its high energetic content, silage effluent is worth to be treated at the digesters. To separate silage effluent from stormwater runoff, the drained outflow of a silo can usually be shifted between digester (silage effluent) or stormwater-system. When a foil covered silo is opened and cut, the drainage line, so far discharging pure silage effluent towards the digester is now collecting rainwater, too. Here, the question arises, if the increased amount of now diluted water can still be operated by the digester or if the drainage has to be switched from silage effluent to the stormwater system with adverse effects on stormwater composition. If the drainage shall be discharged towards the digester, both the hydraulic transport system and the digester must be able to cope with the increased flow. An improvement can already be achieved by installing two shafts, one for the silo effluent and one for the stormwater. For this, the uncut silos have to be covered with a thick foil and spanned in that way, that the stormwater drains directly to a rainwater retention basin and the silage sap drains to a second duct. To manage open silos, more sophisticated drainage systems with a defined throttle flow towards the fermenter and a hydraulically defined overflow towards the stormwater system could achieve source-oriented flow separation.

**Regular sweeping:** The results above show a fast accumulation process of contaminants on the surfaces within few days. A great risk is the surface contamination with silage effluent, which cannot be removed by dry sweeping but is highly soluble in water. In a stormwater event, the accumulated contaminants are washed off. To be fair, not all of the solid fraction of RRM would be washed off at each rainfall. While the sugary silage effluent is washed-off easily, also at lower intensities, the particulate RRM are washed off as function of rain intensity, volume and the substrate itself. Surface pollution rises quickly within few days of accumulation. The organic contamination loads (in this study 2 to 50 g COD/m<sup>2</sup>) strongly differs compared with urban areas with rather low TOC loads of 0.003 to 0.045 g/m<sup>2</sup> (Deletic

and Orr, 2005) with according consequences of stormwater treatment. Usually, the contaminants of COD of road runoff varies between 5 mg/L and 85 mg/L (Helmreich et al., 2010; Kayhanian et al., 2012), whereas COD concentrations of silo surface runoff varies between 500 and 25'000 mg/L due to own measurements of high resolved rainfalls at a biogas plant. The average concentration of silo stormwater runoff was about 3'500 mg/L on usual working days which is 40 times higher than the maximum of road runoff and about 5 times higher than communal waste water. This highly contaminated stormwater runoff would have a considerable impact on the environment if discharged untreated and strongly underlines the relevance of this contaminated silo stormwater runoff.

**Monitoring of surface pollution:** The sampling method, using a wet vacuum cleaner is suitable for an exact measurement of surface pollution in the defined grid but suffers from a limited sampling area. Due to the random contamination pattern, this introduces uncertainties which cannot reliably be quantified by just two parallels. For a reasonable experimental design, the local conditions have to be considered thoroughly. Both sampling methods with fixed and variable sampling points, respectively, are producing comparable results.

In contrast to urban surfaces, the accumulation the contaminants with time is very distinct. Despite the random accumulation pattern and remaining uncertainties, a rather robust estimation of pollutant accumulation is derived from the data assuming a linear increase of area loading.

$$y = a \cdot x + b \quad 3$$

where  $y$  is the total built-up,  $a$  is the daily built-up,  $x$  represents the days and  $b$  is the background loading after cleaning with the street sweeper.

However, these data give an order of magnitude but may differ from plant to plant according to the discussed complex impact parameters.

## 2.5 CONCLUSION

This study showed the pollution potential for stormwater on biogas plants due to the structure and operated substrates on those plants. The surface pollution is system inherent and depend on composition and moisture of the stored substrate as well as operational and meteorological conditions. These lead to spatially and temporally very heterogeneous and

variable loads of contaminants on the surface. In the case of rainfall, the accumulated contaminants are washed-off and lead to a highly contaminated stormwater.

Following conclusions for improving stormwater management on biogas plants can be drawn:

- An intelligent flow separation with an improved drainage system is advisable.
- Regularly cleaning with dry sweeping significantly mitigate the pollution potential of stormwater. In case of wet stored substrate, which is often not avoidable, regular wet sweeping is required to remove surface contamination by silage effluent. Since the accumulation by this source is slower, longer cleaning intervals can be applied. A case adapted combination of dry (e.g. daily) and wet (e.g. weekly) cleaning should be applied in the best practice case. This would not only enhance the profit of a biogas plant due to the recovery of energy containing substrate, furthermore, it would help to protect our environmental by reducing the contaminants on the surface and therefore reducing the potential pollution of storm water.
- But still, as a result of the measuring campaigns it can be noted that a separation of the different water flows from each zone (silage sap, contaminated and not contaminated stormwater) cannot be ensured at each time of the year and every zone can be highly contaminated. Hence, no area can be generally presumed as clean. This raises the question of an appropriate stormwater treatment if discharged to a surface water. The organic nature of the pollutants suggests the application of biologic treatment technologies.

## 2.6 ADDITIONAL THOUGHTS ABOUT SUBSTANCE FLOWS ON A SILO FACILITY

The study showed the danger and variety of surface contamination on agricultural areas like silo facilities. These variety of pollution in combination with intermitted rainfall lead to a complex system that is hard to predict. Instead, measuring the dynamics of runoff events can lead to more insights. To measure these dynamics, a sampler was installed next to the rainwater retention basin and controlled with a rain gauge. The result were high-resolution time series of concentration and runoff. However, this only leads to a mixed concentration from the individual zones defined above, as the runoff from these zones meet and are discharged jointly to the retention basin. Based on the findings regarding the accumulation of surface contamination and monitored dynamics of stormwater-runoff in detail, a model was developed with the software SWMM (StormWater-Management-Model) and calibrated with the monitored events. This allows to estimate the contribution of individual zones.

As a result, it can be stated that the first flush of a rainfall events has the greatest energetical potential and is at the same time the most dangerous for the environmental. Even if the concentration of this first flush is exorbitant high, the flow is only marginal as Fig. 17 shows. A reason of it is the sugary surface from the silage runoff which can be easily cleaned and washed-off due to its good solubility. Following the first flushing, the COD concentration significantly decreased with rapidly increased flows. At this point, the rainwater increasingly dissolves and mobilizes the raw matter losses on the surface. In the evaluation of many rainwater events, it must be stated that no break-even-point in the time series could be found for certainty where the runoff is unproblematic and can be discharged untreated. The variety of the operational conditions on the investigated silo facility (as probably on other facilities, too) is far too great. However, the knowledge about the first flush and the following moderately loaded runoff can be used for a control system.

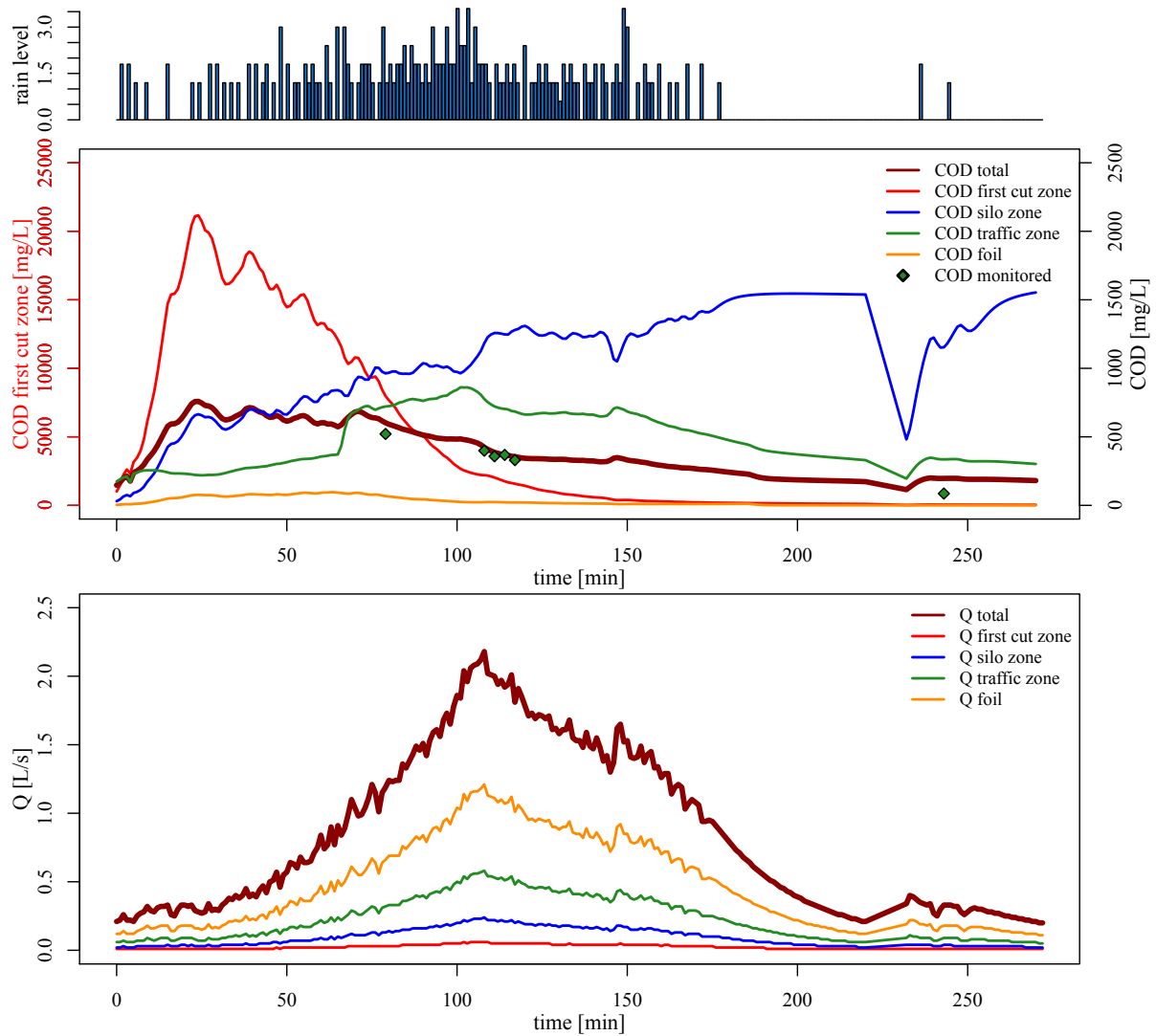


**Fig. 17:** Substance concentrations and flows that have been divided into different zones using SWMM modelling

An essential part in a smart silo management is the extensive division of the silage effluent and the stormwater-runoff. There are two possible techniques to achieve this, a single line and double line drainage concept, respectively. The single line drainage system is already discussed above as this kind of system was part of the considered silo facility. Shortly, it is based on a single drainage sewer and switchable shafts on the traffic area (see Fig. 18, left). As long as a silo remains closed, division of both flows is straightforward. Once a silo is opened, the shaft must be switched to stormwater drainage so that both silage effluent and stormwater flows into the retention basin. This may be a cheap procedure but not an ideal solution.

The double line drainage concept is based on an additional drainage sewer on the silo so that the drainage shaft on the traffic area has not to be switched any more. With a closed silo, it works similar to the single line concept. At a cut silo, open manhole covers for silage effluent have to be replaced with closed ones, depending on the withdrawal progress. Under the stored raw material, the silage effluent can still drain to the digester, whereas on the areas already emptied, the closed silage manhole cover protects the rainwater to drain to the digester as well. The more built-in manholes, the higher the degree of distribution. In this way, a mixing of both flows can be widely avoided.

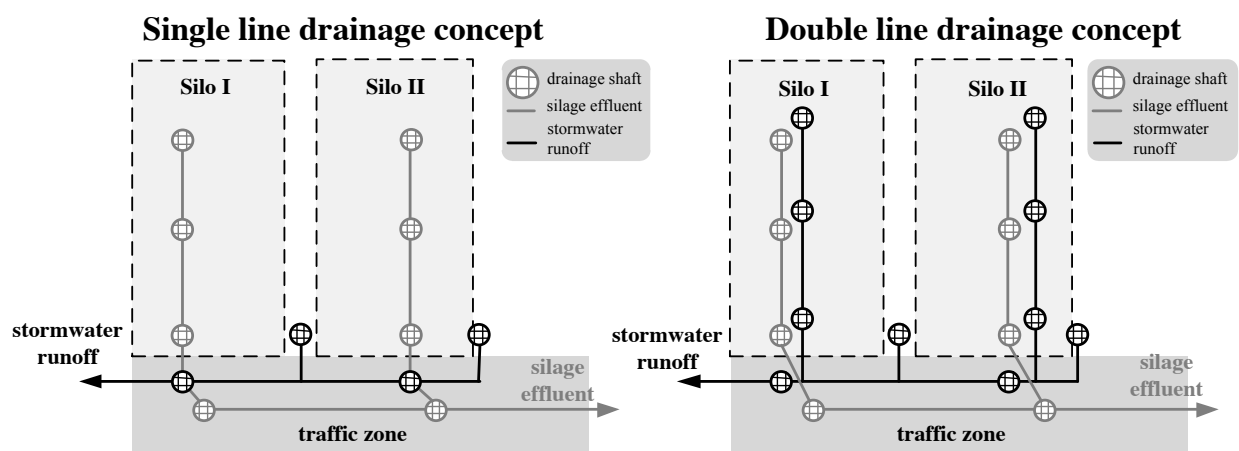


Fig. 18: Possible drainage concepts for silo facilities

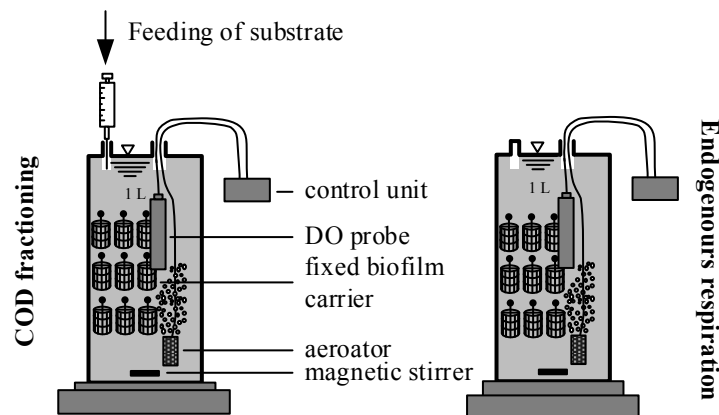


### 3 Degradation kinetics and COD fractioning of agricultural wastewaters from biogas plants applying biofilm respirometry

This chapter is published in:

**Environmental Technology**; 31.12.2019; Volume 42:15; 2391-2401

<https://doi.org/10.1080/09593330.2019.1701570>



Stormwater runoff from agricultural silo facilities can be heavily polluted and needs to be treated before discharged. This study investigates biological treatability and kinetic constants of characteristic silo runoffs applying attached growth systems. For this, respirometry measurements, typically applied in activated sludge systems as suspended growth, were modified by using adapted biofilm carriers. This allows a determination of degradation kinetic of the biofilm system and a COD fractioning at the same time, which are fundamental values for the design of a full-scale plant. To prove the comparability, the developed respirometry method was compared with the state of art using suspended growth systems and domestic wastewater. Both methods showed similar kinetics and the results are comparable to the recommended parameters of the activated sludge model (ASM). As stormwater runoff is usually a mixture from different pollution sources, various, typically occurring substrates are investigated regarding degradation kinetics and COD fractions. Wastewater polluted with digestion residue and solid manure showed similar COD fractions as domestic wastewater with an inert fraction  $S_i$  of 5 to 6% and a comparatively low rapidly degradable fraction  $S_s$  of 21 to 27%. Though, wastewater from corn or whole crop silage showed significant better degradation efficiencies and kinetics with an  $S_i$  of 2 to 3% and rapidly degradable fraction of 56 to 57%. As COD concentrations up to  $5,000 \text{ mg} \cdot \text{L}^{-1}$  for stormwater runoff and up to  $60,000 \text{ mg} \cdot \text{L}^{-1}$  for silage effluent can be expected, the results not only show the necessity but also prove feasibility of biological treatment of stormwater runoff from silo works and provide design parameters for adapted treatment systems.



### 3.1 INTRODUCTION

A central aim of the EU Water Framework Directive, 2000, is to achieve a status of “good ecologic quality” in water bodies. Meanwhile, the second reporting period is underway and still aimed at improving the physical-chemical status of surface waters (Völker et al., 2016). In rural areas, an intensified reduction of emissions from diffusely scattered point sources is now intended by the environmental authorities. Beside small domestic wastewater-treatment-plants without nutrient removal (Cramer et al., 2018), a focus on stormwater runoff from farms and silo plants pollutions is envisaged. Especially large impermeable surfaces of open silos storing biomass for fodder and biogas production are heavily loaded with organics due to material losses during transportation and contaminated by silage effluent (Michael Cramer et al., 2019a). Depending on the respective facility and the season, different substrates are stored in a silo. Stormwater runoff can be predominantly polluted with a single substrate or mixture of different substrates and silage effluent. The silage effluent is evoked by lactic acid fermentation due to an exclusion of oxygen during storage (Gebrehanna et al., 2014) and contains high amounts of organics and nutrients (Faulkner et al., 2011; Holly et al., 2018). At a closed silo, this silage effluent can be energetically used for biogas production (Pacetti et al., 2015; Poeschl et al., 2012). However, as soon as a silo is opened and operated, the silage effluent and material losses lead to a highly polluted surface. In rainfall events, these surface pollutions are washed-off. Current state of the art is to store this stormwater runoff in rainwater retention basins. In best practice case, this runoff is applied to agricultural land. But there are still facilities where this effluent is discharged untreated (Michael Cramer et al., 2019a).

Depending on the location of the facility, field application is often very expensive or not applicable in cases of specialized farms and biogas plants without sufficient land area. Due to the high organic pollution of stormwater (Larson and Safferman, 2009), the untreated discharge of these wastewaters has a severe impact on the ambient water quality. In consequence, the development of suitable treatment technologies for this runoff is urgently required. Well-proved biological treatment systems applied for domestic wastewater may be adapted for this purpose. However, their potential efficacy and appropriate design depend on the biodegradability and kinetic of this special wastewater. Whereas domestic wastewater compounds and their treatment is widely investigated (Alam et al., 2003; Friedrich et al., 2017, 2015; Gujer et al., 1999a; Henze et al., 2000; Sung et al., 2019; Vázquez-López et al., 2019), there is still a lack of research on stormwater runoff polluted with characteristic agricultural substrates and residues.

A useful way for estimating the biodegradability of substrates and kinetic parameter are batch experiments. Commonly, the kinetic parameters are estimated with an automatic system for measuring the oxygen consumption over time (Gujer et al., 1999a). Using this method, the resulting oxygen uptake rate (OUR) can be used for estimating the different fractions of COD (Dulekgurgen et al., 2006; Hocaoglu et al., 2010; Lazrak et al., 2018). Typically, OUR measurements are applied for (and with) activated sludge systems. However, due to the special conditions when treating runoff from agricultural silo facilities, attached growth systems may provide several advantages (long term adaptation of the biofilm on special substrates, robustness against longer starvation periods, energy efficiency, low maintenance effort). For biofilm systems, OUR measurements with activated sludge can be misleading for both the treatability and kinetic parameters, especially if the sludge is taken from a domestic WWTP which is not adapted to the investigated substrates. So, if attached growth systems shall be applied in full scale, respirometry should be adapted to these technologies. A simple method for this biofilm respirometry consists on suspended growth by using settled biomass (Carvallo et al., 2002; Livingston and Chase, 1989). An alternative method uses (manually) detached biomass and therefore disrupted biofilm as pseudo suspended growth system (Ferrai et al., 2010; GRADY et al., 1996; Van Loosdrecht et al., 1990). Though, these methods may come to deviating findings, namely concerning kinetics, compared to attached growth systems. But still, there is only little research with undisturbed biofilm. Some have developed an in-situ method to measure the kinetic with intact biofilm (Ordaz et al., 2012; Riefler et al., 1998).

Summarizing, there is lack of (1) simple approaches for respirometry with intact biofilm for accurate kinetic parameter estimation and (2) information on the aerobic degradability of wastewater polluted with characteristic agricultural substrates and residues. Against this background, the aim of this study is the investigation of a) the biodegradability and b) the kinetics of single substrates typically appearing on silo facility by c) using adapted biofilm carrier. To allow a direct comparison with domestic wastewater, it is useful to apply the standard COD fractions for design and modelling in activated sludge systems. Besides, this work shows a simple applicable respirometry method with biofilm carrier for estimating the biological treatability and kinetic parameters at the same time. To prove its reliability, this method is compared with domestic wastewater fed conventional respirometry with activated sludge.

## 3.2 MATERIAL AND METHODS

### 3.2.1 WASTEWATER PREPARATION

To produce representative wastewaters from silage substrates, various raw materials are taken from the silos of a biogas plant located in Mecklenburg-Vorpommern (Germany). 50.0 g corn silage, 51.5 g whole crop silage, 98.5 g fermentation residue, 55.0 g solid manure and 52.5 g dry chicken faces were dissolved in 1 L water for 2 hours. After dissolving, the solution was separated from coarse materials by a sieve with a pore size of 1 mm. The silage effluent was directly taken from the same silo facility.

### 3.2.2 ANALYTICAL PROCEDURE

The COD is measured with Dr. Hach vessel test LCK 314 and 514 in accordance with measuring procedure ISO 6060-1989. For the dissolved fractions, the samples were filtered with a 0.45  $\mu\text{m}$  filter.

The biological oxygen demand  $\text{BOD}_5$  was measured with a WTW BOD-Oxi-Top TS 606/2-i at controlled temperature of 20°C for 5 days. Each sample was inoculated with 2 mL of activated sludge and measured twice. The BOD of the inoculum (zero sample) was subtracted from the BOD of the samples.

To estimate the inert dissolved COD fraction  $S_i$  as well as rapidly and slowly degradable  $S_s$  and  $X_s$  fractions, respectively, the OUR based method was used. The respirometry measurement described in Fig. 19 is performed to distinguish  $S_s$  and  $X_s$  COD fractions. For this, a 1 L reactor is filled with 13 HEL-X H2X3 high-density-polyethylene biofilm carriers taken from a pilot plant which was operated with mixed stormwater from the same biogas plant at an average volumetric load of  $1.1 \text{ kg}_{\text{COD}} \cdot \text{m}^{-3} \cdot \text{d}^{-1}$  and average surface area load of  $3.4 \text{ g}_{\text{COD}} \cdot \text{m}^{-2} \cdot \text{d}^{-1}$  for six months in order to ensure an adequate adaption of the biofilm. For the biofilm respirometry, the carriers were fixed on a line on top of a magnetic stirrer to ensure a homogeneous mixing. The quality of respirometric measurements depends on the ratio of initial substrate concentration  $S_0$  to initial biomass  $X_0$  (typically expressed as volatile suspended solids)  $S_0/X_0$  (Spérandio and Etienne, 2000). In contrast to activated sludge systems, the  $S_0/X_0$  ratio for biofilm systems can only be estimated or alternatively indicated as  $S_0$  to surface area of the carrier material  $A_0$ . For an adequate measurement of both the kinetic and rapidly degradable COD fraction  $S_s$ , rather high  $S_0/A_0$  ratios of 8 to 10  $\text{g}_{\text{COD}} \cdot \text{m}^{-2}$  were chosen. The investigated substrates also contain organic and ammonia nitrogen.

Therefore, both, biomass growth and nitrification have to be considered for determination of the COD fractioning as both is unavoidable with a high  $S_0/A_0$  ratio.

The dissolved oxygen DO is measured using an optical DO probe from Venier with a time resolution of one second. This high measuring frequency is essential to represent the fast-degradable  $S_s$  fraction in a sufficient resolution. The DO is controlled between 2 and 4  $\text{mg}_{\text{O}_2} \cdot \text{L}^{-1}$  by switching on/off a submerged aerator. The OUR is calculated during each switch-off, i.e. oxygen consumption phase. Before substrate dosage, the biofilm carriers underwent a starvation period of 24 hours. After logging few points of the basic OUR, substrate was added to the reactor for determining the total  $\text{OUR}_{\text{tot}}$ . The  $S_s$  fraction is related to a high OUR, whereas the  $X_s$  fraction to a significantly lower OUR due to the limiting hydrolyzation process of  $X_s$  to  $S_s$ . A parallel reactor without substrate feeding is used for measuring the endogenous  $\text{OUR}_e$ .

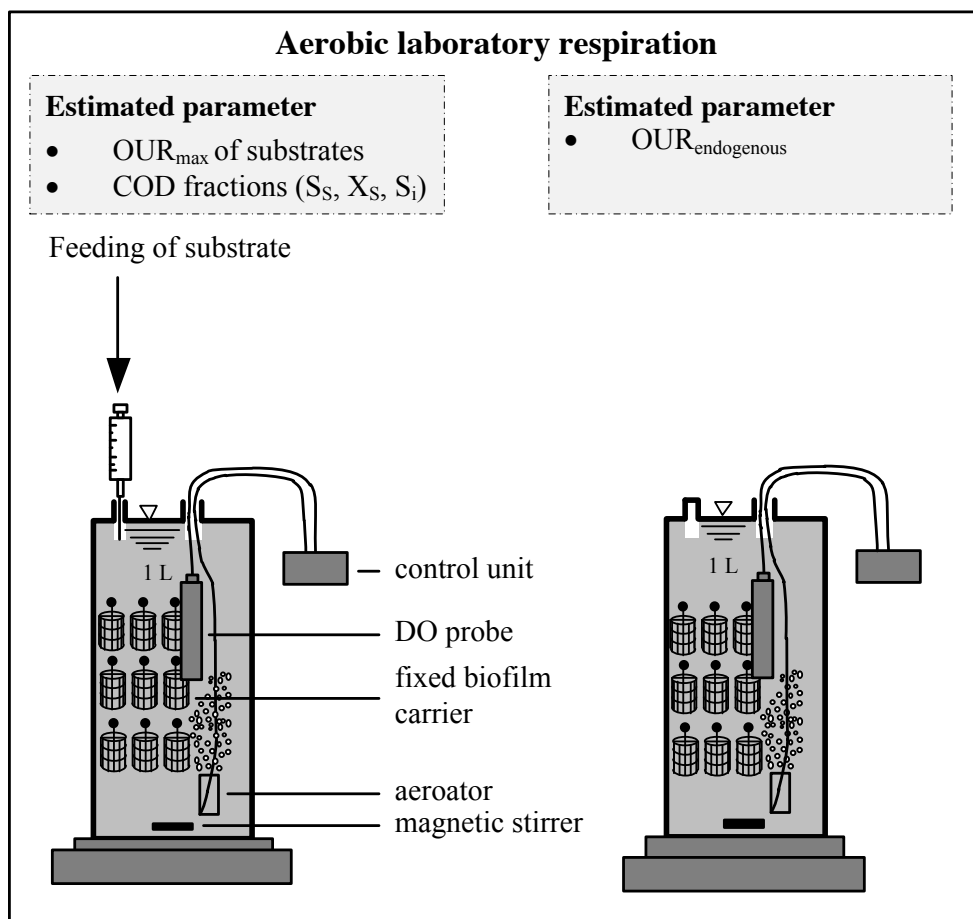


Fig. 19: Schema of the respirometry measurement of the oxygen uptake rate OUR

### 3.2.3 MATHEMATICAL MODEL

For fractioning the homogenized influent  $COD_{h,in}$ , a COD balance has to be done:

$$COD_{h,in} = COD_{f,in} + COD_{p,in} = X_i + S_i + X_S + S_S = COD_{deg} + X_{ES} \quad 3$$

where  $COD_{f,in}$  is the filtrated COD measured with a  $0.45 \mu m$  filter,  $COD_{p,in}$  is the particulate COD,  $X_{ES}$  is the excess sludge as a sum of inert particulate COD  $X_i$  and heterotrophic biomass  $X_H$  ( $X_{ES} = X_{i,BM} + X_H + X_i$ ),  $S_i$  is the dissolved and particulate inert fractions,  $X_S$  and  $S_S$  are the slowly and rapidly degradable fraction, respectively. Inert means in this context non-biodegradable constituents. The particulate  $COD_{p,in}$  is calculated as difference between homogenized  $COD_{h,in}$  and filtrated  $COD_{f,in}$ . Fig. 20 illustrates the influent COD fraction and conversion during biodegradation.

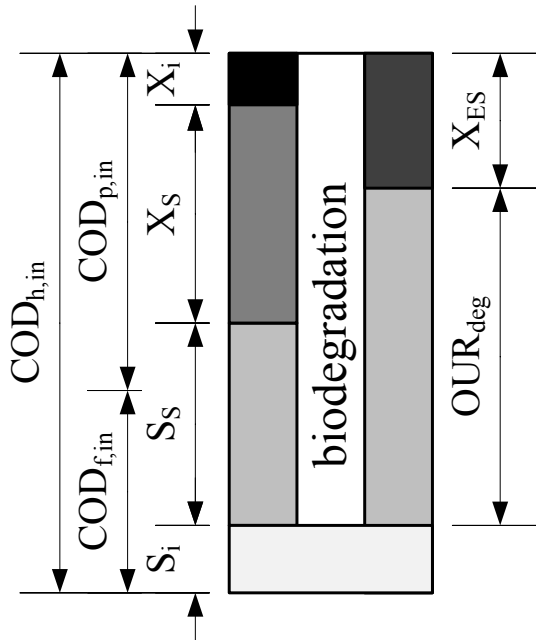


**Fig. 20: COD fractions of influent wastewaters and alteration after biodegradation**

The dissolved inert COD fraction  $S_i$  can be measured as filtrated COD after starvation. The starvation and completed degradation, respectively, can be identified when the  $OUR_{tot}$  equals  $OUR_e$  as seen in the respirogramm. It can be assumed that the COD elimination  $COD_{eli}$  is finished under the particular operational conditions (like sludge age; for further information about  $S_i$  as a function of sludge age see (Friedrich et al., 2016) and the remaining COD equals numerically the  $S_i$  fraction. The time for complete degradation can significantly vary and is strongly driven by the  $X_S$  fraction biodegradability. The higher this fraction, the longer it takes until the COD is completely degraded. The  $S_i$  is calculated as ratio of effluent and influent COD concentration.

The average specific surface area degradation rate  $r_{deg}$  [ $g_{COD} \cdot m^{-2} \cdot d^{-1}$ ] is calculated with eq. 4 with degraded  $COD_{deg}$  as difference of  $COD_{h,in}$  and effluent  $COD_{eff}$  at the required time  $t_{deg}$ .

$$r_{deg} = \frac{COD_{deg}}{t_{deg} \cdot A_{tot}} \quad 4$$

where  $A_{tot}$  [ $m^2$ ] is the total surface area used amount of biofilm carrier  $n$  (here  $n=13$ ), whereas  $A_{tot}$  is the product of the specific packing bed of one carrier [ $m^3 \cdot unit^{-1}$ ], the amount  $n$  [ $unit^{-1}$ ] and the specific surface area of one carrier [ $m^2 \cdot m^{-3}$ ]. The specific packing bed of one carrier was estimated by counting the amount of carriers to completely fill a 5 L reactor and dividing the reactor volume by the counted number (here  $19.38 \text{ mL} \cdot unit^{-1}$ ). The used carrier have a specific surface area  $A_{sp}$  of  $322 \text{ m}^2$  per  $m^3$  bulk material. For the amount of used biofilm carrier, the total surface area  $A_{tot}$  is therefore  $0.08 \text{ m}^2$ . Under starvation conditions, the endogenous respiration can be measured. In the concept of endogenous respiration, the degradation of  $X_H$  is regarded as a first order decay kinetic. In this model,  $b_H$  is regarded as constant for that particular system and  $X_H$  can be expressed as:

$$X_H(t) = X_H(0) \cdot e^{-b_H \cdot t} \quad 5$$

The oxygen-uptake-rate OUR is calculated from the measured dissolved oxygen DO during oxygen consumption phase eq. 6 (Spanjers et al., 1996).

$$OUR = -\frac{dDO}{dt} \quad 6$$

During starvation, the reduction of active biomass can be understood as decrease of endogenous oxygen uptake rate  $OUR_e$  according to Ramdani et al. 2010. However, the heterotrophic organisms  $X_H$  contain an additional undegradable fraction  $f_U$ . Hence, the active biomass can be expressed as  $(1-f_U) \cdot X_H$ . Based on the OUR method, this reduction of active biomass equals:

$$OUR_e = (1 - f_U) \cdot \frac{dX_H}{dt} \quad 7$$

The oxygen consuming parts of COD degradation are those which are not incorporated into excess sludge and can be divided into rapidly and slowly degradable fractions  $S_S$  and  $X_S$ , respectively. The COD utilization can be expressed as difference of bacteria growth and decay. The decay rate  $b_H$  is determined during aerobic biofilm respirometry measurements whereas the yield coefficient for bacteria growth is carried out in separate conventional respirometry using activated sludge. The degradable part of  $X_H$  is the active biomass and

leaves an unbiodegradable part. This remaining unbiodegradable part  $f_U$  is estimated with 0.2 (Gujer et al., 1999a).

Adding the produced effluent to the reactor, the oxygen is consumed by the heterotroph and autotrophic microorganism for COD degradation and nitrification of ammonia. Hence, the total respiration rate  $OUR_{tot}$  is in eq. 8 divided into a part for heterotrophic and autotrophic degradation.

$$OUR_{tot} = \frac{1 - Y_H}{Y_H} \cdot X_H \cdot \mu_H + \frac{4.57 - Y_A}{Y_A} \cdot X_A \cdot \mu_A \quad 8$$

Where  $Y$  is the yield coefficient of heterotrophic (H) and autotrophic (A) microorganism,  $X$  is the biomass and  $\mu$  is the growth rate. To estimate the yield coefficient of heterotrophic microorganism, a respirometry using activated sludge was applied to the different effluent and can be calculated with eq. 8. For autotrophic organism, a  $Y_A$  of 0.24 is assumed (Gujer et al., 1999a).

$$Y_H = \frac{\Delta COD_p - \int (OUR_{tot} - OUR_e)}{\Delta COD_p} - 4.57 \cdot \Delta NO_3 \quad 9$$

Where  $NO_3$ -N is the produced nitrate from the initial ammonia.

The oxygen consumption of  $S_S$  degradation induces a substantial increase of OUR directly after feeding. As soon as the  $S_S$  fraction of the influent is degraded, the hydrolyzation of the  $X_S$  fraction becomes the dominating process. It is considered that this process is not linked with oxygen consumption and therefore, cannot be identified with the OUR method. However, the  $X_S$  fraction is converted into  $S_S$ . Through this  $S_S$  release, the hydrolyzation process is captured indirectly over the oxygen consuming  $S_S$  fraction. During the experiments, no Allylthiourea (ATU) was dosed to avoid the risks of inhibiting heterotrophic processes or nitrification adaption to ATU (Spanjers and Vanrolleghem, 1995). Hence, the oxygen consumption of nitrifying ammonia has to be considered ( $OUR_N$ ). Applying Monod kinetics to the OUR based method by neglecting the particulate adsorbed fraction  $X_{S,AD}$ , the COD fractions can be determined as follows:

$$OUR_{tot} = (1 - Y_H) \cdot \left( \frac{dS_S}{dt} + \frac{dX_S}{dt} \right) + (1 - f_U) \cdot b_H \cdot X_H + OUR_N \quad 10$$

For more details about the mathematical model see (Spérando and Etienne, 2000).

The ammonia of the influent  $S_{NH4,in}$ -N can be either incorporated into biomass or nitrified. This utilization depends on the degraded  $COD_{deg}$  and the nitrogen content of the newly

formed biomass  $i_{N,BM}$ . The nitrogen content is set to  $0.07 \text{ g}_N \cdot \text{g}_{XH}^{-1}$  (Henze et al., 2000). The nitrification leads to an additional OUR. Hence, a nitrogen balance with respect to the formed and decayed biomass is performed in eq. 11 to estimate the amount of nitrified ammonia  $\text{NO}_3\text{-N}$  during the respiration:

$$\text{NO}_3 = S_{\text{NH}_4, \text{in}} - \left( Y_H - (1 - e^{-b_H \cdot t}) \right) \cdot i_{N,BM} \cdot \text{COD}_{deg} \quad 11$$

The oxygen demand for nitrification of ammonia is  $4.57 \text{ g}_{\text{O}_2} \cdot \text{g}_{\text{NH}_4\text{-N}}^{-1}$ . Therefore, the oxygen nitrification rate  $\text{OUR}_N$  can be estimated with eq. 12:

$$\text{OUR}_N = (4.57 - Y_A) \cdot \text{NO}_3 \quad 12$$

Considering eq. 5 and 8 with the simplification that  $X_S$  and  $X_{S,ad}$  equals one single  $X_S$  part, we get the uptake rate for COD degradation  $\text{OUR}_{deg}$ :

$$\text{OUR}_{deg} = \text{OUR}_{tot} - \text{OUR}_e - \text{OUR}_N = (1 - Y_H) \left( \frac{dS_S}{dt} + \frac{dX_S}{dt} \right) \quad 13$$

To distinguish the degradation of  $S_S$  and  $X_S$  and the parallel occurring nitrification, the area of these plateaus has to be integrated. A common way is an integration of OUR at the time after dosage ( $\text{OUR}_{tot}(t_0)$ ) until the first plateau for receiving the  $S_S$  fraction assuming that  $X_S$  hydrolyzation starts only when  $S_S$  is completely degraded (Ekama et al., 1986). However, this approach is quite mechanistic regarding the highly complex biocenosis of activated sludge. In a more reasonable approach, the degradation process of  $X_S$  via hydrolysis starts simultaneously with the  $S_S$  degradation straight after substrate dosage and is best described with a saturation function (Petersen et al., 2003; Spanjers and Vanrolleghem, 1995; Spérandio and Etienne, 2000). Assuming a saturation function for  $X_S$  hydrolyzation and  $\text{NH}_4$  oxidation, additional lines are introduced. Integration of these areas between  $\text{OUR}_{tot}(t_0)$  until  $\text{OUR}_{tot}(t_N)$  and  $\text{OUR}_{tot}(t_{XS})$ , respectively, leads to the oxygen consumption of ammonia oxidation and  $X_S$  degradation. The estimating method of the oxygen demand for nitrification  $\text{OUR}_N$  is in accordance with the findings of (Spanjers and Vanrolleghem, 1995). This also corresponds to the approaches in ASM3, where Hydrolysis is independent from the  $S_S$  concentration. A typical respirogramm is depicted in Fig. 21.



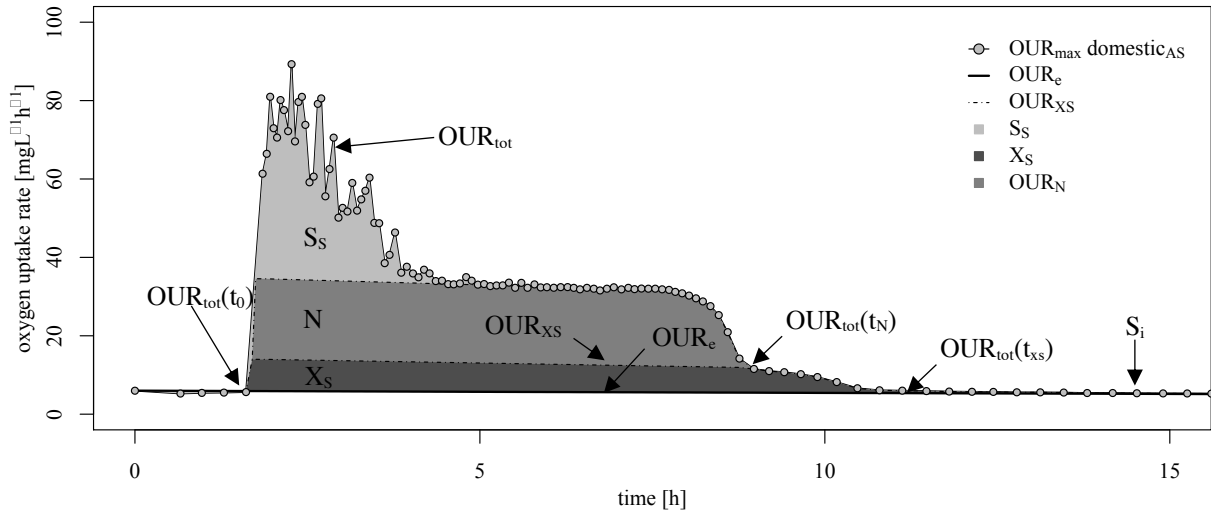


**Fig. 21:** Parameter description for identifying COD fraction with respirometry

### 3.3 RESULTS

#### 3.3.1 ESTIMATING KINETIC CONSTANTS AND COD FRACTIONING

The endogenous decay rate was determined by adjusting the  $OUR_e$  line to the  $OUR$  measuring point within the first hours of starvation and after the degradation is completed as seen in Fig. 22. The best model fit for the  $OUR_e$  line was at a decay rate  $b_H$  of  $0.022\text{ d}^{-1}$  which is surprisingly low with respect to the common proposals as it is just a tenth of the recommended value for activated sludge. A separate paper discussing decay rate in biofilms and other properties in detail (Michael Cramer et al., 2019b). The pollution concentrations of the dissolved raw substrates are shown in Table 6. The good COD to BOD ratio of 1.35 and BOD to  $\text{NH}_4\text{-N}$  ratio of 100:1 of corn or whole crop silage and 100:7 of silage effluent indicate a good degradability of these three wastewaters. It appears to be problematic that the fermentation residue and solid manure contain quite high ammonia concentrations and BOD:N ratio of over 100:35 at a COD:BOD ratio above 4.0. In the case of The initially the fermentation residue, the initially good degradable part of the raw material was digested. Hence, the remaining part should mostly consists of slowly degradable substances. Solid manure contains mainly straw and dry faeces, what explains its poor degradability.

The yield coefficient  $Y_H$  of the effluent varies significantly. Substrates similar to domestic wastewater show also similar  $Y_H$ , like fermentation residue and dry chicken faces with  $Y_H = 0.64$  and  $0.678$ , respectively. On the other hand, corn and whole crop silage have just a poor yield of around  $0.58$ . By contrast, silage effluent shows an astonishing high  $Y_H$  of  $0.87$  wich

is in the range of pure glucose having a  $Y_H$  of 0.90 to 0.91 (Dircks et al., 1999; Goel et al., 1999).

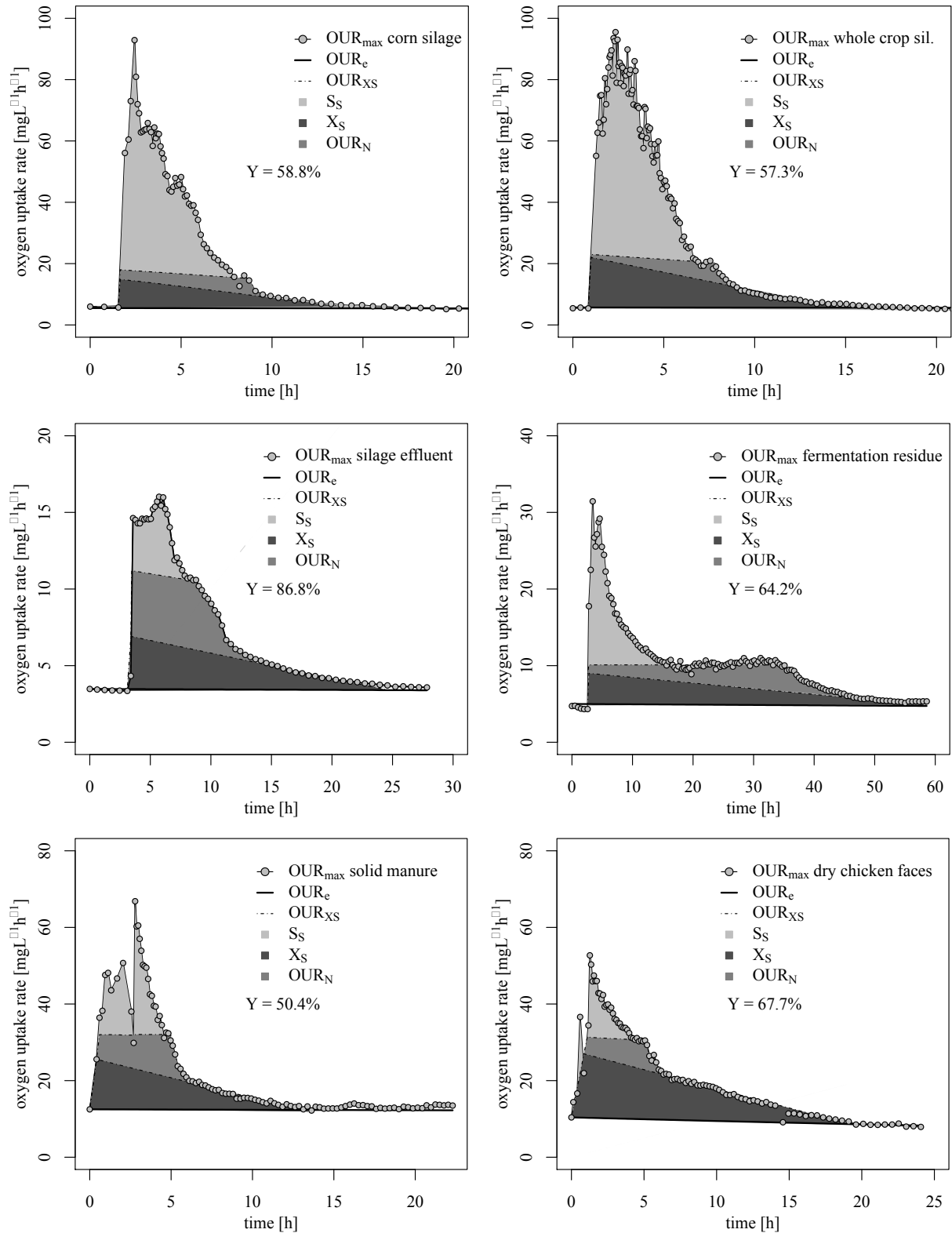


**Fig. 22:** Results of the OUR measurement via respiration method for corn silage (top left), whole crop silage (top right), solid manure (middle left), dry chicken faces (bottom right), silage effluent (bottom left) and fermentation residue (middle right); two replicates

The fractioning of COD shows a significant difference from domestic wastewater. The eliminated COD after 24  $\text{COD}_{\text{eli24h}}$  and 96 hours of degradation  $\text{COD}_{\text{eli96h}}$  are listed in Table 7 and

Table 8. Substrates like corn or whole crop silage show considerable better biodegradability in terms of a high  $S_s$  and low  $S_i$  fraction in comparison with domestic wastewater. Beyond that, these good degradation efficiencies with respect to a low  $S_i$  are linked to high degradation kinetics, allowing high area loadings of about  $15.5 \text{ g}_{\text{COD}} \cdot \text{m}^{-2} \cdot \text{d}^{-1}$  in maximum. Substrates like solid manure and fermentation residue show quite similar degradability kinetic of  $5.5 \text{ g}_{\text{COD}} \cdot \text{m}^{-2} \cdot \text{d}^{-1}$  and COD fractions compared with domestic wastewater.

**Table 6: Properties of the dissolved substrates; two replicates**

substrate	sample nr.	COD <sub>h</sub>	COD <sub>f</sub>	BOD <sub>5</sub>		NH <sub>4</sub>	
		mg/L	mg/L	mg/L	%	mg/L	%
corn silage	s1	6,525	4,194	3,133	47.5±	30	0.45±
	s2	6,421	4,128	3,020	0.9%	29	0.01%
whole crop silage	s1	6,804	5,132	1,976	30.1±	32	0.47±
	s2	6,696	5,050	2,089	0.8%	31	0%
fermentation residue	s1	3,802	2,181	579	15±0. 4%	202	5.3± 0.07%
	s2	3,742	2,147	551		198	
solid manure	s1	2,328	2,214	282	11.6±	102	4.39±
	s2	2,292	2,178	254	0.6%	100	0.04%
dry chicken faces	s1	8,723	6,449	3,528	41.9±	155	1.77±
	s2	8,585	6,347	3,726	1.1%	152	0.02%
silage effluent	s1	60,950	57,829	37,152	61.1±	2,878	4.72±
	s2	59,983	56,911	36,708	0.4%	2,832	0.04%
domestic WW	s1	796	519	341	41.5±	69	8.61±
	s2	784	511	315	1.6%	67	0.11%
ASM3 (Gujer et al., 1999a)	-	260	90	130	50%	16	6.2%

**Table 7: Results of the biodegradation efficiency and kinetic; two replicates**

substrate	sample nr.	COD <sub>f,24h</sub> mg/L	COD <sub>eli,24h</sub> %	COD <sub>f,96h</sub> mg/L	COD <sub>eli,96h</sub> %	Y <sub>H</sub> %	r <sub>tot,deg</sub> g <sup>COD</sup> / d·m <sup>2</sup>	g <sup>COD</sup> / g <sub>VSS</sub>
corn silage	s1	361	94.5± 0%	145	97.8± 0%	58.8%	15.42	-
	s2	357		140				
whole crop silage	s1	166	97.5± 0%	151	97.2± 0.5%	57.3%	15.58	-
	s2	170		225				
fermentation residue	s1	1,028	71.3± 1.4%	355	91.5± 0.9%	64.2%	5.43	-
	s2	1,136		287				
solid manure	s1	619	71.9± 1.3%	476	77.9± 1.5%	50.4%	6.93	-
	s2	679		546				
dry chicken faces	s1	893	91.4± 1.7%	422	94.1± 1%	67.7%	8.16	-
	s2	592		597				
silage effluent	s1	2,552	96± 0.2%	2,261	96.2± 0%	86.2%	26.52	-
	s2	2,261		2,288				
domestic ww with AS	s1	50	93.2± 0.5%	46	94.5± 0.3%	68.7%	-	0.53± 0
	s2	58		41				
domestic ww with adopted AS	s1	40	83.7± 1%	55	78.4± 0.3%	68.7%	5.68	-
	s2	45		57				

\*calculated according to eq. 14

**Table 8: Results of the COD fractioning; two replicates**

substrate	sample nr.	S <sub>S</sub>		X <sub>S</sub>		S <sub>i</sub>		OUR <sub>N</sub>	
		mg/L	%	mg/L	%	mg/L	%	mg/L	%
corn silage	s1	3,737	57.2± 0.1%	2,011	30.8± 0%	145	2.3± 0.2%	30± 0.2	9.6± 0.2%
	s2	3,674		1,977		140			
whole crop silage	s1	3,818	55.7± 0.8%	2,416	35.3± 0.5%	151	2.8± 0.5%	24.2± 0.1	6.2± 0.1%
	s2	3,705		2,345		225			
fermentation residue	s1	1,018	27± 0.4%	1,998	52.9± 0.7%	355	8.5± 0.9%	35.1± 0.3	11.6± 0.3%
	s2	1,016		1,994		287			
solid manure	s1	496	21.1±	1,276	54.3±	476	5.9±	44.4±	18.7±
	s2	479	0.4%	1,234	0.9%	546	0.4%	0.2	0.2%
dry chicken faces	s1	4,118	46.7± 1.1%	3,919	44.4± 1%	422	5.9± 1%	28.1± 0	3± 0%
	s2	3,961		3,770		597			
silage effluent	s1	2,552	25.7± 0.3%	22,675	37± 0.5%	2,261	3.9± 0.1%	17.9± 0.5	33.5± 0.5%
	s2	2,261		22,019		2,288			
domestic ww with AS	s1	117	14.6±	379	47.4±	46	5.5±	73.5±	32.5±
	s2	114	0.1%	370	0.4%	41	0.3%	0.6	0.6%
domestic ww with adopted AS	s1	148	18.4±	371	46.3±	55	7.1±	73.5±	28.2±
	s2	143	0.3%	360	0.7%	57	0.1%	0.4	0.4%
ASM3 (Gujer et al., 1999a)	-	51	19.6%	98	37.5%	30	11.5 %	46.4	31.3 %

### 3.3.2 VERIFYING THE RESULTS OF BIOFILM RESPIROMETRY

For verifying the results of the biofilm respirometry, the method was applied to domestic wastewater and compared with the recommended values of the ASM3 (Gujer et al., 1999b). Furthermore, the respirometry with biofilm carriers is compared with the state of art OUR measurements using activated sludge. Both reactors with biofilm carriers (Fig. 23, left) and with activated sludge (Fig. 23, right) showed nearly the same endogenous OUR of around 5 mg·L<sup>-1</sup> before dosage. Hence, it is assumed that the initial active biomass concentration of the experiment was similar. Activated sludge showed a significant higher maximal OUR. This may be due to diffusional limitations of the biofilm. However, both systems had the same oxygen demand and similar COD fractions. This is not surprising as the same domestic

wastewater was used during the experiments and both the biofilm carrier and activated sludge were well adapted to this wastewater. The results can also be used for a rough comparison of biofilm and activated sludge technology in full scale. For this, the determined kinetics have to be converted to characteristic reference values of biofilm and activated sludge systems, combining a typical sludge concentration in activated sludge tanks of  $3.5 \text{ kg}_{\text{VSS}} \cdot \text{m}^{-3}$  with the measured conversion rate of  $0.54 \text{ kg}_{\text{COD}} \cdot \text{kg}_{\text{VSS}}^{-1} \cdot \text{d}^{-1}$  leads to a surface area degradation rate of  $5.87 \text{ g}_{\text{COD}} \cdot \text{m}^{-2} \cdot \text{d}^{-1}$ .

$$r_{deg} = \frac{3.5 \frac{\text{kg}_{\text{VSS}}}{\text{m}^3} \cdot 0.54 \frac{\text{kg}_{\text{COD}}}{\text{kg}_{\text{VSS}} \cdot \text{d}}}{1'000 \frac{\text{kg}_{\text{COD}}}{\text{g}_{\text{COD}}} \cdot 322 \frac{\text{m}^2}{\text{m}^3}} = 5.87 \frac{\text{g}_{\text{COD}}}{\text{m}^2 \cdot \text{d}} \quad 14$$

This is nearly the same value as measured for the biofilm carriers ( $5.68 \text{ g}_{\text{COD}} \cdot \text{m}^{-2} \cdot \text{d}^{-1}$ ). In other words, with the used carrier material, the required reactor volume for both technologies is very similar.

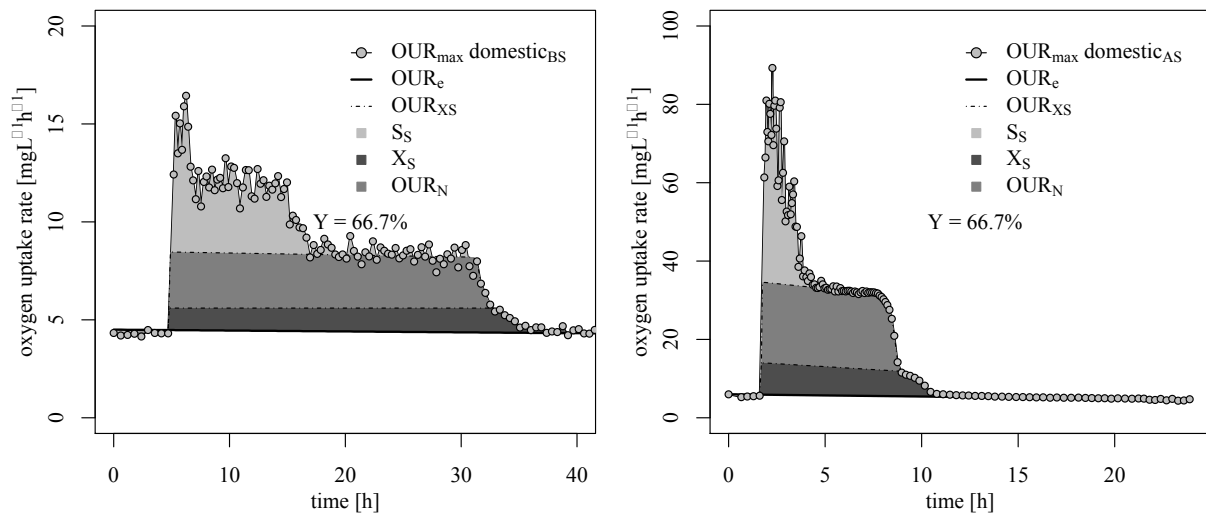


**Fig. 23:** Results of the OUR measurement via respiration method for domestic wastewater with a biofilm carrier system (BS, left) and activated sludge (AS, right); two replicates

### 3.3.3 COMPARISON OF COD FRACTIONS FROM RESPIRATION WITH INFLUENT CONCENTRATIONS

By comparing the particulate and filtrated COD with the calculated fraction from respiration measurement, it can be noted that there is no consistent correlation. It shall be noted that  $X_S$  is in some cases even higher than the particulate COD. This underlines again that  $X$  represents more the status of degradability than the physical phase. Hence, the most reliable way for measuring the COD fraction seems to be the respiration method.

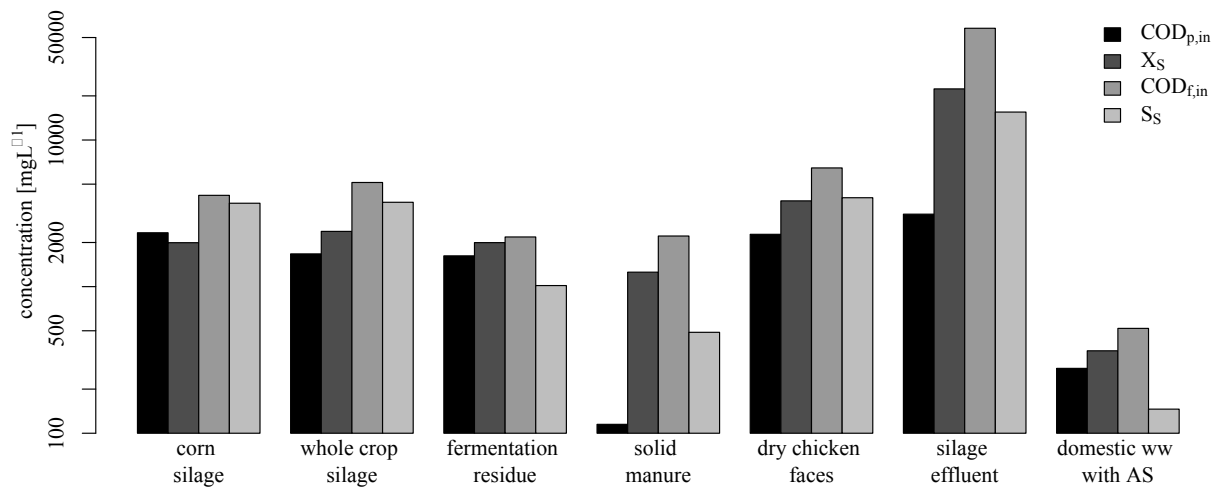


**Fig. 24:** Results of the COD fractioning by respiration measurements

### 3.4 DISCUSSION

The investigated agricultural pollution sources of stormwater showed diverse biodegradabilities. Materials directly from the agricultural field have a good degradability and low  $S_i$  fraction like corn and whole crop silage, whereas materials that were exposed to a digestion process (either in the biogas plant or in the animal body) showed a significantly lower degradability. Furthermore, a stoichiometric good degradability is also linked to high kinetic constants. Despite these relative differences, all wastewaters can be characterized as well biodegradable. Special attention should be paid to the dissolved inert COD ( $S_i$ ), since it defines the achievable effluent value, if biological treatment of stormwater is planned. Partly, extremely high concentrations of silo stormwater runoff of up to  $10.000 \text{ mg} \cdot \text{L}^{-1}$  can occur (Michael Cramer et al., 2019a). With those influent concentrations, only a COD between  $100$  to  $400 \text{ mg} \cdot \text{L}^{-1}$  can be expected in the effluent. This issue needs to be discussed when defining realistic discharge limits for those plants. Generally discharge limits, purely



based on COD, independent from its degradability, may neglect the complex and strongly varying composition of agricultural farm and silo runoff.

The removal rates with respect to a packing bed were calculated by the theoretical specific packing bed of a single biomass carrier and transmitted to the quantity used in the laboratory respiration experiments. This approach is uncertain and the calculated removal rates of per  $\text{m}^2$  packing bed is a rough estimation and has to be verified at a larger scale. Despite these uncertainties, the total removal rate and degradation kinetics of corn and whole crop silage is quite high. Surface area loadings of about  $15.5 \text{ g}_{\text{COD}} \cdot \text{m}^{-2} \cdot \text{d}^{-1}$  would theoretically be possible for pure COD removal. However, stormwater runoff is usually a mixture of different pollution sources. Depending on the real composition, lower volume loads of up to  $5.5 \text{ g}_{\text{COD}} \cdot \text{m}^{-2} \cdot \text{d}^{-1}$  may therefore be required.

### 3.5 CONCLUSION

From the generally good biodegradability of stormwater runoff, following conclusion are drawn:

- COD fractions of stormwater runoff from silo facilities is strongly dependent on the stored substrates. Substrates that undergone a digestive process showed considerably lower degradation kinetics and therefore demand higher reactor volumes as raw materials like manure and fermentation residue compared with corn and whole crop silage.
- An aerobic biological treatment is feasible and will achieve high efficiencies regarding the parameter COD between 95% to 98%
- The definition of discharge limits may be based on expectable remaining concentrations, defined by  $S_i$

Regarding the respirometry using biofilm carriers instead of sludge liquor it can be stated:

- The approach delivers comparable results and is an easy to use method for estimating both kinetic and biodegradability parameters.
- Since the  $S_0/X_0$  ration cannot be exactly given, an alternative ratio e.g.  $S_0/A_0$  may be more appropriate and fits better to design procedures of biofilm systems
- The upscaling of measured kinetics to technical scale would be of great interest but demands further validation.

### 3.6 COMPLEMENTARY THOUGHTS ABOUT DISCHARGE LIMITS BASED ON CONCENTRATIONS

As previously intimated, COD discharge limits solely based on concentration should be reconsidered regarding this specific wastewater. Still, the discharge limits for silo facilities have not yet been incorporated into the regulations and are still under discussion at the agency. For domestic wastewater, a COD limit of  $150 \text{ mg}_{\text{COD}}\text{L}^{-1}$  is set in a comparable size category (German size class I) (AbwV-A1, 2004). As the dissolved inert fraction  $S_i$  is generally a percental part of the influent, a proposed discharge limit of  $150 \text{ mg}_{\text{COD}}\text{L}^{-1}$  cannot be ensured at each time of the year even if the biodegradation of the wastewater is completely degraded to the  $S_i$  fraction. However, this exceeding is not automatically linked to a high oxygen attrition in the water body to be discharged and raises the question if a limiting value only based on concentrations is sufficient for evaluating in this specific case. A different approach can be found in the regulatory standards for stormwater treatment systems. This standard uses the approach of the state of art instead of fixed discharge limits and in many cases requires a case-by-case assessment by the authorities (DWA-A-138, 2005; DWA-M-153, 2007). Applying this can be more useful in this case as it points out the maximum technical possibilities from which a certain performance is expected across the board.

As food for thoughts, measurements based on oxygen attrition can be a solution. A common method from the bygone era is the measurement of biological oxygen demand after 5 days ( $\text{BOD}_5$ ). The measurement is based on pressure differences as a result of  $\text{CO}_2$  production during biological degradation (for details see Metcalf and Eddy, 2014). The main advantage of this method is that it shows real biological activity and the inert fraction is not considered. Therefore, the BOD value would be a better choice for a possible effluent limitation for this specific wastewater as it represents better the possible oxygen attrition in the water bodies. Though, the measurement demands specific equipment, preparation and lasts 5 days. Moreover, a closed balance sheet is not possible with BOD as with the COD.

Facing the disadvantages of the BOD measurement, the OUR method discussed above (see chapter 3.2) can be adapted to measure the remaining oxygen attrition by using biodegraded effluents of a treatment plant instead of raw substances (as in the case of COD fractioning). Unlike BOD measurements, the oxygen attrition is monitored directly and can therefore be converted into a COD value which allows a closed COD balance. Likewise, the active ventilation (deviating from BOD which is based on oxygen diffusion) allows the usage of a high amount of active biomass which further enables a fast degradation of the substrates

within just a couple of hours. Experiments showed, that both measuring BOD and remaining COD attrition with the respiration method lead to similar results. The major advantage of the COD respiration method is the simplicity and low time requirement of less than one day against 5 days for BOD measurements.

If a release from rigid discharge limits is not possible by dealing with an extremely high polluted influent, one solution may be to temporary store the wastewater until more medium or low loaded stormwater arrives to dilute the inert fraction. Usually, extremely high polluted stormwater-runoff is the result of long dry periods with consequential high accumulation of the surface contamination followed by low stormwater-runoff. Thus, medium or poor loaded stormwater results after intensive stormwater-runoff and long rain periods, respectively. Hence, storing the highly polluted runoff requires only little storage space. The integral design of treatment and storage facilities is discussed in detail in chapter 4.6.

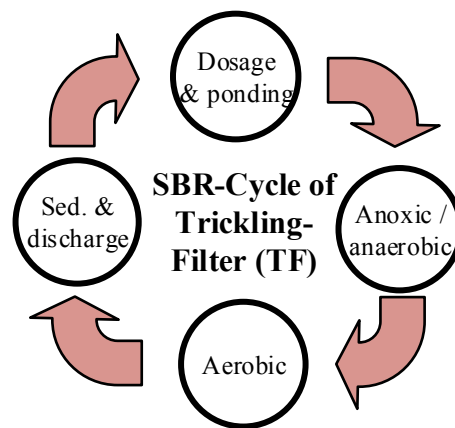


#### 4 Kinetic of Denitrification and Enhanced Biological Phosphorous Removal (EBPR) of a trickling filter operated in a sequence-batch-reactor-mode (SBR-TF)

This chapter is published in:

*Environmental Technology*; 17.12.2019; Volume 42:17; 2631-2640

<https://doi.org/10.1080/09593330.2019.1709564>



Due to their limited ability for nutrient removal, trickling filter systems (TFS) have almost fallen into oblivion today, even though they are robust and energy-efficient treatment systems. The advantage of this process technology, however, is the sessile biomass, which allows long periods of starvation without rinsing out the biomass. Therefore, this technology is promising for treating organic-polluted, intermittent stormwater-runoff. Several combinations with activated sludge systems (ASS) use the trickling filter as pre-treatment, requiring two separate treatment systems. This combines the advantages of both systems, but is paid with increased invest costs and space requirement. Due to these concerns, a trickling filter was developed that allows a nutrient removal without an additional ASS and exemplary tested for treating stormwater runoff of a silo facility. Beside aerobic conditions, anoxic and anaerobic steps have to be ensured during the process for a nutrient removal. For this, the TFS is ponded with a mix of purified wastewater from the secondary clarification tank (containing nitrate) and untreated raw water (containing degradable COD). This allows both, an integration of upstream-denitrification and enhanced-biological-phosphorous-removal (EBPR). During anoxic step, nitrate removal rates of  $0.8 \text{ kg}_{\text{COD}} \cdot \text{m}^{-3} \cdot \text{d}^{-1}$  can be expected, whereas a maximum COD removal rate of  $4.5 \text{ kg}_{\text{COD}} \cdot \text{m}^{-3} \cdot \text{d}^{-1}$  are achieved. To support a complete nitrification of ammonia, a COD removal rate below  $0.5 \text{ kg}_{\text{COD}} \cdot \text{m}^{-3} \cdot \text{d}^{-1}$  is recommended. The anaerobic/aerobic  $\text{PO}_4$  uptake rate of the EBPR was 31%. These results show that a combination of trickling filter with ASS in one single reactor is feasible.

## 4.1 INTRODUCTION

Stormwater-runoffs from agricultural areas like silo facilities are highly polluted. The main sources of this pollution are the surface contamination with silage effluent from lactic acid fermentation and material losses during transportation of raw material (Michael Cramer et al., 2019a). The treatment of this runoff has two major concerns. For one thing, the inflow to the treatment plant is rain-dependent, so that a partial absence of rain leads to a significant spread of effluent load or to long periods of starvation. Furthermore, high loadings of COD and nutrients like nitrogen (N) and phosphorous (P) in the effluent require a controlled reduction of nitrogen and phosphorous fractions to maintain discharge limits (Michael Cramer et al., 2019c). Facing both concerns simultaneously is not a straightforward task. As the runoff showed an excellent degradability, there is a call of a robust treatment system for this specific wastewater.

Attached growth systems like trickling filter immobilize biomass on biofilm carrier (Daigger and Boltz, 2011; Gavrilescu and Macoveanu, 2000) so that it can withstand longer starvation periods without losing significant biomass. Though, due to continuous aerobic conditions and reduced excess sludge production, these systems lack nutrient removal (Metcalf and Eddy, 2014). Contrary, activated sludge systems (ASS) like sequence-batch-reactors (SBR) are removing nutrients efficiently by introducing anoxic and anaerobic steps or zones (Hu et al., 2002; Obaja et al., 2004). However, decay during long starvation periods can lead to a critical sludge concentration in ASS which inhibits the settling properties of the sludge (Metcalf and Eddy, 2014). Thus, the secondary clarification can fail in sludge retention, fostering the loss of ASS, namely in case of increased hydraulic loads in stormwater conditions. Comparing these concerns, a combination of both systems seems to be a promising approach.

The state of art of biological nutrient removal is based on a) nitrification of ammonia, b) denitrification of nitrate and c) biological P removal (Gujer et al., 1999b; Petersen et al., 2003; Van Haandel and Van Der Lubbe, 2007). Nitrogen removal consist of nitrification and denitrification where the involved organism groups form symbiotic communities in the biofilm (Martiny et al., 2005). In low loaded systems (i.e. limited growth of heterotrophic MO), chemo-litho-autotrophic organisms oxidize ammonia ( $\text{NH}_4$ ) to nitrate ( $\text{NO}_3$ ) under strictly aerobic conditions (nitrification). Simplified, nitrification can be regarded as two main oxidation steps: i) ammonia to nitrite and ii) nitrite to nitrate. During absence of dissolved oxygen (anoxic conditions) and available degradable COD, a large ratio of

ordinary heterotrophic organism are able to perform denitrification by reducing nitrate to elementary nitrogen  $N_2$  with the aid of chemical oxygen demand (COD) as electron donor. Several denitrification processes are used in ASS (upstream-, intermittent, simultaneous denitrification (Van Haandel and Van Der Lubbe, 2007)). Different approaches of combinations of trickling filter with activated sludge systems called ASS/TF have been evaluated in separate reactors (Nourmohammadi et al., 2013; Wanner et al., 1988) or in hybrid reactors where a trickling filter is integrated above an activated sludge reactor (Majumder and Gupta, 2003) with the aim of using benefits of both systems like the reduced energy consumption and nutrient removal. All systems have a pre-treatment with a trickling filter in common, whereby the nitrogen removal was integrated with either a pre- or a post-denitrification with an external substrate feed. These process concepts are energy-saving but also more cost- and space-intensive. For further details of nitrogen removal and the involved microorganism see (Fleck et al., 2018; Lazrak et al., 2018; Li et al., 2018).

Another main aspect of wastewater treatment is the P-removal, which can be designed differently in ASS. One promising approach is the enhanced biological phosphorous removal (EBPR). The EBPR has been extensively investigated (Chen et al., 2004; Gujer et al., 1999b; Seviour et al., 2003; Siegrist et al., 2002) and is now state of art in wastewater treatment plant. Common EBPR processes are the BardenPho or the UCT process (Barnard, 1976). It consists of alternating anaerobic and aerobic conditions. Introducing an additional anaerobic zone or step into the biological process of AS supports the growth of phosphorous accumulating organism (PAO). During absence of dissolved oxygen DO together with a simultaneous oversupply of COD, PAOs are synthesizing poly-hydroxy-alkanoates PHA as storage product which results in  $PO_4$  release (Siegrist et al., 2002). This additional storage product leads to an immediate growth as soon as the subsequent aerobic step starts and therefore, enhances the net growth rate of PAOs towards other organism groups (López-Vázquez et al., 2008; Oehmen et al., 2007; Seviour et al., 2003; Siegrist et al., 2002; Van Loosdrecht et al., 1997) and therefore, the P to VSS ratio decreases in this step. These qualities lead to a significant selection advantage and enriches the activated sludge with PAOs. In this subsequent aerobic step, the P is re-incorporated into the biomass as polyphosphate, resulting in an increased ratio of P to VSS. This P release in anaerobic conditions and enhanced P reuptake in aerobic conditions which results in a positive net removal of P, is known as enhanced biological phosphorous removal EBPR. Typical anaerobic time periods for introducing an EBPR are known between 0.5 to 3.0 h (Chen et



al., 2004; López-Vázquez et al., 2008), whereas the P content of the volatile suspended solids ranges from 5 to 47 %, depending on the enrichment of PAOs (Hu et al., 2002).

The present work aimed to investigate a combination of ASS with TF but in a single reactor in order to save aeration energy, costs and space at the same time. For this purpose, a trickling filter was designed in pilot scale for treating stormwater runoff from a biogas plant which allows a ponding for introducing anoxic/anaerobic steps. The study was focused on the nutrient removal by operating the trickling filter in a sequence batch mode (SBR-TF) with integrated denitrification and EBPR.

## 4.2 MATERIAL AND METHODS

### 4.2.1 REACTOR DESIGN OF SBR-TF SYSTEM

The developed SBR-TF system consist of a primary clarification, a trickling filter and a combined storage and secondary clarification tank as depicted in Fig. 25. The solids from the raw wastewater are removed during primary clarification and disposed as primary sludge to the post-treatment. The liquid phase is distributed to the trickling filter with a rotary sprinkler for homogenous spreading of the wastewater over the surface. As media for the trickling filter, biofilm carrier with a specific surface area of 322 m<sup>2</sup> per m<sup>3</sup> bulk material were used. To ensure a sufficient aeration, the air is supplied by a fan to enhance the chimney draft effect. The fan is installed above the highest filling level to avoid a contact with liquids during filling step. Depending on the SBR-step, the wastewater could take two pathways: a) during denitrification (DN) step, the wastewater is pumped from the sump of the trickling filter directly back to the rotary sprayer (Fig. 25, 2b) and b) during aerobic steps, the wastewater is pumped from the sump towards the combined storage and secondary clarification tank (3a see Fig. 25).

Therefore, the combined tank has two tasks: a) Providing sufficient water volume for a complete filling of the tricking filter (2a see Fig. 25) and b) separating clarified water from excess sludge (4 see Fig. 25). The clarified water is discharged to the water body (5 see Fig. 25), whereas the excess sludge is discharged to the sludge post treatment.

The SBR-TF was fed with stormwater runoff from a biogas plant for 6 months. As biomass inoculum, activated sludge from a domestic wastewater treatment plant with about 400,000 population equivalents were used. The adaptation time of the biomass in the trickling filter to the stormwater runoff was 1 month.

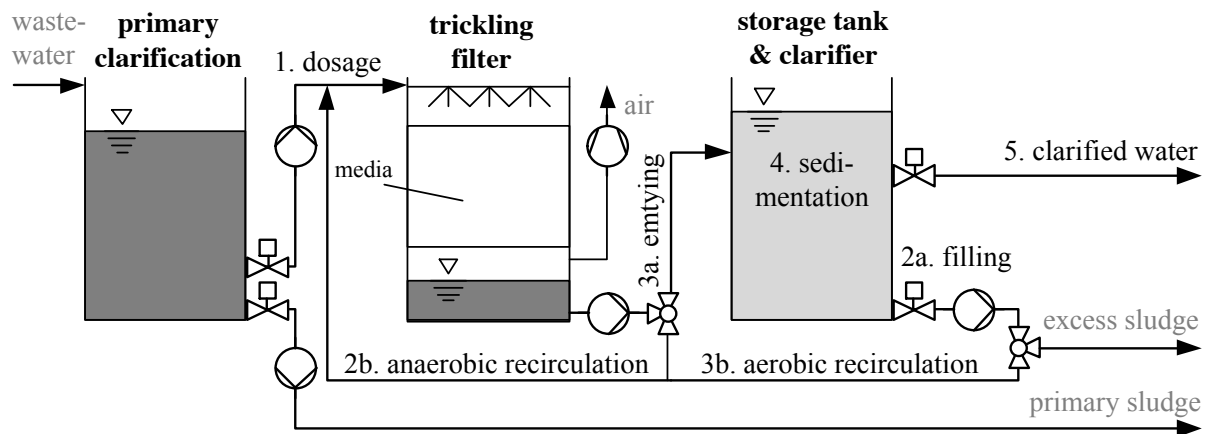


**Fig. 25: Reactor design of the trickling filter system**

#### 4.2.2 CONCEPT OF SBR-TF WITH INTEGRATED DN AND EBPR

To combine the advantages of ASS with a trickling filter for enhanced nutrient removal, it is based on the concept of a sequence-batch-reactor (SBR). This concept consists of four steps as shown in Fig. 26.

1) Wastewater dosage and filling: Pretreated wastewater during primary clarification is fed to the trickling filter. The amount fed depends on the COD and N concentration of the wastewater to ensure a maximum volumetric load supporting nitrification. The range of exchange volume during these experiments varied between 20 and 50 % of the trickling filter and the volumetric load between  $0.3$  and  $1.5 \text{ kg}_{\text{COD}} \cdot \text{m}^{-3} \cdot \text{d}^{-1}$ , respectively.

2) Denitrification and EBPR: After the dosage step, the trickling filter is filled with treated wastewater from the storage tank up to the highest level of the filter, in order to minimize the ingress of oxygen (step 1B, Fig. 26). This treated wastewater has a high nitrate but a low COD concentration from the previous cycle. A denitrification (DN) of nitrate is supported by both dosed, rapidly degradable COD from raw wastewater and high nitrate concentration from the previous step, together with a inhibition of oxygen diffusion through the surface through ponding of the trickling filter, the nitrate is reduced to elementary nitrogen by ordinary heterotrophic organism. To provide the biofilm homogenously with nitrate and substrate, the wastewater is recirculated within the trickling filter during step 2. As soon as the nitrate is completely consumed, the anoxic conditions switches to anaerobic conditions. The additional anaerobic time was set to about 90 minutes to support the P release of PAOs whereas the total time amount for this step 2 (DN plus EBPR) was set to 120 minutes.

3) Nitrification and aerobic COD removal: The ponded trickling filter is emptied into the storage tank and the aerobic step is initiated. Here, the wastewater is recirculated from the

storage tank back to the trickling filter during aerobic recirculation, treated in the filter by the biofilm and emptied again into the storage tank. In this step, the COD is completely degraded and the remaining ammonium which is not incorporated into biomass is nitrified. This process is oxygen driven and the air supply pipes inhibit the chimney draft effect as they are build up at the top of the filter. To improve the oxygen diffusion and therefore the chimney draft effect, the fan impeller was turned on. With this construction, the limiting step is not the aeration itself but still the oxygen transfer into the biofilm is driven by diffusion. As soon as the dissolved oxygen concentration increases, the oxygen transfer to the liquid phase is faster than the oxygen consumption of the organism and indicates the termination of this step. To verify this, the concentration of dissolved oxygen and redox potential is measured in the recirculation water prior to the rotary sprayer. The initial time amount of this step (nitrification and COD removal) was set to 180 minutes.

4) Sedimentation: At last in the sedimentation step, the clarified water is separated from the excess sludge in the combined storage and clarification tank. The sedimentation time is set to 45 minutes and the clarified water is discharged via gravity flow at a fixed water level. After discharge, the cycle starts again with wastewater dosage and ponding (step 1).

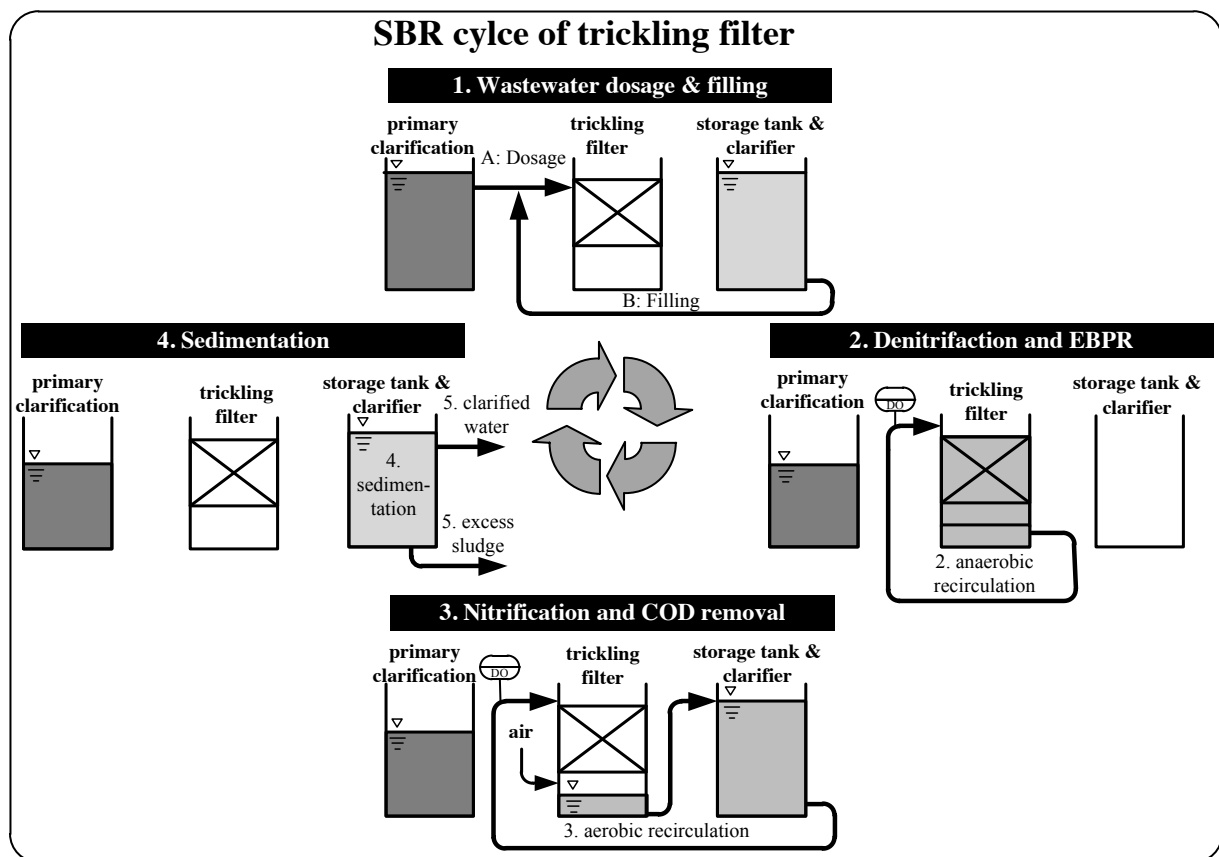


Fig. 26: Principle of the SBR trickling filter process

### 4.2.3 MATHEMATICAL MODEL

The nitrified ammonium  $\text{NO}_3$  is defined by the difference of the influent ammonium concentration  $\text{NH}_{4,\text{in}}$  and the incorporation into biomass. The total  $\text{NH}_4$  incorporation into biomass can be calculated with a term for bacteria growth and decay. The required nitrification demand is calculated with eq. 15.

$$\text{NO}_3 = \text{NH}_{4,\text{in}} - \left( Y_H - (1 - e^{-b_H \cdot t_{\text{TS}}}) \right) \cdot i_{\text{N,BM}} \cdot \text{COD}_{\text{deg}} \left[ \frac{\text{mg}}{\text{L}} \right] \quad 15$$

where  $Y_H$  is the yield factor for heterotrophic microorganisms,  $b_H$  is the decay rate,  $t_{\text{TS}}$  is the sludge age,  $i_{\text{N,BM}}$  is the nitrogen content of biomass and  $\text{COD}_{\text{deg}}$  the degraded COD. For  $Y_H$ ,  $b_H$ , and  $i_{\text{N,BM}}$ , typical values of biofilm system are estimated with  $Y_H = 0.53$ ,  $b_H = 0.022 \text{ d}^{-1}$  (Michael Cramer et al., 2019c) and  $i_{\text{N,BM}} = 0.07 \text{ g}_{\text{N}}/\text{g}_{\text{COD,BM}}$  (Henze et al., 2000).

The stoichiometric oxygen equivalent of nitrate is 2.86. Considering a yield factor  $Y_H$ , the nitrate degradation rate  $r_{\text{V,NO}_3}$  can be converted to a COD degradation rate  $r_{\text{V,COD}}$ :

$$r_{\text{V,COD}} = \frac{r_{\text{V,NO}_3} \cdot 2.86}{1 - Y_H} \left[ \frac{\text{kg}}{\text{m}^3 \cdot \text{d}} \right] \quad 16$$

With this, the theoretical COD removal rate can be determined for a specific wastewater from the nitrogen removal rate by knowing the specific  $Y_H$ . Furthermore,  $Y_H$  can be determined with eq. 17 under oxygen-limited conditions by rearranging eq. 2.

$$Y_H = 1 - \frac{r_{\text{V,NO}_3} \cdot 2.86}{r_{\text{V,COD}}} \left[ \frac{\text{kg}}{\text{m}^3 \cdot \text{d}} \right] \quad 17$$

### 4.2.4 ANALYTICAL PROCEDURE

To measure the concentration of  $\text{NH}_4$ ,  $\text{NO}_3$ ,  $\text{PO}_4$  and dissolved COD, the samples are filtered with  $0.45 \mu\text{m}$  filters and measured with Dr. HACH vessel tests LCK303, LCK339, LCK049 and LCK514. To verify the statistical confidence of these measurements, domestic wastewater was initial measured with triplicate measurements (Table 9). For online-monitoring of DO and redox potential, an optical probe for DO and redox probe from VENIER is used and integrated in a measuring line prior to the rotary sprayer.

Table 9: Triple measurements of domestic wastewater using HACH cuvette tests

parameter	measurement 1	measurement 2	measurement 3	standard deviation
COD	902	910	914	4.99
NH4-N	14.6	14.6	14.3	0.14
NO3-N	1.09	1.03	1.01	0.03
PO4-P	5.49	5.45	5.55	0.04

4.2.5 WASTEWATER PROPERTIES

The wastewater was taken from a rainwater retention tank of a biogas plant. The characteristics of the wastewater is listed in Table 10. For the case that no stormwater runoff was available at that time, a synthetic wastewater was produced. For this, rainwater from roofs were harvested in a container and mixed with raw material typically used in the biogas plant for 24h. During this time, the COD and nutrients are partly dissolved in a way similar to stormwater wash-off. Finally, the solids were separated with a sieve. The typical COD:N:P ratio is depicted in Fig. 27.

Table 10: Characteristic of raw wastewater from the biogas plant

Inflow concentration	COD mg <sup>3</sup> ·L <sup>-1</sup>	PO4-P mg <sup>3</sup> ·L <sup>-1</sup>	TN mg <sup>3</sup> ·L <sup>-1</sup>	NH4-N mg <sup>3</sup> ·L <sup>-1</sup>	pH	Conductivity mS/cm
stormwater runoff	58-77'890	2.9-1'010	20-2'855	13.4-433	7.3-8.5	0.2-12.2

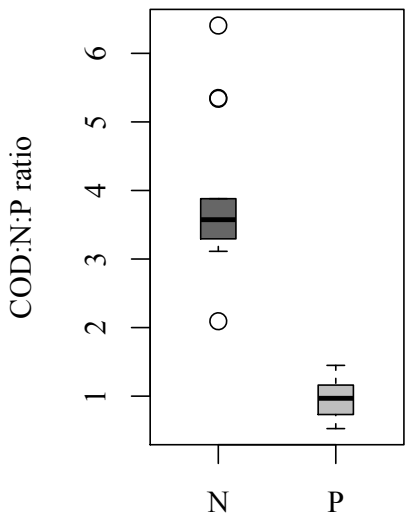


Fig. 27: Characterization of COD:N:P ratio as 100:N:P of raw wastewater

## 4.3 RESULTS

### 4.3.1 COD-REMOVAL EFFICIENCY

The SBR-TF was operated for 6 months at a volumetric loading between 0.5 and 0.8  $\text{kg}_{\text{COD}}\cdot\text{m}^{-3}\cdot\text{d}^{-1}$  (Fig. 28, left). During the first 3 months, the biofilm carriers were adapted to the wastewater. After this adaption time, the COD removal rate was constantly above 85%. However, the COD degradation efficiency showed a range about  $\pm 8\%$  after adaption period. In contrast to domestic wastewater, COD fractions of stormwater runoff are subject to certain fluctuations where inert fractions can vary between 5 and 15% (Michael Cramer et al., 2019c).

To verify the maximum performance regarding a COD removal rate, the volumetric loading was increased stepwise. As shown in Fig. 28 (right), the COD removal efficiency decreased with increasing loading. At a removal rate above  $1.0 \text{ kg}_{\text{COD}}\cdot\text{m}^{-3}\cdot\text{d}^{-1}$ , the removal efficiency is below 70%. Compared to literature, this elimination rate is in the lower mid-range (Metcalf and Eddy, 2014). Typically, at volumetric loadings of 0.6 to  $1.6 \text{ kg}_{\text{COD}}\cdot\text{m}^{-3}\cdot\text{d}^{-1}$ , removal efficiency of 80 to 90 % can be expected. In the state of art, trickling filters are operated strictly under aerobic conditions. By combining steps of the SBR process like a sedimentation and an anaerobic step, the effective time for degradation decreases as does the removal rate. However, to ensure a total COD degradation efficiency of 90% with this process technology, a volumetric loading below  $0.8 \text{ kg}_{\text{COD}}\cdot\text{m}^{-3}\cdot\text{d}^{-1}$  is sufficient if a complete nitrification is not an issue. This volumetric loading includes an anoxic, aerobic and anaerobic step for the denitrification. Typically, the COD degradation kinetics during denitrification step is reduced since the energy yield of “nitrate respiration” is lower and not all ordinary heterotrophic organisms are able to perform it. Hence, the maximum volumetric loading for just COD removal without anoxic step would be correspondingly higher. Assuming an anoxic kinetic COD decrease to 75% (Ekama and Wentzel, 1999), a volumetric COD loading of  $1.1 \text{ kg}_{\text{COD}}\cdot\text{m}^{-3}\cdot\text{d}^{-1}$  can be expected under solely aerobic conditions.

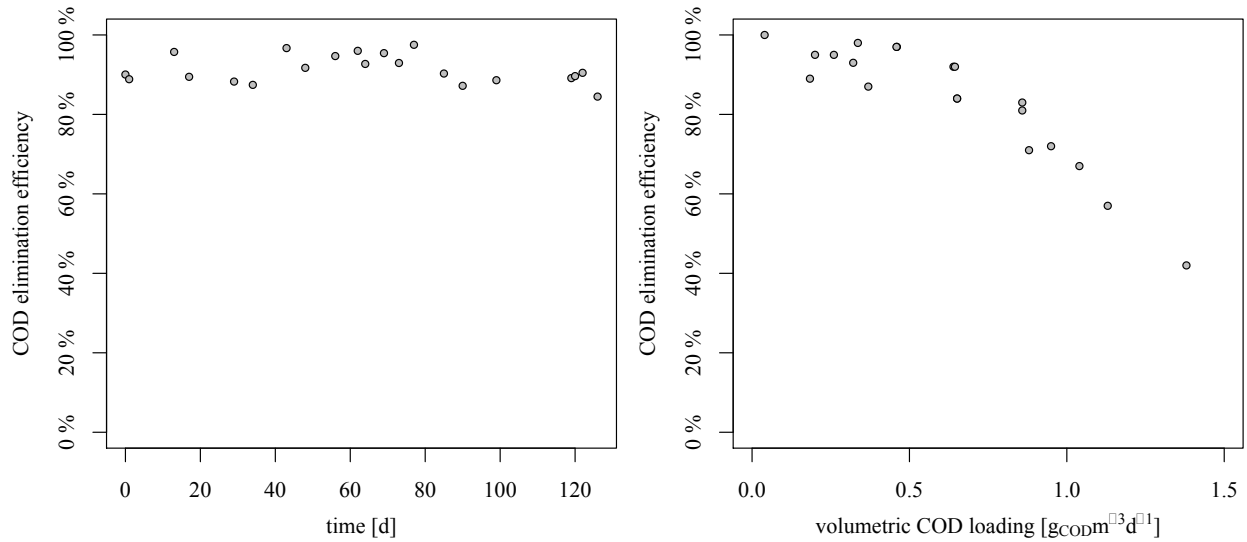


**Fig. 28: COD removal efficiency of SBR-pilot plant with both synthetic wastewater and stormwater runoff**

#### 4.3.2 NITROGEN REMOVAL EFFICIENCY WITH NITRIFICATION AND DENITRIFICATION

According to the high oxygen demand and poor growth rate of nitrifying bacteria, a low volumetric loading is required for complete nitrification. The recommendation for nitrifying trickling filter for domestic wastewater is between  $0.16$  to  $0.4 \text{ kgCOD} \cdot \text{m}^{-3} \cdot \text{d}^{-1}$  for a nitrification rate of minimum 90 % (Daigger and Boltz, 2011; Metcalf and Eddy, 2014). As depicted in Fig. 29 on the left, a volumetric loading below  $0.5 \text{ kgCOD} \cdot \text{m}^{-3} \cdot \text{d}^{-1}$  showed a nitrification efficiency of 90 %. This high possible volumetric loading is not only related to the good oxygen supply during aerobic conditions but also to the lower COD:N ratio of 100:3.5 which demands less nitrification capacity. Therefore, the identified maximum COD loading for a high nitrification rate is slightly above literature values.

After the nitrification and the following sedimentation step, the treated wastewaterwater is discharged and one cycle is completed. Depending of the exchange volume, the remaining wastewater has still a high nitrate concentration (exchange volume of  $1/3$  means a reduction of  $2/3$  of the initial N plus additional  $\text{NH}_4$  biomass incorporation), that has to be denitrified in the upstream DN. For this, raw sewage is fed to the trickling filter and filled with wastewater. As soon as the oxygen is consumed, the upstream denitrification takes place. For this nitrogen removal via denitrification, the ammonia has to be nitrified in the previous cycle. If a high volumetric COD loading inhibits the nitrification, the total nitrogen removal decreases to a minimum of 20 to 35 % by biomass incorporation (depending on the COD:N ratio) as shown in Fig. 29 (right). This allows an estimation of the amount of formed biomass,

as prerequisite of a biomass balance in biofilm systems (Tränckner et al., 2008). Lowering the volumetric COD loading enhances the nitrification rate and simultaneously the total nitrogen removal rate. The nitrification rate is thus directly related to the total nitrogen removal which proofs a well performing integrated denitrification. The denitrification of nitrate is carried out by heterotrophic microorganism which show typically high degradation kinetics due to their known high growth rates. Hence, the nitrification can be stated as the limiting step, so the volumetric COD loading has to be adjusted to a sufficient nitrogen removal rate.

Due to the high pollution concentrations of 2'000 to 4'000  $\text{mg}_{\text{COD}}\cdot\text{L}^{-1}$ , the exchange volume of raw wastewater was between 13 and 22%. Since the treated wastewater is discharged after the aerobic step, the ammonia fed into the respective cycle can only be nitrified. Hence, the maximum theoretical nitrogen removal efficiency is derived from the fed ammonia, the volumetric exchange rate and the ammonia biomass incorporation. At a volumetric loading of  $0.5 \text{ kg}_{\text{COD}}\cdot\text{m}^{-3}\cdot\text{d}^{-1}$  and a nitrification efficiency of 90%, a maximum theoretical nitrogen removal efficiency of 70 to 79% is achievable. However, the determined total nitrogen removal efficiency was above 90%. This unexpected high TN removal efficiency can only arise from simultaneous nitrification and denitrification (SND) during aerobic step caused by oxygen diffusion limitations effects in the biofilm.

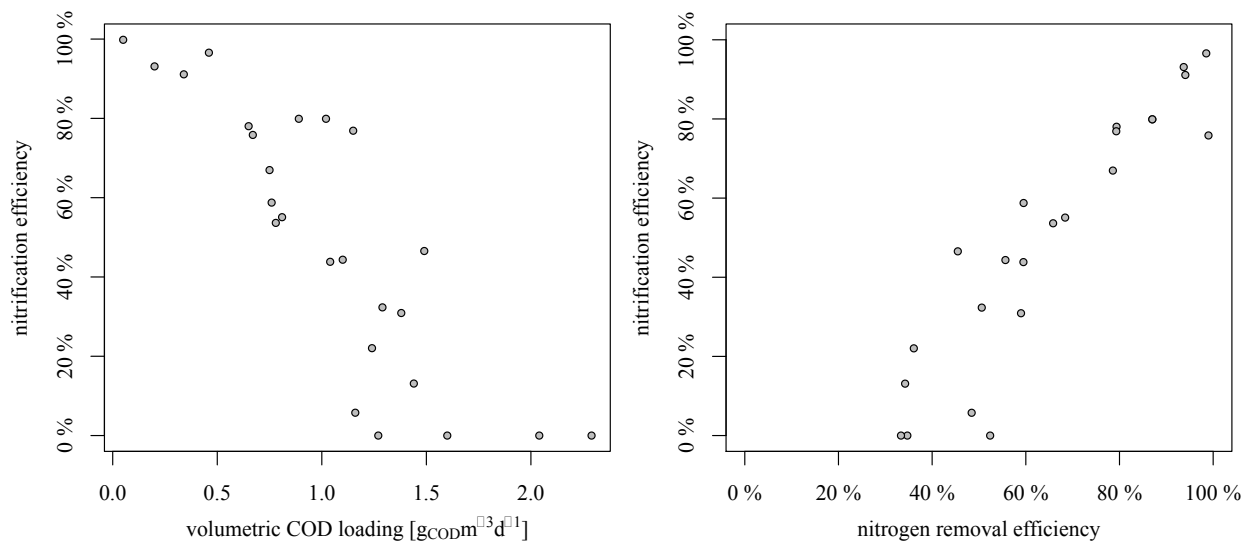


**Fig. 29: Results of the nitrification and nitrogen removal efficiency**



### 4.3.3 ENHANCED BIOLOGICAL PHOSPHORUS REMOVAL EBPR

For verification of an EBPR, a complete SBR cycle was measured. In the first step of the cycle, the nitrate is reduced to elementary nitrogen in the preceding denitrification. As a result of the SND under aerobic conditions discussed above, the nitrate concentration had to be manually increased to  $35 \text{ mg}\cdot\text{L}^{-1}$  with  $\text{KNO}_3$  to verify the denitrification step as nearly no nitrate was measurable after the aerobic step. During the denitrification step, the COD removal efficiency is particularly high due to adsorption effects. The substrate is stored in the cells of ordinary heterotrophic organisms and leads to a significant COD concentration decrease.

The anaerobic step begins when nitrate is completely reduced and the PAO organism are releasing  $\text{PO}_4$ . As seen in Fig. 30, the maximum  $\text{PO}_4$  release was reached after 60 minutes. During this release, the P to volatile suspended solids (VSS) ratio P/VSS decreased from 15.7% to 10.4 %. After a steady state of  $\text{PO}_4$  release was reached, the aerobic step was manually started (step 3: Nitrification and COD removal, Fig. 26). However, in this plant design the oxygen transfer to the liquid phase is limiting the aerobic removal. In turn, the raising dissolved oxygen concentration is an indicator for the progress of COD removal and nitrification. As soon as DO concentration exceeds  $2 \text{ mg}\cdot\text{L}^{-1}$ , the COD concentration and  $\text{PO}_4$  uptake reached steady state, respectively. When this steady state is reached, the wastewater treatment is completed. The net P removal after an aerobic step was  $20.7 \text{ mg}\cdot\text{L}^{-1}$  whereas the total biological P removal efficiency was 64.4%. Typically, the nitrate concentration would increase during this step without SND.

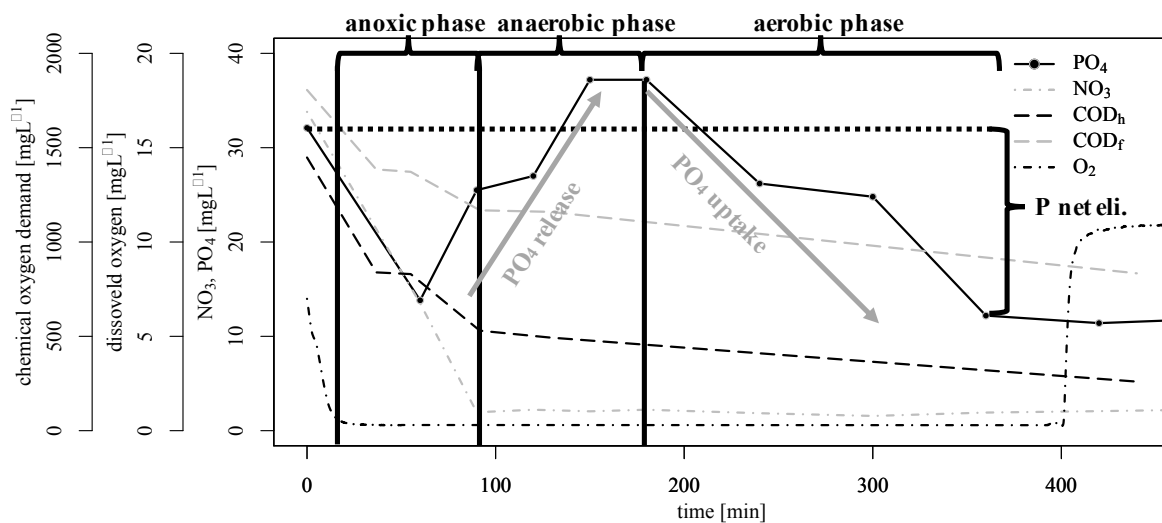


**Fig. 30:** High-resolved measurement of a SBR cycle for verifying an EBPR

#### 4.3.4 DEGRADATION KINETICS

To verify the maximum degradation rates of COD and  $\text{NO}_3$ , high amounts of both were fed to the SBR-TF. The kinetic parameters of COD and nutrient removal were calculated as the mean of the positive slope of the concentration over time (Fig. 31). The resulting COD and  $\text{NO}_3$  degradation rates  $r_C$  according to Fig. 31 are  $2.14 \pm 0.04 \text{ mg}_{\text{COD}} \cdot \text{min}^{-1}$  and  $0.377 \pm 0.02 \text{ mg}_{\text{NO}_3} \cdot \text{min}^{-1}$ . These specific kinetics  $r_C$  refer to the volume of trickling filter reactor, here  $V_{\text{WW}} = 0.077 \text{ m}^3$ . From aspects of comparability, these values have to be converted into a volumetric removal rate  $r_V$  referring the volumetric amount of biofilm media, here  $V_{\text{TF}} = 0.0544 \text{ m}^3$ . To convert the  $r_C$  to a volumetric degradation rate  $r_V$ , the packed bed volume of the trickling filter  $V_{\text{TF}}$  and volume of wastewater  $V_{\text{WW}}$  have to be considered:

$$r_V = r_C \cdot \frac{V_{\text{WW}}}{V_{\text{TF}}} \left[ \frac{\text{kg}}{\text{m}^3 \cdot \text{d}} \right] \quad 18$$

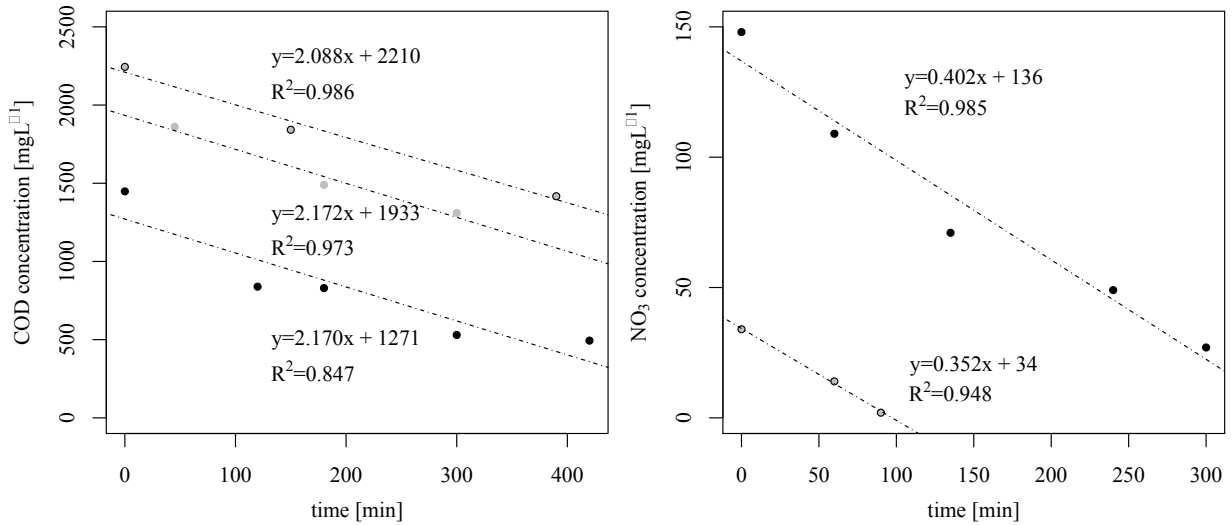


**Fig. 31: Results of COD and  $\text{NO}_3$  degradation kinetics**

The results of the maximum degradation rates are shown in Table 11. Despite the process-related limiting oxygen transfer and reduced active time caused by the integrated SBR mode (anaerobic step, sedimentation), the determined maximum COD degradation rate of  $4.5 \text{ kg}_{\text{COD}} \cdot \text{m}^{-3} \cdot \text{d}^{-1}$  is in the mid-range compared to literature (Daigger and Boltz, 2011; Naz et al., 2015). However, this high degradation rate can also be explained with the good degradation rates of specific stormwater runoffs due to increased rapidly degradable fraction compared to domestic wastewater like silage effluent and corn silage (Michael Cramer et al.,

2019c). COD removal and denitrification are both realized with heterotrophic microorganism. The identified anoxic/aerobic  $\text{PO}_4$  uptake rate was 31 % and therefore in the midrange of literature values (

Table 12). As the total VSS is unknown in biofilm systems, volumetric kinetic rates are used instead of sludge loading rates for the SBR/TF system.

**Table 11: Results of degradation kinetics**

$r_{V,COD}$	$r_{V,NO_3}$	COD/NO <sub>3</sub>
$kg_{COD} \cdot m^{-3} \cdot d^{-1}$	$kg_{COD} \cdot m^{-3} \cdot d^{-1}$	-
4.537	0.798	5.114

**Table 12: Results of P-release and uptake rates documented in literature**

	Aerobic P-uptake rate	Anoxic P-release rate	Anoxic/ aerobic uptake rate
	$\frac{\text{mg}}{\text{L}} \cdot \frac{\text{h}^{-1}}{\text{L}}$ $\frac{\text{mg}}{\text{g}_{\text{vss}} \cdot \text{L}^{-1}} \cdot \frac{\text{h}^{-1}}{\text{L}}$	$\frac{\text{mg}}{\text{L}} \cdot \frac{\text{h}^{-1}}{\text{L}}$ $\frac{\text{mg}}{\text{g}_{\text{vss}} \cdot \text{L}^{-1}} \cdot \frac{\text{h}^{-1}}{\text{L}}$	%
SBR/TF (López- Vázquez et al., 2008)	2.05	6.56	31
(Van Loosdrecht et al., 1997)	1.9-5.9	6.2-19.2	23-48
	1.2-1.6	4.0-6.0	20-40

#### 4.4 DISCUSSION

The study proved that the trickling filter system in SBR mode is suitable for wastewater treatment. The results showed that the SBR-TF combined the advantages of both systems as simplicity and reduced energy demand due to the missing forced aeration of trickling filter and enhanced biological nutrient removal efficiency of activated sludge systems. However, each SBR cycle requires the trickling filter to be ponded for the denitrification step to avoid oxygen diffusion as well as a back pumping to the secondary clarification tank for the aerobic step. This pumping time reduces the active time for degradation and therefore requires a larger plant design as well as an enhanced control technology compared with typical trickling filter.

A COD degradation rate of stormwater runoff of  $4.5 \text{ kg}_{\text{COD}} \cdot \text{m}^{-3} \cdot \text{d}^{-1}$  was achieved. With domestic wastewater, a theoretical COD removal rate of  $6.4 \text{ kg}_{\text{COD}} \cdot \text{m}^{-3} \cdot \text{d}^{-1}$  is achievable. Typical ranges of degradation kinetics of trickling filter with plastic packings are between 1.6 and  $8.0 \text{ kg}_{\text{COD}} \cdot \text{m}^{-3} \cdot \text{d}^{-1}$  (Metcalf and Eddy, 2014). These differences between both wastewaters can be explained with the lower yield coefficient of stormwater-runoff. A lower  $Y_H$  and a specifically higher oxygen demand can inhibit the degradation kinetic if oxygen supply is limited. The kinetic parameters and  $Y_H$  for this specific wastewater is discussed in a different paper (Michael Cramer et al., 2019c). Due to the plant design of the pilot plant, however, oxygen limitations have arisen. Nevertheless, The SBR concept allows an efficient nutrient removal at a low energy level which is comparable to activated sludge systems. Furthermore, this degradation kinetic is related to the total operation time. As this time also includes an anaerobic and anoxic step, the mere COD degradation would be higher.

Prerequisite for denitrification is a stable nitrification in the aerobic step. For nitrification rates above 90 %, a volumetric loading below  $0.5 \text{ kg}_{\text{COD}} \cdot \text{m}^{-3} \cdot \text{d}^{-1}$  should be applied to the system. Concerning biofilm nitrification, this is consistent with the findings of (Daigger and Boltz, 2011; Majumder and Gupta, 2003; Metcalf and Eddy, 2014). As soon as the ammonia is nitrified, the aerobic step can be terminated. As good indicator for detecting this state, the increase of dissolved oxygen can be used. Hence, the nitrification rate limits the total nitrogen removal efficiency. However, the determined TN removal was significantly higher than the theoretical possible, indicating a simultaneous nitrification and denitrification during aerobic step. This simultaneous nitrification and denitrifications depending on the biofilm thickness is well known (Matsumoto et al., 2007; Viridis et al., 2011). Hence, the total denitrification process in these experiments has to be divided into two steps, one happening in the anaerobic step and one simultaneous nitrification and denitrification during aerobic step. This thick biofilm is caused by the high specific surface area of the carrier of  $322 \text{ m}^2 \cdot \text{m}^{-3}$  and the fixed sprayer with suboptimal water distribution. This effect can be an advantage in cases of wastewaters with high ammonia content but can also be avoided by using carrier with less specific surface area, rotary sprayer and increased hydraulic loads. However, thick biofilm layers are not typical for conventional trickling filter, as the layer are either flushed out or consumed by predators like fly larvae.

#### 4.5 CONCLUSION

According to the results, the following conclusions are drawn:

- Ponding of trickling filter allows a nutrient removal due to the integration of anoxic/anaerobic steps. For this, the TFS has to be operated in a SBR-mode. This allows a direct integration of nutrient removal in the trickling filter instead of an additional ASS reactor and therefore reduces the construction costs compared to typical ASS/TF combinations.
- By integrating nutrient removal into a trickling filter, the advantages of biofilm and activated sludge systems are combined in a robust and energy-efficient process. However, this ponding and emptying of the trickling filter demand additional time and reduces the degradation rates and therefore enhances the required reactor volume.

- For a sufficient nitrification rate  $> 90\%$ , a volumetric loading of below  $0.5 \text{ kg}_{\text{COD}} \cdot \text{m}^{-3} \cdot \text{d}^{-1}$  is recommended. For implementing EBPR an anaerobic contact time of 60 minutes is recommended.
- Due to the simple technology and low energy costs, SBR-trickling filters may be attractive for rural areas and regions where requirements for nutrient removal coincide with the need for robustness and low operational effort.

#### 4.6 CONTINUING THOUGHTS OF STORMWATER TREATMENT ON SILO FACILITIES

The paper showed a possible solution dealing with stormwater runoff from silo facilities exemplary applied on a biogas plant. Though, a reliable treatment technology is not a stand-alone solution in this case. Instead, a holistic approach is required. For this, considering a smart control system for both the water management and the stormwater retention basin is essential. Considering the knowledge about the heavily polluted first flush of a rain event, a possible smart control system may include an energetic use by recycling the first flush in the digester (Fig. 32). For this purpose, either a time or volume control can be performed by constructive adjustment of the retention basin. The medium loaded runoff is then treated by the developed treating system discussed above.

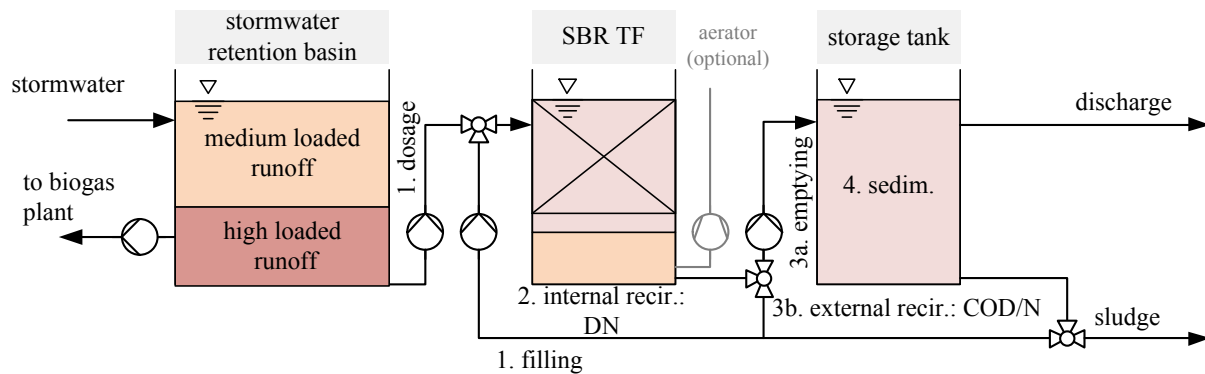


**Fig. 32:** Concept of stormwater treatment system

In contrast to domestic wastewater, the inflow from stormwater treatment systems is only intermittent. The danger when operating a trickling filter during long dry periods is 1) that it dries out due to evaporation effects if the same water is trickled over and over again and 2) the decay as a result of decay. To prevent a drying of the biomass, the trickling filter must be trickled continuously which is ensured by the external recirculation with already degraded wastewater from the storage tank (Fig. 32). The control concept must therefore maintain a defined water level in the retention basin for this case (Fig. 33). As soon as this level is reached, no further discharge is allowed and exclusively the external recirculation is active as no further degradation of N and P through denitrification and EBPR is expected at this point. From this point, the water level drops slightly due to evaporation alone. The evaporation losses are compensated with a dosage from the water reserve of the retention basin. Hence, the minimum volume of the retention basin is defined by the evaporation losses during the dry periods. However, in periods of sufficient rainfall (mostly autumn and spring time), the runoff is treated and discharged.



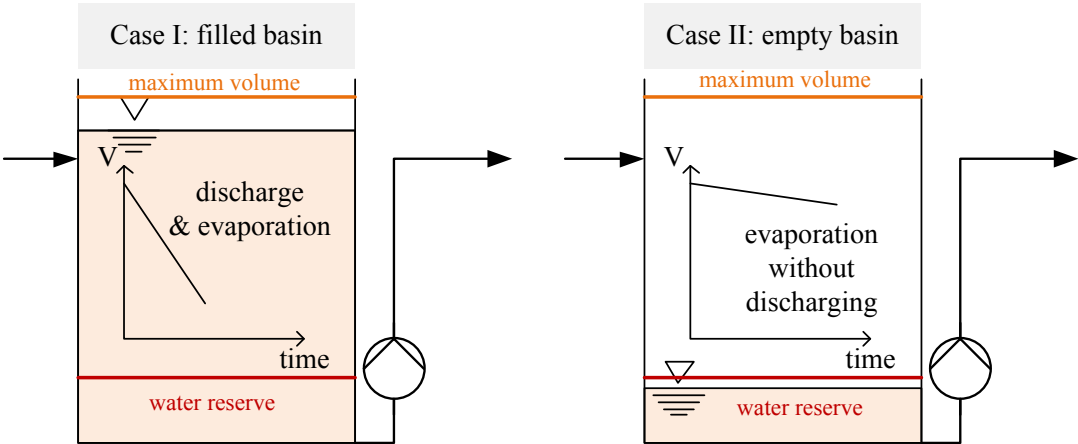


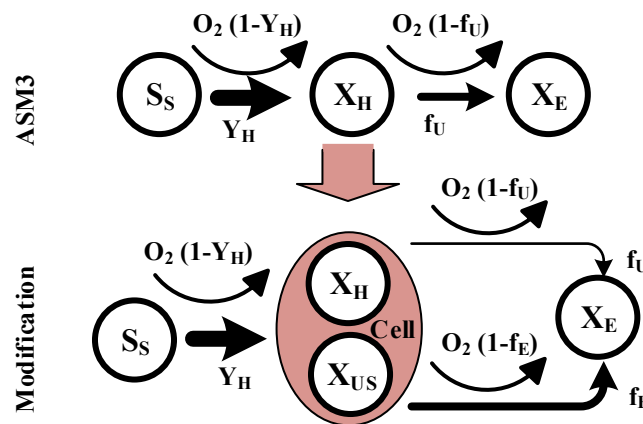
**Fig. 33:** Control concept of stormwater retention basin

## 5 Development of decay in Biofilms under Starvation Conditions – Rethinking of the Biomass Model

This chapter is published in:

Water; 27.4.2020; Volume 12:5; 1249

<https://doi.org/10.3390/w12051249>



The study investigates the decay of heterotrophic biomass in biofilms under starvation conditions based on measurements of the oxygen uptake rate (OUR). Original incentive was to understand the preservation of active biomass in SBR-trickling filter systems (SBR-TFS), treating event-based occurring, organically polluted stormwater. In comparison with activated sludge systems, the analyzed biofilm carrier of SBR trickling filters showed an astonishing low decay rate of  $0.025 \text{ d}^{-1}$ , that allows the biocenosis to withstand long periods of starvation. In activated sludge modeling, biomass decay is regarded as first order kinetics with a 10 times higher constant decay rate ( $0.17\text{--}0.24 \text{ d}^{-1}$ , depending on the model used). In lab-scale OUR measurements, the degradation of biofilm layers led to wavy sequence of biomass activity. After long starvation, the initial decay rate (comparable to activated sludge model (ASM) approaches) dropped by a factor of 10. This much lower decay rate is supported by experiments comparing the maximum OUR in pilot-scale biofilm systems before and after longer starvation periods. These findings require rethinking of the approach of single-stage decay rate approach usually used in conventional activated sludge modelling, at least for the investigated conditions: the actual decay rate is apparently much lower than assumed, but is overshadowed by degradation of either cell-internal substrate and/or the ability to tap “ultra-slow” degradable chemical oxygen demand (COD) fractions. For the intended stormwater treatment, this allows the application of technical biofilm systems, even for long term dynamics of wastewater generation.

## 5.1 INTRODUCTION

Biological wastewater treatment is based on the accumulation of a complex consortium of microorganisms in suspended systems (activated sludge), as biofilms attached to carriers (biofilm systems), or a combination of both. Provided optimal living conditions and substrate supply, the performance of those systems is mainly dependent on mass of metabolic active microorganisms. In situations with strongly varying loading (e.g., periodic wastewater generation, treatment of organic polluted stormwater), the varying substrate supply can lead to strong variations of active biomass and related substrate transformation rates. Especially long starvation conditions may lead to a significant decrease of performance due to biomass decay. This needs to be assessed when designing treatment technologies for those conditions.

Bacteria (as the most relevant group for substrate metabolism in activated sludge and biofilm systems) apply various adaptation strategies to starvation. The most prominent are altering the macromolecular composition (Daigger and Grady, 1982; Hood et al., 1986) and reducing the cell size (Morita, 1993; White, 2000). Besides, a reduction of the protein synthesizing system, the ribosomes, has been observed. This process, known as ribophagy is so far not completely understood, but simplified, the degradation of ribosomes seems to serve as a source of energy supply (Cebollero et al., 2012; MacIntosh and Bassham, 2011; White, 2000). It can be postulated that periodic changing substrate supply will perform a selective pressure on the biocenosis and define the phenotypic state of the bacteria (Kurland and Mikkola, 1993). However, these complex starvation-survival response strategies of bacteria can hardly be considered when describing biologic wastewater treatment mathematically.

Instead, the extensive variety of organism groups and their individual response to the environment needs to be streamlined, the governing biological processes, which again can only be described in a strongly simplified way. Currently, mathematical modeling of aerobic biologic wastewater treatment is based on the concepts developed in the activated sludge models (Henze et al., 2000). This also applies for biofilm systems with additional challenge of describing matter transport through the biofilm and related formation layers with different environmental conditions and processes (Gikas and Livingston, 1997; Henze et al., 2000; Wanner and Gujer, 1986). In activated sludge modelling (ASM), the variety of heterotrophic bacteria families is summarized in these models as one group ( $X_H$ ), expressed as chemical oxygen demand (COD).

The dynamics of heterotrophic biomass and the associated COD degradation are mostly mathematically described by combining growth and decay kinetics, both with a first order

dependence on active biomass. Regarding decay, two different approaches were proposed and alternatively applied in activated sludge and biofilm modeling: (i) endogenous respiration model (Gujer et al., 1999a; McKinney, 1960) and (ii) the death-regeneration model (Dold et al., 1980; Wanner et al., 1988; Wanner and Morgenroth, 2004).

In the first commonly used endogenous respiration approach as shown in Fig. 34, the active biomass can be directly consumed for providing maintenance energy for microorganisms as a consequence of decay (McKinney, 1960). As result of decay, a fraction ( $f_u$ ) remains as endogenous residue  $X_E$ .

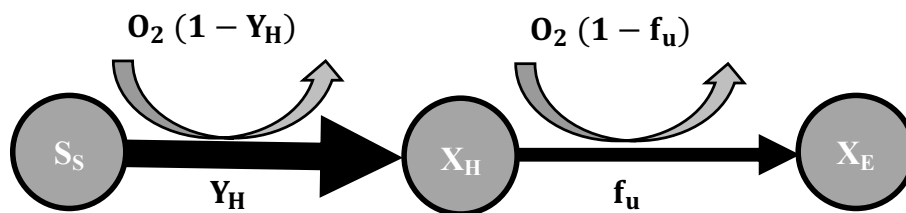


**Fig. 34: Principle of the endogenous respiration model.**

The death-regeneration model was introduced by Dold, Ekama, and Marais (1980). In this approach, heterotrophic microorganisms are releasing an unbiodegradable endogenous residue fraction  $X_E$  and a biodegradable COD fraction  $X_S$  during decay, which is then consumed by an organism, justifying oxygen consumption under starvation conditions (Fig. 35). As a by-product of these decayed bacteria and, therefore, released bioavailable  $X_S$  fraction, new growth is obtained, which is called regeneration. With this approach, increasing respiration rate after anaerobic periods can firstly be explained with the substrate release as a consequence of decay. If decay is an independent process, it would not stop under anaerobic conditions and, therefore, the substrate would accumulate, which then can be oxidized under aerobic conditions.

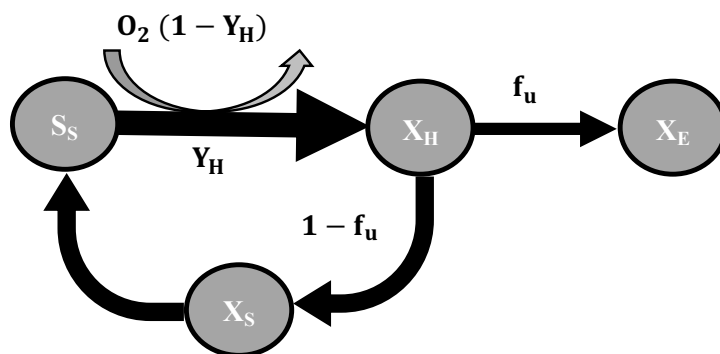


**Fig. 35: Principle of the death-regeneration model.**

According to this model, the decay rate  $b_H$  must become larger than in the endogenous respiration approach to compensate for regeneration. The decay rate from the respiration model  $b'$  can be converted to the death-regeneration model with Equation 19: for this, an endogenous residue factor  $f_U$  of 0.08 was assumed (Dold et al., 1980).

$$b = \frac{b'}{1 - Y_H \cdot (1 - f_U)} [d^{-1}] \quad 19$$

where  $Y_H$  is the heterotrophic biomass yield,  $b$  and  $b'$  is the decay rate within the death-regeneration and endogenous respiration approach, respectively. Applying the proposed biological constants of ASM (Gujer et al., 1999a), the corresponding decay rate for domestic wastewater is  $b = 0.62 d^{-1}$  and  $b' = 0.24 d^{-1}$ .

A simple and well-established method to evaluate the activity of heterotrophic microorganism  $X_H$  is measuring the respiration rate, expressed as biological oxygen uptake rate (OUR). With slight variations, the same method is commonly used for various research questions (Di Trapani et al., 2011; Ramdani et al., 2010; Spanjers and Vanrolleghem, 1995; Tränckner et al., 2008). In the state of the art, OUR is measured with respirometers under strictly controlled conditions to avoid side-effects. The magnificent advantage of this method is highly time resolved and low-cost measuring of kinetic parameters and COD fractions as it is just based on measuring dissolved oxygen. Fig. 36 shows in a schematic way the conversion of COD fraction in the raw water (left) and into biomass (right) during the biological process. The influent  $COD_{h,in}$  can either be degraded, which can be measured with the oxygen respiration rate for degradation  $OUR_{deg}$  or incorporated into biomass as excess sludge  $X_{ES}$ .

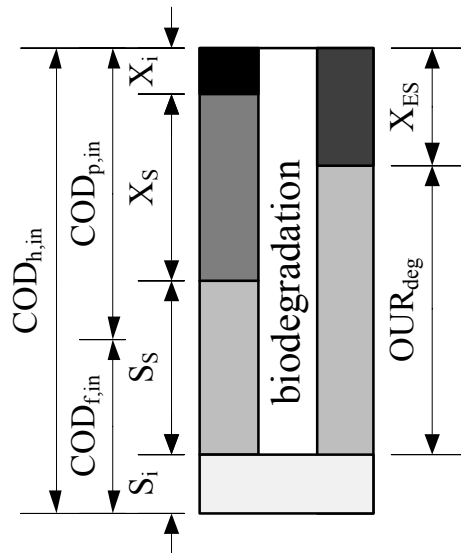


**Fig. 36: Chemical oxygen demand (COD) fractions during biological treatment (Michael Cramer et al., 2019c).**

For a long time it had been generally assumed that the decay rate is a constant and independent from substrate supply conditions (expressed for activated sludge systems by the sludge retention time SRT) for the particular biological environmental (Henze et al., 2000; G.v.R. Marais and Ekama, 1976; McKinney, 1960; Ramdani et al., 2010). Besides, the endogenous residue fraction  $X_E$  and yield coefficient for heterotrophic organism  $Y_H$  is regarded to be constant for a particular substrate in the ASM. These are rather mechanistic assumptions and only valid for systems with rather low load variations. Current research in activated sludge systems proved that both the  $X_E$  fraction (Friedrich et al., 2016) and the decay rate  $b_H$  (Friedrich et al., 2015) are a function of sludge retention time SRT (i.e., function of substrate supply). Due to this observation at extreme conditions of low COD, the question arises if organisms can adapt their decay rate and the assumption of a constant decay rate has to be reconsidered or if the existing ASM has to be extended with an additional very slowly degradable COD fraction (consisting of “hard” external COD and/or cell-internal reserves) and according degradation process. Consequently, this would mean that the actual decay leading to cell death would occur at a lower rate than previously calculated. This is important for the activity and sludge production of all systems running with permanent or periodically occurring starvation conditions.

Those conditions occur for example in systems that treat rainwater runoff with high organic pollution. A practical application is stormwater-runoff from agricultural silo facilities which can be heavily contaminated by organic and nutrient pollutants and has to be treated before discharge into surface waters (Michael Cramer et al., 2019a). In contrast to domestic

wastewater, the inflow to a treatment facility is rain dependent with dry weather periods of several weeks to months. Although, storage devices prior to a treatment plant can dampen these dynamics and biologic treatment systems should be able to survive starvation periods of several weeks and recover quickly in case of rain events. Attached growth systems are for those conditions interesting as they combine rather simple and robust technology with a certain ability to cope with load dynamics (Buitrón and Moreno-Andrade, 2011; Ye et al., 2012).

Applied to the original question, the development of active heterotrophic biomass (here, in attached growth systems) under long lasting starvation conditions, the main objectives of this paper are

- The quantification of cell-decay rate under starvation conditions;
- To identify and quantify degradation of a “new” COD fraction, made accessible under those conditions;
- To quantify the recovery of the biofilm after starvation.
- To verify the results achieved under lab-scale conditions a pilot plant for treating stormwater runoff with high organic pollution is operated, accordingly.

## 5.2 MATERIAL AND METHODS

### 5.2.1 DESIGN OF WASTEWATER TREATMENT PLANT

Stormwater-runoff and silage effluent of a biogas plant was treated by an SBR trickling filter system (SBR-TFS) which is based on a trickling filter and a secondary clarification and storage tank. A compact description is given here. The entire process of SBR trickling filter is discussed in (Michael Cramer et al., 2019b).

Fig. 37 shows a principle schema of the treatment system. In contrast to conventional trickling filters (see e.g., (Metcalf and Eddy, 2014)), the SBR-TFS is operated as a sequence-batch-reactor (SBR) to allow anaerobic phases for a systematic nutrient removal. Like typical SBR as known from activated sludge systems (ASS), the process is divided into an anaerobic and aerobic step. The anaerobic step acts as an upstream denitrification. During this step, the trickling filter is firstly fed with stormwater-runoff from the combined retention and primary clarification tank (rich in COD, ammonia, and phosphorous) and distributed

with a rotary sprayer for a homogeneous spread all over the surface. After dosage, the trickling filter is filled up with treated water from the combined storage and secondary clarification tank (containing nitrate from the previous cycle) to the highest level to avoid oxygen diffusion during anaerobic recirculation (step 2b). The completely ponded system is then internally recirculated to achieve denitrification (and anaerobic P-release, if enhanced biological removal shall be performed). The aerobic phase follows the anaerobic phase in which the wastewater in the trickling filter is emptied into the storage tank. In this phase, the trickling filter sump is constantly pumped into the storage tank and back to the rotary sprayer of the trickling filter until COD degradation and nitrification are completed (step 3b). Distributing the water over a high surface area of the biofilm carrier provides a sufficient oxygen supply through diffusion. The final step is the sedimentation, separating the activated sludge from the clarified water, which is finally discharged.

For the decay experiments, a small-scale SBR-TFS was operated. The steps of one SBR cycle including anoxic, anaerobic, and aerobic conditions are presented in Fig. 38. The total volume of the trickling filter was 80 L with a packing bed volume of 54 L and a specific surface area of the biofilm carrier of  $322 \text{ m}^2 \cdot \text{m}^{-3}$ . During the starvation period, no stormwater was added and the SBR-TFS was only operated with the same treated wastewater.

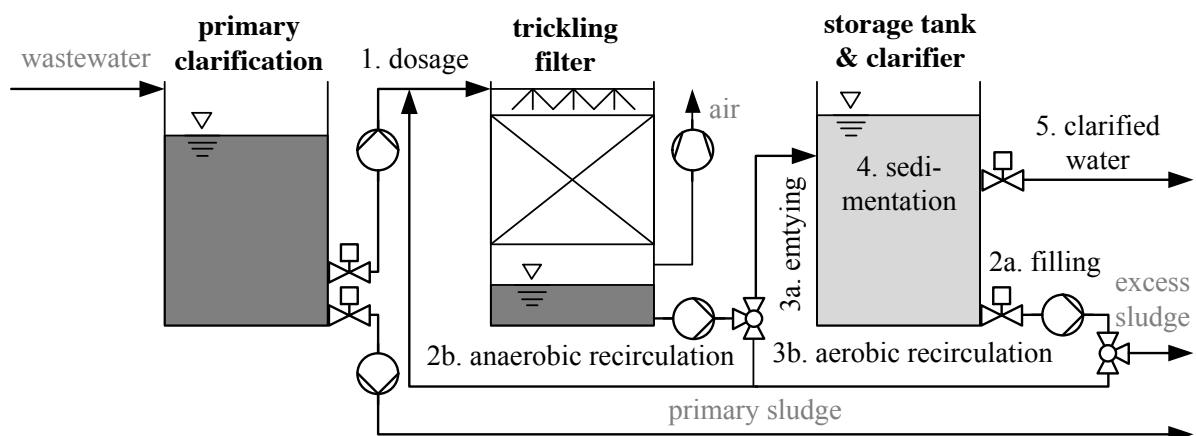


**Fig. 37:** Principle schema of the trickling filter system (Michael Cramer et al., 2019b).



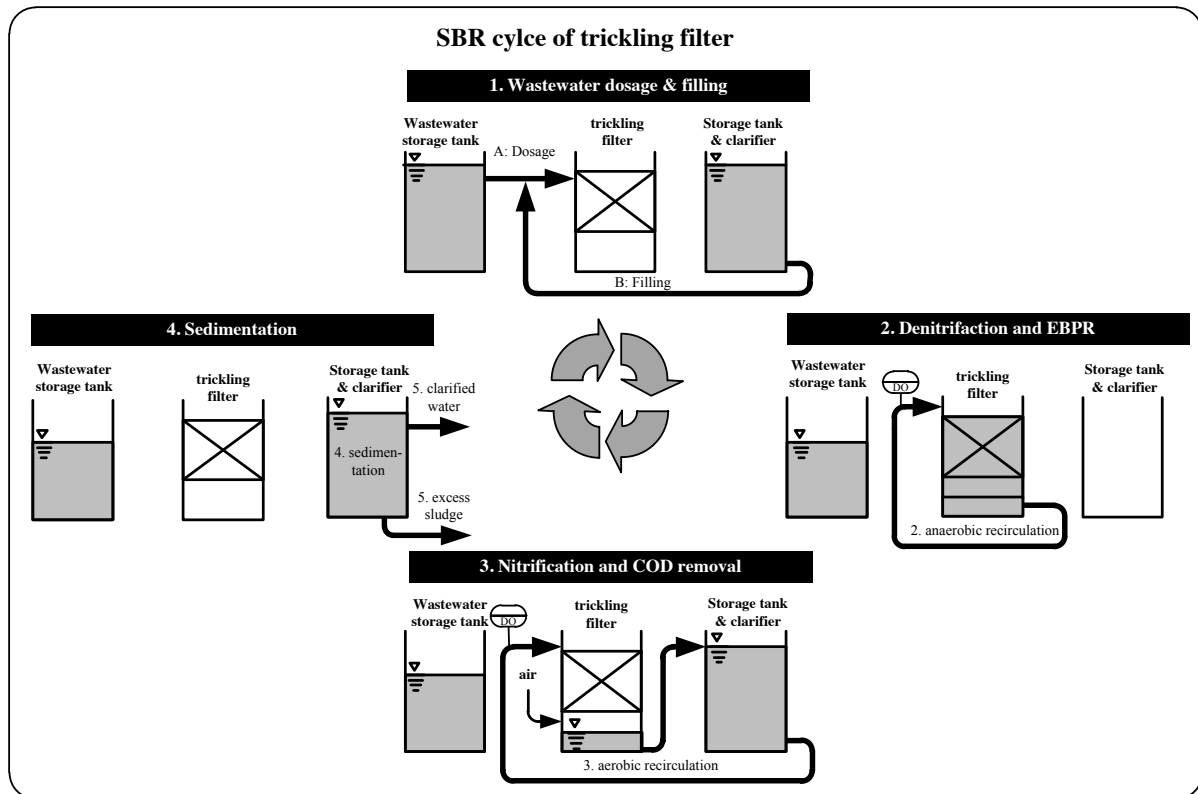


**Fig. 38:** Steps of one SBR cycle (Michael Cramer et al., 2019b).

### 5.2.2 ANALYTICAL PROCEDURE

For measuring the decay rate of attached growth system, a modified OUR method was used for aerobic respiratory in laboratory scale. The schema is presented in Fig. 39, left. OUR tests have been developed and widely applied for activated sludge systems (Friedrich and Takacs, 2013; Gujer et al., 1999a). In order to meet the conditions in the SBR-TFS system closely, activated sludge was replaced by 13 biofilm carrier fixed on a line in a 1 L reactor filled with tap water. The carriers were taken from the pilot plant described above, which was operated for 6 months to treat stormwater-runoff from a biogas plant. A magnetic stirrer provided a homogenous mixture. The dissolved oxygen DO was measured with an optical DO probe (time resolution: 1 s) and controlled in a range of 2–4 g m<sup>-3</sup>. OUR was calculated for each switch-off phase by a linear regression of the declining DO. During the starvation period, the reactor filled with biofilm carriers was aerated without substrate supply. From the resulting respirogramm during starvation, the endogenous respiration rate OUR<sub>e</sub> was calculated according to (Michael Cramer et al., 2019c), (see “mathematical model” below, section 2.3).

For measuring maximum growth rates, the bacteria were fed with silage effluent as highly degradable substrate (Michael Cramer et al., 2019c). The substrate was injected into the

reactor after 3, 4, 7, and 13 days of continuous starvation. After each dosage, the starvation period started again. After substrate dosage, the maximum respiration rate  $OUR_{max}$  was calculated from the respirogramm in the same way as  $OUR_e$ . Assuming a typical value for  $f_U$  and a substrate specific yield coefficient, the growth rate can be calculated from the endogenous and maximum  $OUR$  according to the mathematical model, described below.

In addition to the laboratory respiration tests, the oxygen consumption was measured in the pilot-scale trickling filter (Fig. 39, right). To allow ponding, the aeration aperture at the bottom of the trickling filter is connected to a riser pipe, ending above the highest filling level. At aerobic conditions the same pipe is empty and provides air supply. To avoid unintended limitation of aeration, a fan on top of the rising pipe is sucking air through the unsubmerged trickling filter. For measuring the  $OUR$  in the trickling filter, an optical DO probe was installed in a measuring section of the recirculation pipe shortly before the rotary sprayer. The  $OUR$  measurement was performed in three succeeding steps: (1) the treated wastewater in the secondary clarification was aerated to oxygen saturation with an external aerator. (2) The oxygen saturated water was pumped to the trickling filter to the upper level. To minimize oxygen diffusion, the rotary sprayer was temporary replaced with a pipe that plunged into the water. (3) The water in the filled-up trickling filter was recirculated and the oxygen decline was recorded. This procedure results in one single  $OUR$  measuring point and was repeated each 2 days.

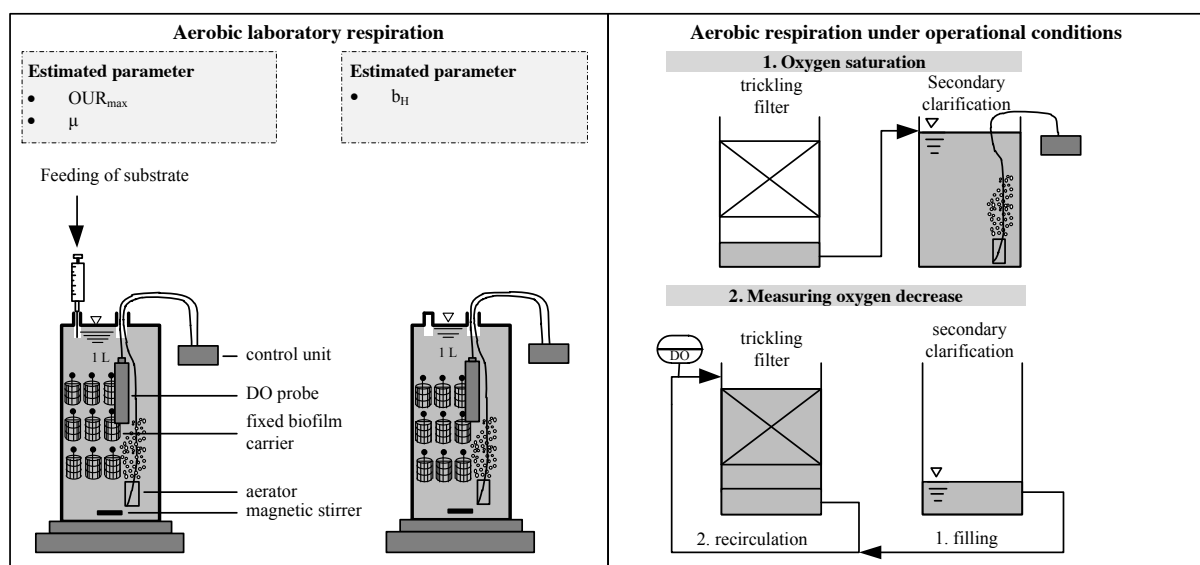


Fig. 39: Schema of the respirometry measurement of the oxygen uptake rate.

### 5.2.3 MATHEMATICAL MODEL

For mathematical derivation of endogenous decay rate based on the OUR method, see (Michael Cramer et al., 2019c). For endogenous respiration, OUR corresponds to the change of  $X_H$ , reduced by an endogenous residue factor  $f_U$ :

$$\text{OUR}_e = (1 - f_U) \cdot \frac{dX_H}{dt} [\text{g} \cdot \text{m}^{-3} \cdot \text{d}^{-1}] \quad 20$$

The net growth of heterotrophic bacteria  $X_H$  is the difference of growth and decay. Both growth and decay can be described as first order kinetics of actual biomass concentration. Additionally, there is a substrate dependency for the growth, usually expressed by a Monod kinetics (Equation 21).

$$\frac{dX_H}{dt} = \mu_{\max} \cdot \frac{S}{K_S + S} \cdot X_H - b_H \cdot X_H [\text{g} \cdot \text{m}^{-3} \cdot \text{d}^{-1}] \quad 21$$

where  $b_H$  is the decay rate of heterotrophic organism,  $\mu$  is the bacteria growth rate,  $S$  is the substrate concentration, and  $K_S$  is the substrate saturation coefficient.

The bacteria growth is stoichiometrically linked to the oxygen demand Equation 22:

$$\text{OUR}_{\text{growth}} = \mu_{\max} \cdot \frac{1 - Y_H}{Y_H} \cdot X_H [\text{g} \cdot \text{m}^{-3} \cdot \text{d}^{-1}] \quad 22$$

Substrate utilization results in oxygen consumption with respect to bacteria growth and endogenous respiration. With this in mind, the maximum oxygen consumption rate  $\text{OUR}_{\max}$  at time  $t(0)$  can be determined with Equation 23:

$$\text{OUR}_{\max}(0) = \left( \mu_{\max} \cdot \frac{1 - Y_H}{Y_H} + (1 - f_U) \cdot b_H \right) \cdot X_H [\text{g} \cdot \text{m}^{-3} \cdot \text{d}^{-1}] \quad 23$$

Substituting  $X_H$  in Equation 23 by the rearranged Equation 20 results in:

$$\text{OUR}_{\max}(0) = \left( \mu_{\max} \cdot \frac{1 - Y_H}{Y_H} + (1 - f_U) \cdot b_H \right) \frac{\text{OUR}_e(0)}{(1 - f_U) \cdot b_H} [\text{g} \cdot \text{m}^{-3} \cdot \text{d}^{-1}] \quad 24$$

Equation 24 can be arranged to calculate the maximum growth rate from respirometry:

$$\mu_{\max} = \frac{Y_H}{1 - Y_H} \cdot (1 - f_U) \cdot b_H \cdot \left( \frac{\text{OUR}_{\max}(0)}{\text{OUR}_e(0)} - 1 \right) [\text{g} \cdot \text{m}^{-3} \cdot \text{d}^{-1}] \quad 25$$

The substrate specific yield coefficient  $Y_H$  of silage effluent was separately determined with 0.87 (Michael Cramer et al., 2019c). This rather high yield is attributable to its sugar-like

ingredients as glucose have a yield coefficient of 0.90–0.91 (Dircks et al., 1999). The decay rate  $b_H$  was calculated from the respirogram and for  $f_U$ , a typical value of 0.2 for heterotrophic biomass was assumed (Gujer et al., 1999a).

### 5.3 RESULTS

#### 5.3.1 DECAY RATE DURING STARVATION

Typically, the decay rate of heterotrophic organism is graphically expressed as a logarithmical decrease of endogenous respiration for activated sludge system. However, for the investigated attached growth systems, this is hardly applicable as Fig. 40 shows. The time series shows that repeatedly a logarithmical decrease of on average 15 h is followed by an exponential increase of on average 10 h with continuously decreasing amplitude. As the used biofilm carrier were grown with a thick biofilm, it seems that the organism makes organic compounds inside the biofilm stepwise accessible as substrate. The processes leading to periodic OUR increase are not clear yet. Working hypotheses are (i) hydrolysis of slowly degradable substrate in the biofilm and decay products, (ii) usage of intracellular storage of the organisms themselves and ribophagia or a combination of both. Layering and diffusional processes may be influencing, too (Kuenen et al., 1986; Kwok et al., 1998).

According to the black line in Fig. 40, the best model fit for endogenous decay rate during the time period of OUR decrease at the beginning of the experiment is the recommended decay rate of  $0.24 \text{ d}^{-1}$  as widely applied and proved in activated sludge modelling (ASM1) (G.v.R. Marais and Ekama, 1976). Considering both parts of the wavy respirogram, the decreasing and increasing OUR, a net decay rate  $b_{H+stor}$  of  $0.17 \text{ d}^{-1}$  in accordance with ASM3 would fit best for a certain time period, here 6–7 days. To express this switch of decay rate, the apparent OUR under endogenous condition is divided into OUR obtained by degradation of an additional fraction  $X_{US}$  (gray dot pointed line, Fig. 40) and OUR obtained by base decay rate  $b_H$  of active biomass (black dot pointed line, Fig. 40). The total OUR is therefore the sum of both (gray dotted line). After this time period, the modelled net decay rate changes significantly to a lower value of  $0.025 \text{ d}^{-1}$ , nearly a tenth of the conventionally applied decay rates. From this time on, all storage fractions are consumed and the sole decay rate is obtained (black dot pointed line).

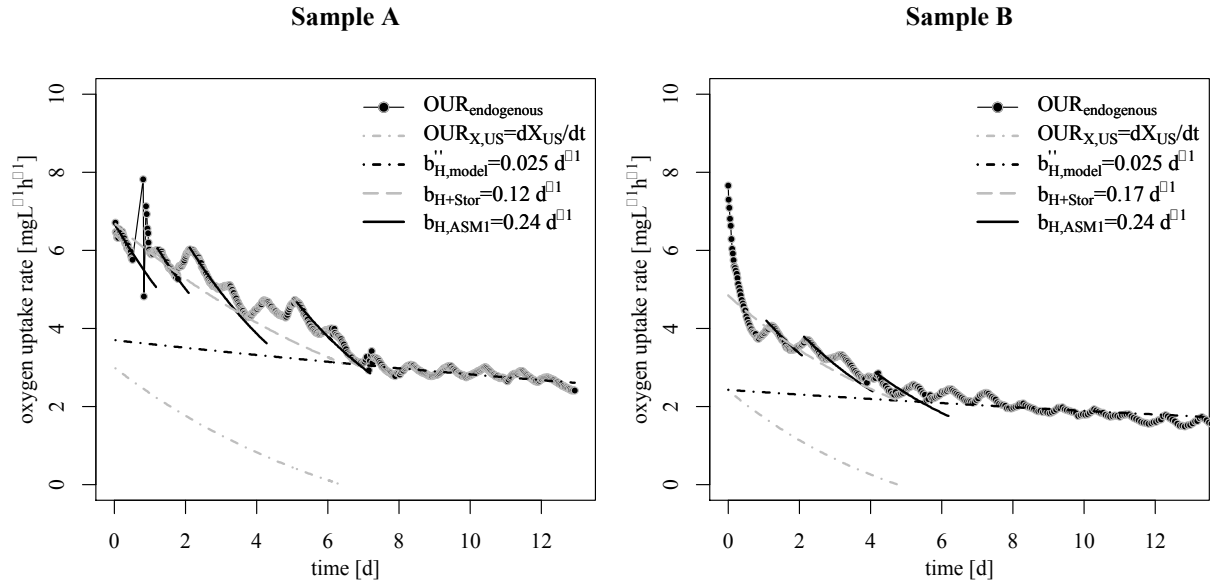


**Fig. 40:** Alternation of decay rate during starvation of biofilm carrier.

If the proposed concept of a base decay and a degradation of “ultra-slowly” degradable  $X_{US}$  applies, the net decay rate after substrate feed as sum parameter of decay and  $X_{US}$  degradation should be the same as in the beginning of the experiment ( $0.17 \text{ d}^{-1}$ ) and then fall back to the base decay rate  $b_H$  as soon as this additional storage fraction is consumed ( $0.025 \text{ d}^{-1}$ ). To answer this, substrate was fed in excess to ensure an accumulation of  $X_{US}$  after 18 days of starvation. As Fig. 41 shows, the brutto decay rate  $b_{H+stor}$  increased again from  $0.025$  (before day 18) to  $0.17 \text{ d}^{-1}$  after substrate feed. After complete consumption of  $X_{US}$ , the decay rate during OUR decreased to  $0.025 \text{ d}^{-1}$  once more ( $=b_H$ ). Precisely, degradation of an addition fraction extended the base decay rate  $b_H$  by this storage fraction, which can be expressed again with the degradation rate  $b_{H+stor}$ . Hence, the best model fit for modelling the overall process for the base decay rate is  $0.025 \text{ d}^{-1}$  in addition with a consumption rate ( $=b_{H+stor}$ ) for  $X_{US}$  of  $0.17-0.025 \text{ d}^{-1}$ . This shows that the alternation is only temporary and therefore can be related with an additional degradation process of the new fraction  $X_{US}$ .

Sample A

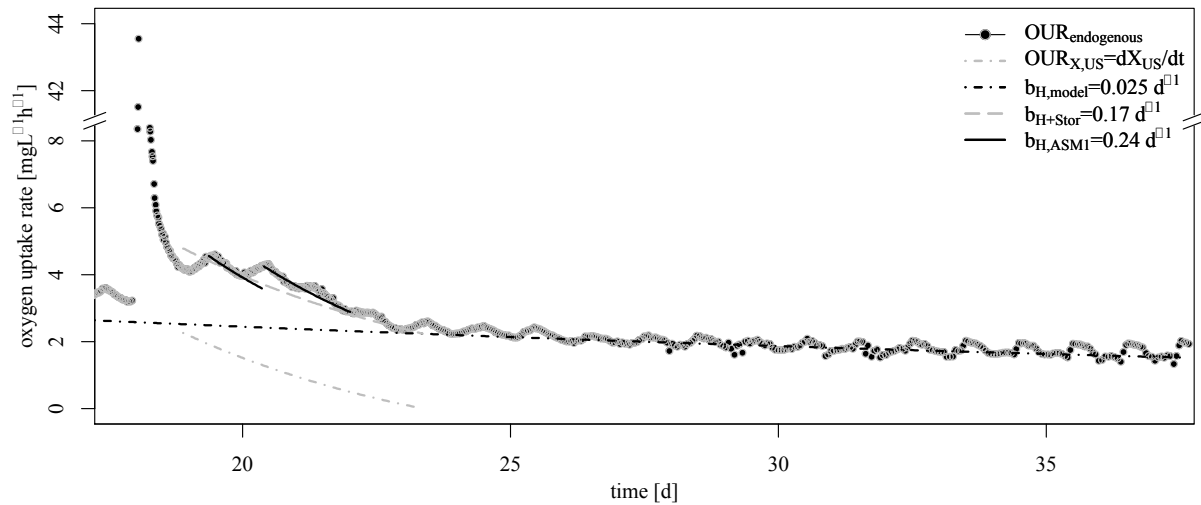


**Fig. 41: Results of endogenous OUR after substrate feeding.**

### 5.3.2 VERIFICATION OF THE LOW DECAY RATE IN PILOT SCALE

The validity of at least two decay mechanisms—(1) a fast decay rate controlled by the availability of an additional  $X_{US}$  fraction and (2) a base decay rate in “real” starvation conditions—should be provable under operational conditions of the pilot plant. The proof can be performed with two experimental concepts: (i) decline of the “operational” OUR under starvation conditions and (ii) measuring maximum biomass activity after starvation. The latter experiment assumes that the identified base decay rate should preserve the biomass activity on a much higher level than calculated with the commonly proposed decay rate.

According to the schema of Fig. 39 on the right, respirometry measurements were performed in the pilot plant. For this, the wastewater in the storage tank was aerated until oxygen saturation occurred and filled back to the highest level in the trickling filter. After filling, the inner recirculation was started to measure the dissolved oxygen decrease within the trickling filter. This decrease lasts up to 3 h, depending on the prior starvation period and the associated endogenous respiration rate (Fig. 42). The figure illustrates the parametrized sequencing decay model after 9 days of starvation. Until the fourth day of starvation, the best model fit is a net decay rate of  $0.14 \text{ d}^{-1}$ , including degradation of “ultra-slow” degradable COD fraction  $X_{US}$  (gray dotted line) and pure decay (black dotted line). At this point,  $X_{US}$  is consumed and the decay rate decreases to the base decay rate of  $0.022 \text{ d}^{-1}$ . Separating both processes would yield a decay rate for the storage products of  $0.14 \text{ d}^{-1}$  ( $-0.022 \text{ d}^{-1}$ ). In

conclusion, the results show that the findings of a low decay rate are indeed representative under real operational conditions for treating stormwater-runoff from silo facilities.

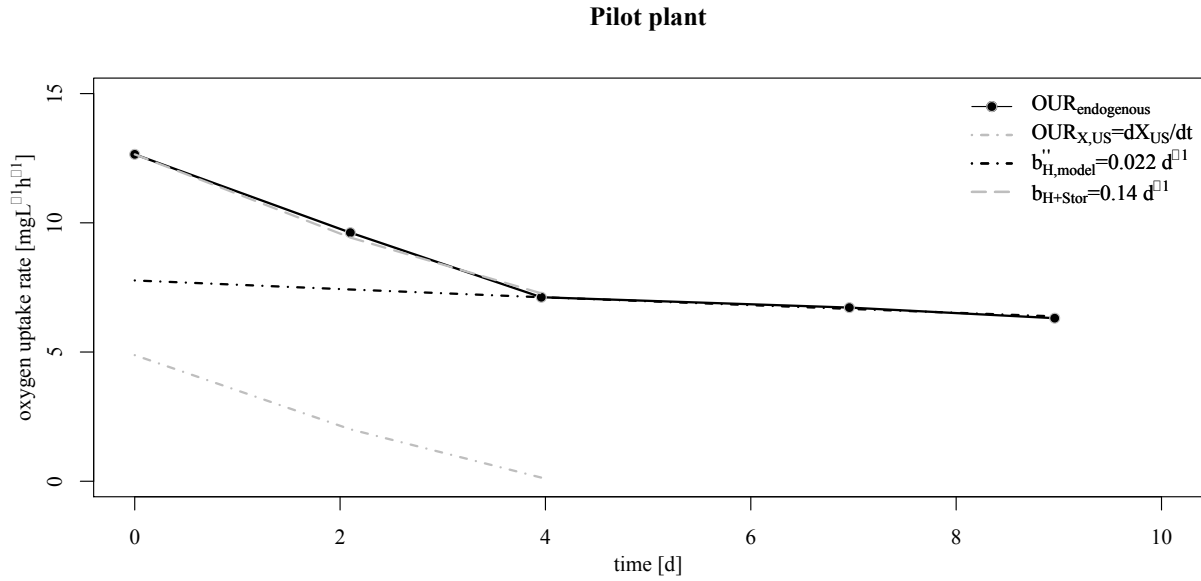


**Fig. 42: Results of respirometry measurement in a pilot scale trickling filter.**

Under starvation conditions, the decrease of  $OUR_{max}$  represents (according to Equation 23) directly the reduction of active biomass  $X_H$ . Knowing the initial  $OUR_{max}(0)$  and decay rate  $b_H$ ,  $OUR_{max}$  at certain times of starvation can be calculated with Equation 26:

$$OUR_{max,calc.}(t) = OUR_{max}(0) \cdot e^{-b_H \cdot t} [g \cdot m^{-3} \cdot d^{-1}] \quad 26$$

For this, silage effluent was dosed into the reactor after 5, 8, and 13 days of continuous starvation as depicted in Fig. 43. As shown in Fig. 43 on the left, the observed and calculated  $OUR_{max}$  according to Equation 26 are nearly the same even after 13 days of continuous starvation. Therefore, it can be inferred that the decay rate of about  $0.025 d^{-1}$  is true and is suitable for an adequate prediction of biomass decrease under long starvation periods. The respirogramm for the case of 13 days of continuous starvation is shown in Fig. 43 on the right. Based on the measurements of  $OUR_e$  and  $OUR_{max}$  and considering Equation 25, a growth rate  $\mu_{max}$  of  $7.9 d^{-1}$  results at a constant  $Y_H$  and  $f_U$  at a temperature of  $25 ^\circ C$ . However, with respect to typical growth rates of  $6 d^{-1}$  at  $20 ^\circ C$ , a growth rate of approximately  $8.5 d^{-1}$  would be expected. Therefore, the estimated rate is within the expected range.

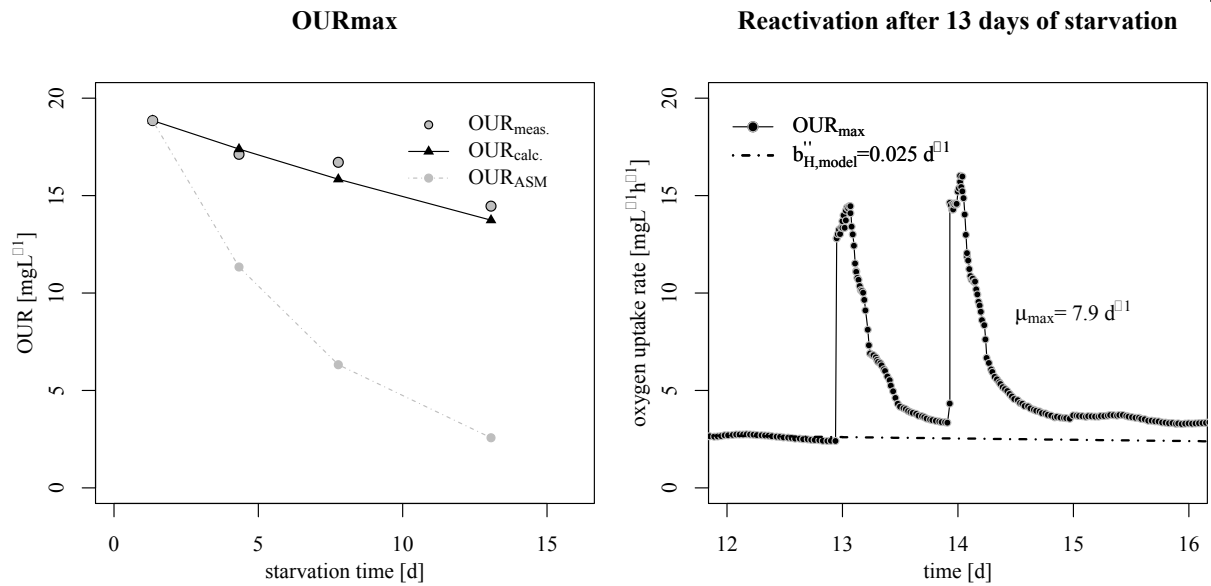


**Fig. 43:** Reactivity of microorganism after starvation.

#### 4. Discussion

The results showed that long starvation periods in the investigated biofilms are linked to a significant lower decay rate of just a tenth of the recommended decay rate used in the ASM (Gujer et al., 1999a). Experiments with activated sludge support these findings (Friedrich et al., 2016, 2015). Actually, both decay rate and particulate inert fraction are rather a function of nutritional state than a constant. For rather steady state substrate supply as common in domestic wastewater treatment plants, this functional relationship is neither detectable nor relevant. However, for long or permanent extreme starvation conditions, the approach of the ASM is not sufficient to explain an alternation of the decay rate. This limitation could be overcome by slight changes of the modelling concept. The actual decay (as irreversible die-off of biomass) needs to be described with the observed much lower decay rate, but is superimposed by decay of “ultra-slow degradable” substrate  $X_{US}$ , which is not “tapped” under normal conditions. The identity of  $X_{US}$  is not clear yet. It can be thought as (i) cell internal reserve substrate or (ii) hardly accessible external substrate or a mix of both. From a modelling perspective, taking it as external substrate is the simplest approach, since  $X_{US}$  formation is in this case decoupled from bacterial growth. This conceptual idea could also explain the wavy decline of decay, especially if combined with the death-regeneration approach. Transformation processes within the rather thick biofilm used in our experiments were probably diffusion controlled and oxygen limited in deeper layers. The diffusion limitation and oxygen penetration into the biofilm are presented in the Supplementary Materials. However, in the death-regeneration approach, decay is defined to be independent from oxygen supply. Therefore, independent from the aerobic state,



biodegradable fractions are released by decay of organism but not used due to oxygen limitation. The biodegradable fractions are preserved in the inward layer of the biofilm carrier. The preserved COD fractions in the lower layers would lead to an increased respiration rate as soon as the upper layer is fully decayed. This short-term regrowth is followed by aerobic decay of the newly formed biomass, leading to the wave-like behavior of the observed respiration rates. This layering effect causing diffusion limitations is often associated with a simultaneous nitrification and denitrification in biofilm systems (Cramer et al., 2020; Viridis et al., 2011). In contrast to the biofilm experiments in this study, experiments with activated sludge will probably not allow such a clear distinction between decay of  $X_{US}$  and actual decay of biomass due to the stochastic distribution of both fractions. Accordingly, respirometry measurement would show a more continuous adaptation of the decay rate.

The extension of the death-regeneration approach by an “ultra-slow” degradable  $X_{US}$  fraction as an external substrate is illustrated in Fig. 44. It can be made available via hydrolyzation to a slow degradable fraction  $(1 - f_E)$  and is then consumed as  $S_S$ . A small ratio  $f_E$  remains as endogenous residue  $X_E$ . The hydrolyzation itself is poorly understood, yet, due to the variety of substrates and apart from this, the experiments in the literature are mainly accomplished with pure substrates (Hauduc et al., 2013). Most model concepts (for instance ASM1, ASM2d, ASM3) are based on a one step hydrolyzation. In the approach proposed here, the  $X_{US}$  fraction is firstly hydrolyzed into  $X_S$  and further hydrolyzed into  $S_S$ . However,  $X_{US}$  hydrolyzation is inhibited by the concentration of the better accessible  $X_S$  and will only be degraded under real starvation conditions when  $X_S$  is fully degraded. Once  $X_{US}$  is consumed, only the base decay rate is obtained. Mathematically, this can be considered with an inversed Monod kinetic (Equation 28). The key idea behind this is that the term for  $X_{US}$  is “inactive” as long as  $X_S$  is still available (Equation 27 is above zero). With decreasing  $X_S$ , the term becomes more and more “active” and is most active when  $X_S$  drops to zero. Now,  $X_{US}$  becomes the limiting step measured in respirometry. As soon as  $X_{US}$  is degraded also, the term reaches zero and only the base decay rate is active (see Equation 25).

$$\frac{dX_S}{dt} = X_H \cdot k_h \cdot \left( \frac{X_S/X_H}{K_S + X_S/X_H} \right) [g \cdot m^{-3} \cdot d^{-1}] \quad 27$$

$$\frac{dX_{US}}{dt} = X_H \cdot k_h \cdot \left( \frac{X_{US}/X_H}{K_S + X_{US}/X_H} \cdot \frac{K_S}{K_S + X_S/X_H} \right) [g \cdot m^{-3} \cdot d^{-1}] \quad 28$$

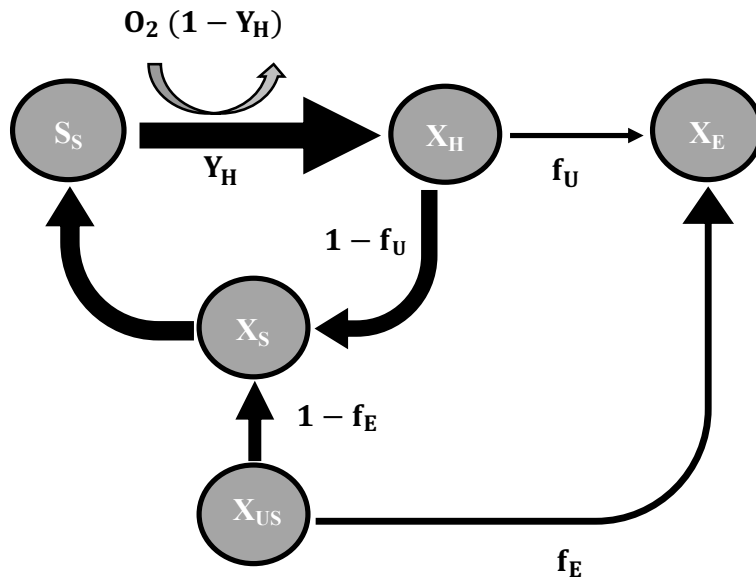


**Fig. 44:** Extending of the death-regeneration model

Similar to the death-regeneration approach, the endogenous approach can be extended in a similar way (Fig. 45). Here, the possibility of a cell internal storage fraction was exemplarily used to integrate the additional  $X_{US}$  fraction. In this approach, the fast-degraded substrate during endogenous conditions (illustrated with a bold line) internal storage fraction  $X_{US}$  is directly degraded into the endogenous residue  $X_E$ , without prior hydrolysis. Both base decay and  $X_{US}$  consumption are running parallel. The degradation rate of  $X_{US}$  can be expressed as the sum decay rate of storage product and base decay rate  $b_{H+stor}$  discussed above minus the base decay rate ( $b_{H+stor} - b_H$ ). The irreversible decay of active biomass is running in parallel with the observed much lower decay rate  $b_H$  (illustrated with a thin line). Summarizing, as long as  $X_{US}$  is still available as substrate, the brutto degradation rate  $b_{H+stor}$  is suitable as best model fit for describing the OUR decrease with time. As soon as  $X_{US}$  is fully degraded, the sole decay rate  $b_H$  is obtained.

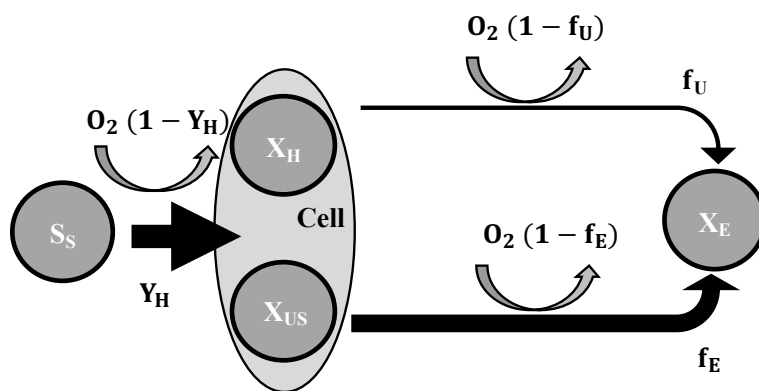


**Fig. 45:** Adjusting of the endogenous respiration model.

$$\frac{dX_H}{dt} = -X_H \cdot b_H [g \cdot m^{-3} \cdot d^{-1}]. \quad 29$$

$$b_H = 0.025 d^{-1}$$

$$\frac{dX_{US}}{dt} = X_H \cdot k_h \cdot \left( \frac{X_{US}/X_H}{K_{US} + X_{US}/X_H} \right) = -X_H \cdot (b_{H+stor} - b_H) [g \cdot m^{-3} \cdot d^{-1}] \quad 30$$

$$b_{H+stor} = 0.17 d^{-1}$$

$$\frac{dX_E}{dt} = f_E \cdot X_{US} \cdot (b_{H+stor} - b_H) + f_U \cdot X_H \cdot b_H [g \cdot m^{-3} \cdot d^{-1}] \quad 31$$

$$f_U = 0.20$$

$$f_E = 0.48$$

A classification of  $X_{US}$  as a cell internal COD fraction or as an external fraction which can be made available to heterotrophic organism by a multi-step hydrolyzation depends on the model approach taken and can both be easily integrated. Compared to the complex adaptation of microorganisms to varying nutritional and environmental conditions, both approaches are still rather conceptual but would sufficiently describe the observed change of decay rate.

## 5.4 CONCLUSIONS

The aim of this work was to quantify the reduction of biomass activity in biofilm systems suffering from periodic starvation conditions. For this, two experimental approaches were combined: (i) OUR experiments with biofilm carriers taken from a pilot-scale trickling filter, (ii) adapted OUR experiments of the complete trickling filter. According to the findings of this work, the following conclusions are drawn:

- Starvation of biofilm carrier was characterized by wavy increase and decrease of endogenous respiration, ending at a surprisingly low base decay rate. Justifying this effect with either the existing death-regeneration model or the endogenous respiratory model is not a straightforward task;
- A possible explanation approach is the layering and the associated oxygen diffusion limitations, which preserves the lower layers from real degradation of COD but not from decay;

- However, even taking these biofilm specific conditions apart: the base decay rate is considerably lower than the recommended value in existing ASM;
- This lower decay rates allow a conservation of biological activity over long starvation periods as shown by reactivation experiments at the pilot SBR trickling filter;
- To explain these findings, the common one step decay model needs be divided into at least two processes: (i) a fast degradation of cell internal reserves and/or hardly degradable external COD, named here as “ultra-slow” degradable COD  $X_{US}$  and (ii) the net decay of active biomass;
- Based on recent publications, it can be assumed that these findings are transferrable to activated sludge systems;
- The findings have practical consequences for aerobic biologic reactors suffering from long starvation conditions: (i) they should survive those conditions better than commonly presumed, (ii) biomass production is larger and aeration demand is lower than commonly presumed.

These findings seem to unmask a so far not relevant simplification of biological processes leading to knowledge a gap between reality and the model (Hauduc et al., 2013). It became only evident here, due to the changed viewpoint of a new treatment challenge: intermittent runoff with high organic pollution. However, other investigations with activated sludge show similar findings (Friedrich et al., 2016), too. It should be worthwhile to revise the current approaches before extrapolating it to uninvestigated operational conditions.

## Supplementary Material

General, a zero-order rate expression  $r_F$  can be seen as a product of a rate constant  $k_{0,F}$  and active biomass  $X_H$  (Morgenroth, 2008). If no substrate is present, this rate expression equals the endogenous oxygen uptake rate  $OUR_e$ :

$$r_F = k_{0,F} \cdot X_H = OUR_e \text{ [g} \cdot \text{m}^{-3} \cdot \text{d}^{-1}] \quad 32$$

With this in mind, a critical characteristic length  $L_{crit}$  of the biofilm can be expressed with Equation 33. For a detailed derivation of the equations, see (Morgenroth, 2008).

$$L_{crit} = \sqrt{\frac{D_F}{OUR_e}} \text{ [mm]} \quad 33$$

With  $D_F$  as diffusion coefficient in the biofilm [ $\text{m}^2 \cdot \text{d}^{-1}$ ]. For oxygen, the  $D_F$  can be set as  $2.1 \cdot 10^{-4} \text{m}^2 \cdot \text{d}^{-1}$ . Regarding typical  $OUR_e$  within the monitored range of  $18\text{--}2 \text{ g} \cdot \text{m}^{-3} \cdot \text{d}^{-1}$ , a critical length  $L_{crit}$  of  $1.0\text{--}1.9 \text{ mm}$  results. The used biofilm carrier showed a biofilm thickness  $L_F$  of  $6.0\text{--}8.0 \text{ mm}$ . Therefore, the quotient  $L_F/L_{crit}$  is above 4, which is indicating a mass transport limitation within the biofilm (Morgenroth, 2008). The penetration depth  $\beta L_F$  is expressed with Equation 34:

$$\beta L_F = \sqrt{\frac{2 \cdot C_{O_2} \cdot D_F}{k_0 \cdot X_H}} \text{ [mm]} \quad 34$$

With  $C_{O_2}$  [ $\text{g} \cdot \text{m}^{-3}$ ] as concentration in the liquid phase, here oxygen. Again, replacing the rate expression with the oxygen uptake rate results in Equation 35:

$$\beta L_F = \sqrt{\frac{2 \cdot C_{O_2} \cdot D_F}{OUR_e}} \text{ [mm]} \quad 35$$

The range of oxygen during the aerobic batch experiments was between  $2$  and  $4 \text{ g} \cdot \text{m}^{-3}$ . The comparison of biofilm thickness and oxygen penetration is presented in Fig. 46. Concerning a decrease of the endogenous  $OUR$  with time due to a degradation of  $X_H$ , the oxygen penetration depth slightly increases with time. However, there is still a gap of  $1.5 \text{ mm}$  between oxygen penetration and minimal biofilm thickness which can be seen as anaerobic.

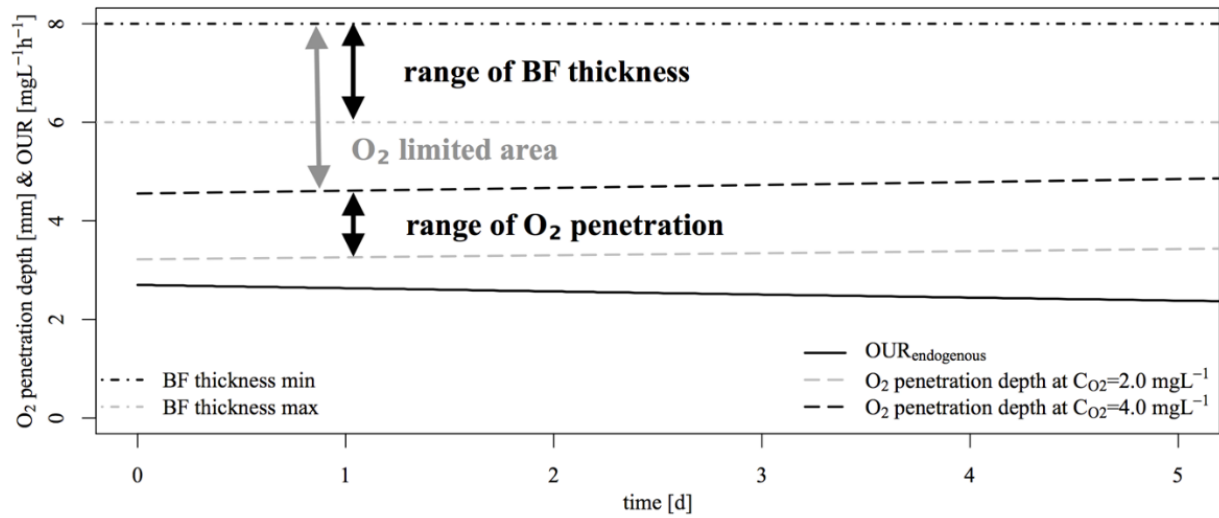


Fig. 46: Diffusion limitation with respect of oxygen penetration into the biofilm.

## 6 Summary

### 6.1 FINAL CONCLUSION

The regulatory standards in Germany regarding stormwater runoff was discussed in chapter 1.2. The study of this specific stormwater runoff gave many insights. Unlike stormwater as described in the previously accepted standards and our initial considerations, this runoff has a high percentage of N and P in addition to a possibly very high COD load. During this research project, a new ad-hoc-working group was initiated by the Country-Working-Group-Water (German LAWA) to meet these insights and to create a new awareness regarding stormwater runoff from silo facilities (LAWA, 2018). The final report from the ad-hoc-working-group pointed out the real danger of this stormwater runoff from silo facilities and indicated a strict distinction to stormwater runoff as describes in the currently accepted rules and regulations (see (DWA-A-102-1, 2020; DWA-M-153, 2007)). Moreover, an efficient operation and management of silo plants for the reduction of the pollution load was shown pictorially. However, there was a lack of possible technical treatment options and discussion of potential future regulations of the effluent standards.

From both an economic and environmental perspective, a silo management is required. A smart silo management should insist on a deep awareness of the two different water flows, the energetically highly potential silage effluent and the medium to highly loaded stormwater runoff. Though, an adequate separation of these water flows during daily operations is a challenge. Regular cleaning and sweeping are strongly recommended since it noticeably reduces the stormwater runoff load. Depending on the moisture content of the stored raw material, an additional wet cleaning procedure from time to time provide a deep cleaning where the surface cleaning with a dry sweeper fails. However, these cleaning procedures can only reduce the problem and a treatment is still necessary as no area can be regarded as clean.

This thesis showed the biological treatability of stormwater runoff from silo facilities. Though, the runoff showed good degradation ability of the contaminants and low inert fraction there are yet no official discharge limits for this specific wastewater. This work may help to define one by the authorities.

However, small rain events after long dry periods are problematic. The first flush is often heavily contaminated, and if not enough medium to low polluted runoff follows, the discharge can show quite high COD concentrations ( $>200 \text{ mg} \cdot \text{L}^{-1}$ ) after treatment even

with a degradation efficiency of over 98%. Here the question arises if discharge limits as known from domestic wastewater treatment plants are the right way to go or if the predefinition of technical standards would be a better solution.

It appeared that under specific circumstances approach of the ASM is not sufficient to describe real life of microorganism, resulting from a simplification. This simplification of biological processes consequently lead to uncertainties in the modelling (Hauduc et al., 2013). However, it could be shown that the approach of decay in the ASM is rather a sum parameter of a “base” decay rate and degradation. For this newly introduced fraction, two possible approaches for extending the existing ASM are presented in this thesis. Firstly, a two-step hydrolysis of an additional external substrate ensures a substrate supply at the time of need as soon as all storage fractions are degraded. Second, an additional cell internal fraction is permanently degraded but with rather high kinetic with respect to the decay kinetic. Both concepts can improve the decay approach of the commonly used ASM as they particularly better describe the first rapid degradation.

## 6.2 PERSPECTIVE

### 6.2.1 IMPLEMENTATION OF A TREATMENT SYSTEM

The proposed treatment concept is in direct competition with application to the field. The case of field application requires a sufficiently large retention basin volume, considering that it is not possible to apply throughout the full year. Implementing a treatment system or using field application as a proper solution is therefore a matter of costs. The further away the field is or the farmer has no access to it in the first place, the more profitable it is to treat it on site. Though, the evaluation standards and treatment systems for stormwater used in urban runoff do not apply due to the different characteristics of stormwater in this case. The treatment concept has to face with high amounts of nutrients, depending on the stored raw matter. Furthermore, for implementing a treatment system, a separation of the highly polluted silage runoff and low to medium polluted stormwater runoff is strongly recommended and would significantly reduce the treatment costs. Appropriate treatment, however, involves embedding biological treatment in a meaningful holistic concept, similar to a combined sewer system with stormwater overflow basins (Tränckner, 2019). In addition, appropriate regulations must be introduced or adapted to reflect the state of the art.



### 6.2.2 RESEARCH AND DEVELOPMENT

For deriving general dimensioning approaches for the developed plant design, long-term monitoring of semi-technical or full-scale plants operating under real conditions on silo facilities is necessary. The duration should exceed a whole year to monitor seasonal influences on the biomass activity. These seasonal influences involve temperature and rain and snow fall events, respectively. Furthermore, other technology systems could also provide a certain capability to meet the requirements discussed above like retention soil filter and constructed wetlands, respectively. Both can face intermittent stormwater runoffs and adequately degrade COD and P could be restrained within limits. Though, denitrification is not straightforward with these systems.

The findings regarding a rethinking of biomass modelling refer to a specific substrate under specific circumstances like intermittent switching between starvation and highly loaded substrate inflow, operated with a newly developed plant design. In order to find international acceptance in the science community, these finds should be verified with domestic wastewater as this has been and is still extensively tested worldwide. Though, the question if the wave behavior of the respiration rate can be traced back to an additional internal storage fraction or external slow degradable fraction still remains.

## References

- AbwV-A1, 2004. Verordnung über Anforderungen an das Einleiten von Abwasser in Gewässer (Abwasserverordnung - AbwV) Anhang 1 Häusliches und kommunales Abwasser.
- Acosta, J.A., Faz, A., Kalbitz, K., Jansen, B., Martínez-Martínez, S., 2014. Partitioning of heavy metals over different chemical fraction in street dust of Murcia (Spain) as a basis for risk assessment. *J. Geochemical Explor.* 144, 298–305. <https://doi.org/10.1016/j.gexplo.2014.02.004>
- Alam, M.Z., Fakhru'l-Razi, A., Molla, A.H., 2003. Biosolids accumulation and biodegradation of domestic wastewater treatment plant sludge by developed liquid state bioconversion process using a batch fermenter. *Water Res.* 37, 3569–3578. [https://doi.org/10.1016/S0043-1354\(03\)00260-4](https://doi.org/10.1016/S0043-1354(03)00260-4)
- Barbosa, A.E., Fernandes, J.N., David, L.M., 2012. Key issues for sustainable urban stormwater management. *Water Res.* 46, 6787–6798. <https://doi.org/10.1016/j.watres.2012.05.029>
- Barnard, J., 1976. A review of biological phosphorus removal in the activated sludge process. *Water Sa* 2, 136–144.
- Buitrón, G., Moreno-Andrade, I., 2011. Biodegradation kinetics of a mixture of phenols in a sequencing batch moving bed biofilm reactor under starvation and shock loads. *J. Chem. Technol. Biotechnol.* 86, 669–674. <https://doi.org/10.1002/jctb.2566>
- Capodaglio, A.G., Callegari, A., 2016. Domestic wastewater treatment with a decentralized, simple technology biomass concentrator reactor. *J. Water, Sanit. Hyg. Dev.* 6, 507–510. <https://doi.org/10.2166/washdev.2016.042>
- Carvalho, L., Carrera, J., Chamy, R., 2002. Nitrifying activity monitoring and kinetic parameters determination in a biofilm airlift reactor by respirometry. *Biotechnol. Lett.* 24, 2063–2066.
- Cebollero, E., Reggiori, F., Kraft, C., 2012. Reticulophagy and ribophagy: Regulated degradation of protein production factories. *Int. J. Cell Biol.* 2012, 1–9. <https://doi.org/10.1155/2012/182834>
- Chen, Y., Randall, A.A., McCue, T., 2004. The efficiency of enhanced biological phosphorus removal from real wastewater affected by different ratios of acetic to propionic acid.

- Water Res. 38, 27–36. <https://doi.org/10.1016/j.watres.2003.08.025>
- Cheng, J., Yuan, Q., Youngchul, K., 2017. Evaluation of a first-flush capture and detention tank receiving runoff from an asphalt-paved road. *Water Environ. J.* 31, 410–417. <https://doi.org/10.1111/wej.12258>
- Cramer, M., Koegst, T., Tränckner, J., 2018. Multi-criterial evaluation of P-removal optimization in rural wastewater treatment plants for a sub-catchment of the Baltic Sea. *Ambio* 47. <https://doi.org/10.1007/s13280-017-0977-8>
- Cramer, Michael, Rinas, M., Kotzbauer, U., Tränckner, J., 2019a. Surface contamination of impervious areas on biogas plants and conclusions for an improved stormwater management. *J. Clean. Prod.* 217, 1–11. <https://doi.org/10.1016/j.jclepro.2019.01.087>
- Cramer, M., Tränckner, J., Kotzbauer, U., 2020. Kinetic of denitrification and enhanced biological phosphorous removal (EBPR) of a trickling filter operated in a sequence-batch-reactor-mode (SBR-TF). *Environ. Technol. (United Kingdom)* 1–10. <https://doi.org/10.1080/09593330.2019.1709564>
- Cramer, Michael, Tränckner, J., Kotzbauer, U., 2019b. Denitrification and Enhanced Biological Phosphorous Removal (EBPR) with a trickling filter operated in a sequence-batch-reactor-mode (SBR-TF). *Environ. Technol. (United Kingdom)*.
- Cramer, Michael, Tränckner, J., Schelhorn, P., Kotzbauer, U., 2019c. Degradation kinetics and COD fractioning of agricultural wastewaters from biogas plants applying biofilm respirometry. *Environ. Technol. (United Kingdom)*.
- Daigger, G.T., Boltz, J.P., 2011. Trickling Filter and Trickling Filter-Suspended Growth Process Design and Operation: A State-of-the-Art Review. *Water Environ. Res.* 83, 388–404. <https://doi.org/10.2175/106143010X12681059117210>
- Daigger, G.T., Grady, C.P.L., 1982. An assessment of the role of physiological adaptation in the transient response of bacterial cultures. *Biotechnol. Bioeng.* 24, 1427–1444. <https://doi.org/10.1002/bit.260240614>
- Deans, E.A., Svoboda, I.F., 1992. Aerobic Treatment of Silage Effluent Experiments. *Bioresour. Technol.* 40, 23–27.
- Deletic, A., Orr, D.W., 2005. Pollution Buildup on Road Surfaces. *J. Environ. Eng.* 131, 49–59. [https://doi.org/10.1061/\(ASCE\)0733-9372\(2005\)131:1\(49\)](https://doi.org/10.1061/(ASCE)0733-9372(2005)131:1(49))

- Di Trapani, D., Capodici, M., Cosenza, A., Di Bella, G., Mannina, G., Torregrossa, M., Viviani, G., 2011. Evaluation of biomass activity and wastewater characterization in a UCT-MBR pilot plant by means of respirometric techniques. *Desalination* 269, 190–197. <https://doi.org/10.1016/j.desal.2010.10.061>
- Dircks, K., Pind, P.F., Mosbæk, H., Henze, M., 1999. Yield determination by respirometry - The possible influence of storage under aerobic conditions in activated sludge 25, 69–74.
- Dold, P.L., Ekama, G., Marais, G. v. R., 1980. A General Model for the Activated Sludge Process. *Water Res. Public Heal. Eng.* 12, 47–77.
- Dulekgurgen, E., Doğruel, S., Karahan, Ö., Orhon, D., 2006. Size distribution of wastewater COD fractions as an index for biodegradability. *Water Res.* 40, 273–282. <https://doi.org/10.1016/j.watres.2005.10.032>
- DWA-A-102-1, 2020. Grundsätze zur Bewirtschaftung und Behandlung von Regenwetterabflüssen zur Einleitung in Oberflächengewässer – Teil 1: Allgemeines.
- DWA-A-138, 2005. Planung, Bau und Betrieb von Anlagen zur Versickerung von Niederschlagswasser.
- DWA-A-792, 2018. Technische Regel wassergefährdender Stoffe (TRwS) – Jauche-, Gülle- und Silagesickersaftanlagen (JGS-Anlagen).
- DWA-M-153, 2007. Handlungsempfehlungen zum Umgang mit Regenwasser.
- Egodawatta, P., Ziyath, A.M., Goonetilleke, A., 2013. Characterising metal build-up on urban road surfaces. *Environ. Pollut.* 176, 87–91. <https://doi.org/10.1016/j.envpol.2013.01.021>
- Ekama, G.A., Dold, P.L., Marais, G.R., 1986. Procedures for determining influent COD fractions and the maximum specific growth rate of heterotrophs in activated sludge systems. *Water Sci. Technol.* 18, 91–114. <https://doi.org/10.2166/wst.1986.0062>
- Ekama, G.A., Wentzel, M.C., 1999. Denitrification kinetics in biological N and P removal activated sludge systems treating municipal wastewaters. *Water Sci. Technol.* 39(6), 69–77.
- Faulkner, J.W., Zhang, W., Geohring, L.D., Steenhuis, T.S., 2011. Nutrient transport within three vegetative treatment areas receiving silage bunker runoff. *J. Environ.*

- Manage. 92, 587–595. <https://doi.org/10.1016/j.jenvman.2010.09.020>
- Fedje, K., 2015. Life Cycle Assessment of Phosphorus Sources from Phosphate ore and urban sinks : Sewage Sludge and MSW Incineration fly ash. *Int. J. Environ. Res.* 9, 133–140.
- Ferrai, M., Guglielmi, G., Andreottola, G., 2010. Environmental Modelling & Software Modelling respirometric tests for the assessment of kinetic and stoichiometric parameters on MBBR biofilm for municipal wastewater treatment. *Environ. Model. Softw.* 25, 626–632. <https://doi.org/10.1016/j.envsoft.2009.05.005>
- Fleck, L., Ferreira Tavares, M.H., Eyng, E., Orssatto, F., 2018. Optimization of the nitrification process of wastewater resulting from cassava starch production. *Environ. Technol.* (United Kingdom) 3330, 1–10. <https://doi.org/10.1080/09593330.2018.1472300>
- Friedrich, M., Jimenez, J., Pruden, A., Miller, J.H., Metch, J., Takács, I., 2017. Rethinking growth and decay kinetics in activated sludge - Towards a new adaptive kinetics approach. *Water Sci. Technol.* 75, 501–506. <https://doi.org/10.2166/wst.2016.439>
- Friedrich, M., Takacs, I., 2013. A new interpretation of endogenous respiration profiles for the evaluation of the endogenous decay rate of heterotrophic biomass in activated sludge. *Water Res.* 7. <https://doi.org/10.1016/j.watres.2013.06.043>
- Friedrich, M., Takács, I., Tränckner, J., 2016. Experimental Assessment of the Degradation of “Unbiodegradable” Organic Solids in Activated Sludge. *Water Environ. Res.* 88, 272–9. <https://doi.org/10.2175/106143016X14504669767779>
- Friedrich, M., Takács, I., Tränckner, J., 2015. Physiological adaptation of growth kinetics in activated sludge. *Water Res.* 85, 22–30. <https://doi.org/10.1016/j.watres.2015.08.010>
- Fuchsz, M., Kohlheb, N., 2015. Comparison of the environmental effects of manure- and crop-based agricultural biogas plants using life cycle analysis. *J. Clean. Prod.* 86, 60–66. <https://doi.org/10.1016/j.jclepro.2014.08.058>
- Galanos, E., Gray, K.R., Biddlestone, A.J., Thayanithy, K., 1995. The Aerobic Treatment of Silage Effluent: Effluent Characterization and Fermentation. *J. Agric. Eng. Res.*
- Gavrilescu, M., Macoveanu, M., 2000. Attached-growth process engineering in wastewater treatment. *Bioprocess Eng.* 23, 95–106. <https://doi.org/10.1007/s004490050030>

- Gebrehananna, M.M., Gordon, R.J., Madani, A., Vanderzaag, A.C., Wood, J.D., 2014. Silage effluent management: A review. *J. Environ. Manage.* 143. <https://doi.org/10.1016/j.jenvman.2014.04.012>
- Gikas, P., Livingston, A.G., 1997. Specific ATP and specific oxygen uptake rate in immobilized cell aggregates: Experimental results and theoretical analysis using a structured model of immobilized cell growth. *Biotechnol. Bioeng.* 55, 660–673. [https://doi.org/10.1002/\(SICI\)1097-0290\(19970820\)55:4<660::AID-BIT8>3.0.CO;2-F](https://doi.org/10.1002/(SICI)1097-0290(19970820)55:4<660::AID-BIT8>3.0.CO;2-F)
- Goel, R., Mino, T., Satoh, H., Matsuo, T., 1999. MODELING HYDROLYSIS PROCESSES CONSIDERING INTRACELLULAR. *Water Sci. Technol.* 39, 97–105. [https://doi.org/10.1016/S0273-1223\(98\)00779-3](https://doi.org/10.1016/S0273-1223(98)00779-3)
- Goonetilleke, A., Egodawatta, P., Kitchen, B., 2009. Evaluation of pollutant build-up and wash-off from selected land uses at the Port of Brisbane, Australia. *Mar. Pollut. Bull.* 58, 213–221. <https://doi.org/10.1016/j.marpolbul.2008.09.025>
- GRADY, C.P.L., SMETS, B.F., BARBEAU, D.S., 1996. VARIABILITY IN KINETIC PARAMETER ESTIMATES: A REVIEW OF POSSIBLE CAUSES AND A PROPOSED. *Water Res.* 30, 742–748.
- Gujer, W., Henze, M., Mino, T., Loosdrecht, M.C.M. Van, 1999a. Activated sludge model No. 3. *Water Sci. Technol.* [https://doi.org/10.1016/S0273-1223\(99\)00405-9](https://doi.org/10.1016/S0273-1223(99)00405-9)
- Gujer, W., Henze, M., Mino, T., Van Loosdrecht, M.C.M., 1999b. Activated sludge model no. 3. *Water Sci. Technol.* 39, 183--193.
- Haider, S., Svardal, K., Vanrolleghem, P.A., Kroiss, H., 2003. The effect of low sludge age on wastewater fractionation (SS, SI). *Water Sci. Technol.* 47, 203–209. <https://doi.org/10.2166/wst.2003.0606>
- Hauduc, H., Rieger, L., Oehmen, A., van Loosdrecht, M.C.M., Comeau, Y., Hédut, A., Vanrolleghem, P.A., Gillot, S., 2013. Critical review of activated sludge modeling: State of process knowledge, modeling concepts, and limitations. *Biotechnol. Bioeng.* 110, 24–46. <https://doi.org/10.1002/bit.24624>
- Helmreich, B., Hilliges, R., Schriewer, A., Horn, H., 2010. Runoff pollutants of a highly trafficked urban road - Correlation analysis and seasonal influences. *Chemosphere* 80, 991–997. <https://doi.org/10.1016/j.chemosphere.2010.05.037>
- Henrich, C.-D., Marggraff, M., 2013. Energy-efficient Wastewater Reuse – The

- Renaissance of Trickling Filter Technology. Proc. 9th Int. Conf. Water Reuse 27–31.
- Henze, M., Gujer, W., Van Loosdrecht, M.C.M., Mino, T., 2000. Activated sludge models ASM1, ASM2, ASM2d and ASM3. IWA Publ.
- Herbert, D., 1958. Recent progress in microbiology, in: Proc. 7th Int. Congr. Stockholm.
- Herngren, L., 2005. Build-up and wash-off process kinetics of PAHs and heavy metals on paved surfaces using simulated rainfall.
- Hocaoglu, S.M., Insel, G., Cokgor, E.U., Baban, A., Orhon, D., 2010. COD fractionation and biodegradation kinetics of segregated domestic wastewater: Black and grey water fractions. J. Chem. Technol. Biotechnol. 85, 1241–1249. <https://doi.org/10.1002/jctb.2423>
- Holly, M.A., Larson, R.A., 2016. TREATMENT OF SILAGE RUNOFF USING VEGETATED FILTER STRIPS. Am. Soc. Agric. Biol. Eng. 59, 1645–1650. <https://doi.org/10.13031/trans.59.11600>
- Holly, M.A., Larson, R.A., Cooley, E.T., Wunderlin, A.M., 2018. Silage storage runoff characterization: Annual nutrient loading rate and first flush analysis of bunker silos. Agric. Ecosyst. Environ. 264, 85–93. <https://doi.org/10.1016/j.agee.2018.05.015>
- Hood, M.A., Guckert, J.B., White, D.C., Deck, F., 1986. Effect of nutrient deprivation on lipid, carbohydrate, DNA, RNA, and protein levels in *Vibrio cholerae*. Appl. Environ. Microbiol. 52, 788–793. <https://doi.org/10.1128/aem.52.4.788-793.1986>
- Hu, Z.R., Wentzel, M.C., Ekama, G.A., 2002. Anoxic growth of phosphate-accumulating organisms (PAOs) in biological nutrient removal activated sludge systems. Water Res. 36, 4927–4937. [https://doi.org/10.1016/S0043-1354\(02\)00186-0](https://doi.org/10.1016/S0043-1354(02)00186-0)
- Huttunen, S., Manninen, K., Leskinen, P., 2014. Combining biogas LCA reviews with stakeholder interviews to analyse life cycle impacts at a practical level. J. Clean. Prod. 80, 5–16. <https://doi.org/10.1016/j.jclepro.2014.05.081>
- J. M. A. Stekar, 1998. Silage effluent and water pollution., in: Conference on Nutrition of Domestic Animals Zadravec-Erjavec Days.
- Juretschko, S., Timmermann, G., Schmid, M., Schleifer, K.H., Pommerening-Röser, A., Koops, H.P., Wagner, M., 1998. Combined molecular and conventional analyses of nitrifying bacterium diversity in activated sludge: *Nitrosococcus mobilis* and

- Nitrospira-like bacteria as dominant populations. *Appl. Environ. Microbiol.* 64, 3042–3051. <https://doi.org/10.1128/aem.64.8.3042-3051.1998>
- Kayhanian, M., Fruchtman, B.D., Gulliver, J.S., Montanaro, C., Ranieri, E., Wuertz, S., 2012. Review of highway runoff characteristics: Comparative analysis and universal implications. *Water Res.* 46, 6609–6624. <https://doi.org/10.1016/j.watres.2012.07.026>
- Khunjar, W.O., Pitt, P.A., Bott, C.B., Kartik, C., 2014. Nitrogen, in: *Activated Sludge-100 Years and Counting*. IWA publishing.
- Kuenen, J.G., B. B. Jorgensen, Revsbech, N.P., 1986. Oxygen Microprofiles of Trickling Filter Biofilms 20, 1589–1598.
- Kurland, G.C., Mikkola, R., 1993. The Impact of Nutritional State on the Microevolution of Ribosomes, Starvation in Bacteria, in: S. Kjelleberg (Ed.), *Plenum Press*. pp. 225–237.
- Kwok, W.K., Picioreanu, C., Ong, S.L., Van Loosdrecht, M.C.M., Ng, W.J., Heijnen, J.J., 1998. Influence of biomass production and detachment forces on biofilm structures in a biofilm airlift suspension reactor. *Biotechnol. Bioeng.* 58, 400–407. [https://doi.org/10.1002/\(SICI\)1097-0290\(19980520\)58:4<400::AID-BIT7>3.0.CO;2-N](https://doi.org/10.1002/(SICI)1097-0290(19980520)58:4<400::AID-BIT7>3.0.CO;2-N)
- Larson, R.A., Safferman, S.I., 2009. Storm water runoff characterization from animal feeding operations. *Am. Soc. Agric. Biol. Eng. Annu. Int. Meet. 2009, ASABE 2009 7*.
- LAWA, 2018. Abschlussbericht - Empfehlungen für den Umgang mit Niederschlagswasser von Biogasanlagen und von Fahrsilos in der Landwirtschaft. *LAWA Ad hoc AG Biogasanlagen 36*.
- Lazrak, A., Mandi, L., Djeni, T.N., Neffa, M., Ouazzani, N., 2018. Assessing biomass diversity and performance of an activated sludge process treating saline table olive processing wastewater. *Environ. Technol. (United Kingdom)* 0, 1–12. <https://doi.org/10.1080/09593330.2018.1447603>
- Leslie Grady, C.P., Daigger, G.T., 1999. *Biological wastewater treatment*.
- Li, Z.H., Zhu, Y.M., Zhang, Y.L., Zhang, Y.R., He, C.B., Yang, C.J., 2018. Characterization of aerobic granular sludge of different sizes for nitrogen and phosphorus removal. *Environ. Technol. (United Kingdom)* 0, 1–10. <https://doi.org/10.1080/09593330.2018.1483971>
- Lijó, L., González-García, S., Bacenetti, J., Fiala, M., Feijoo, G., Moreira, M.T., 2014.



- Assuring the sustainable production of biogas from anaerobic mono-digestion. *J. Clean. Prod.* 72, 23–34. <https://doi.org/10.1016/j.jclepro.2014.03.022>
- Livingston, A.G., Chase, H.A., 1989. Modeling Phenol Degradation in a Fluidized-Bed Bioreactor. *Am. Inst. Chem. Eng.* 35, 1980–1992. <https://doi.org/10.1002/aic.690351209>
- López-Vázquez, C.M., Hooijmans, C.M., Brdjanovic, D., Gijzen, H.J., Van Loosdrecht, M.C.M., 2008. Factors affecting the microbial populations at full-scale enhanced biological phosphorus removal (EBPR) wastewater treatment plants in The Netherlands. *Water Res.* 42, 2349–2360. <https://doi.org/10.1016/j.watres.2008.01.001>
- Lopez, C., Pons, M.N., Morgenroth, E., 2006. Endogenous processes during long-term starvation in activated sludge performing enhanced biological phosphorus removal. *Water Res.* 40, 1519–1530. <https://doi.org/10.1016/j.watres.2006.01.040>
- MacIntosh, G.C., Bassham, D.C., 2011. The connection between ribophagy, autophagy and ribosomal RNA decay. *Autophagy* 7, 662–663. <https://doi.org/10.4161/auto.7.6.15447>
- Majumder, P.S., Gupta, S.K., 2003. Hybrid reactor for priority pollutant nitrobenzene removal. *Water Res.* 37, 4331–4336. [https://doi.org/10.1016/S0043-1354\(03\)00436-6](https://doi.org/10.1016/S0043-1354(03)00436-6)
- Marais, G.v.R., Ekama, G.A., 1976. The activated sludge process Part 1 - steady state behaviour. *Water Sa* 2, 163–200.
- Marais, G. v. R., Ekama, G.A., 1976. The activated sludge process – part I: Steady state behaviour. *Water Sa* 2, 163–200. <https://doi.org/10.1007/s41742-017-0037-z>
- Martiny, A.C., Albrechtsen, H., Arvin, E., Molin, S., 2005. Identification of Bacteria in Biofilm and Bulk Water Samples from a Nonchlorinated Model Drinking Water Distribution System: Detection of a Large Nitrite-Oxidizing Population Associated with *Nitrospira* spp. *Appl. Environ. Microbiol.* 71, 8611–8617. <https://doi.org/10.1128/AEM.71.12.8611>
- Matsumoto, S., Terada, A., Tsuneda, S., 2007. Modeling of membrane-aerated biofilm: Effects of C / N ratio, biofilm thickness and surface loading of oxygen on feasibility of simultaneous nitrification and denitrification. *Biochem. Eng. J.* 37, 98–107. <https://doi.org/10.1016/j.bej.2007.03.013>
- McCarty, P.L., Bae, J., Kim, J., 2011. Domestic wastewater treatment as a net energy producer-can this be achieved? *Environ. Sci. Technol.* 45, 7100–7106.

<https://doi.org/10.1021/es2014264>

- McKinney, R.E., 1960. Complete mixing activated sludge. *Water Sew. Work.* 107, 69.
- Metcalf, E., Eddy, M., 2014. *Wastewater engineering: treatment and Resource recovery*, Mic Graw-Hill, USA.
- Moisio, T., 1994. Lactic acid fermentation in silage preserved with formic acid. *Anim. Feed Sci. Technol.* 47, 107–124.
- Morgenroth, E., 2008. Modelling Biofilms, in: Henze, M., van Loosdrecht, M.C.M., Ekama, G.A., Brdjanovic, D. (Eds.), *Biological Wastewater Treatment: Principles, Modelling and Design*. pp. 456–492.
- Morita, R.Y., 1993. Bioavailability of energy and the starvation state, in: Springer. Boston, pp. 1–23.
- Murphy, L.U., Cochrane, T.A., O’Sullivan, A., 2015. Build-up and wash-off dynamics of atmospherically derived Cu, Pb, Zn and TSS in stormwater runoff as a function of meteorological characteristics. *Sci. Total Environ.* 508, 206–213. <https://doi.org/10.1016/j.scitotenv.2014.11.094>
- Naz, I., Saroj, D.P., Mumtaz, S., Ali, N., Ahmed, S., 2015. Assessment of biological trickling filter systems with various packing materials for improved wastewater treatment. *Environ. Technol. (United Kingdom)* 36, 424–434. <https://doi.org/10.1080/09593330.2014.951400>
- Nielsen, P.H., McMahon, K.D., 2014. Microbiology and microbial ecology of the activated sludge process, in: *Activated Sludge–100 Years and Counting*. pp. 53–75.
- Nourmohammadi, D., Esmaeeli, M.B., Akbarian, H., Ghasemian, M., 2013. Nitrogen removal in a full-scale domestic wastewater treatment plant with activated sludge and trickling filter. *J. Environ. Public Health* 2013, 6. <https://doi.org/10.1155/2013/504705>
- Obaja, D., MacÉ, S., Mata-Alvarez, J., 2004. Biological nutrient removal by a sequencing batch reactor (SBR) using an internal organic carbon source in digested piggery wastewater. *Bioresour. Technol.* 96, 7–14. <https://doi.org/10.1016/j.biortech.2004.03.002>
- Oehmen, A., Lemos, P.C., Carvalho, G., Yuan, Z., Keller, J., Blackall, L.L., Reis, M.A.M., 2007. Advances in enhanced biological phosphorus removal: From micro to macro

- scale. *Water Res.* 41, 2271–2300. <https://doi.org/10.1016/j.watres.2007.02.030>
- Ordaz, A., Oliveira, C.S., Quijano, G., Ferreira, E.C., Alves, M., Thalasso, F., 2012. Kinetic and stoichiometric characterization of a fixed biofilm reactor by pulse respirometry. *J. Biotechnol.* 157, 173–179. <https://doi.org/10.1016/j.jbiotec.2011.10.015>
- Pacetti, T., Lombardi, L., Federici, G., 2015. Water-energy Nexus: A case of biogas production from energy crops evaluated by Water Footprint and Life Cycle Assessment (LCA) methods. *J. Clean. Prod.* 101, 1–14. <https://doi.org/10.1016/j.jclepro.2015.03.084>
- Petersen, B., Gernaey, K., Henze, M., Vanrolleghem, P.A., 2003. CALIBRATION OF ACTIVATED SLUDGE MODELS: A CRITICAL REVIEW OF EXPERIMENTAL DESIGNS PETERSEN. *Biotechnol. Environ. Wastewater Treat. Model. waste gas Handl.* 101–186.
- Poeschl, M., Ward, S., Owende, P., 2012. Environmental impacts of biogas deployment - Part II: Life Cycle Assessment of multiple production and utilization pathways. *J. Clean. Prod.* 24, 184–201. <https://doi.org/10.1016/j.jclepro.2011.10.030>
- Ramdani, A., Dold, P.L., Délérís, S., Lamarre, D., Gadbois, A., Comeau, Y., 2010. Biodegradation of the endogenous residue of activated sludge. *Water Res.* 44, 2179–2188. <https://doi.org/10.1016/j.watres.2009.12.037>
- Ramírez-Arpide, F.R., Demirer, G.N., Gallegos-Vázquez, C., Hernández-Eugenio, G., Santoyo-Cortés, V.H., Espinosa-Solares, T., 2018. Life cycle assessment of biogas production through anaerobic co-digestion of nopal cladodes and dairy cow manure. *J. Clean. Prod.* 172, 2313–2322. <https://doi.org/10.1016/j.jclepro.2017.11.180>
- Ravina, M., Genon, G., 2015. Global and local emissions of a biogas plant considering the production of biomethane as an alternative end-use solution. *J. Clean. Prod.* 102, 115–126. <https://doi.org/10.1016/j.jclepro.2015.04.056>
- Riefler, R.G., Ahlfeld, D.P., Smets, B.F., 1998. Respirometric Assay for Biofilm Kinetics Estimation: Parameter Identifiability and Retrievability. *Biotechnol. Bioeng.* 57. [https://doi.org/https://doi.org/10.1002/\(SICI\)1097-0290\(19980105\)57:1<35::AID-BIT5>3.0.CO;2-W](https://doi.org/https://doi.org/10.1002/(SICI)1097-0290(19980105)57:1<35::AID-BIT5>3.0.CO;2-W)
- Seviour, R.J., Mino, T., Onuki, M., 2003. The microbiology of biological phosphorus removal in activated sludge systems. *FEMS Microbiol. Rev.* 27, 99–127.

[https://doi.org/10.1016/S0168-6445\(03\)00021-4](https://doi.org/10.1016/S0168-6445(03)00021-4)

- Siegrist, H., Rieger, L., Koch, G., Kühni, M., Gujer, W., 2002. The EAWAG Bio-P module for activated sludge model No. 3. *Water Sci. Technol.* 45, 61–76. [https://doi.org/10.1016/S0043-1354\(01\)00110-5](https://doi.org/10.1016/S0043-1354(01)00110-5)
- Spanjers, H., Vanrolleghem, P., 1995. Respirometry as a tool for rapid characterization of wastewater and activated sludge. *Water Sci. Technol.* [https://doi.org/10.1016/0273-1223\(95\)00184-O](https://doi.org/10.1016/0273-1223(95)00184-O)
- Spanjers, H., Vanrolleghem, P., Olsson, G., Dold, P.L., 1996. Respirometry in control of the activated sludge process. *Water Sci. Technol.* 34, 117–126. [https://doi.org/10.1016/0273-1223\(96\)84211-9](https://doi.org/10.1016/0273-1223(96)84211-9)
- Spérandio, M., Etienne, P., 2000. Estimation of wastewater biodegradable COD fractions by combining respirometric experiments in various So/Xo ratios. *Water Res.* 34, 1233–1246. [https://doi.org/10.1016/S0043-1354\(99\)00241-9](https://doi.org/10.1016/S0043-1354(99)00241-9)
- Sung, H.N., Katsou, E., Statiris, E., Anguilano, L., Malamis, S., 2019. Operation of a modified anaerobic baffled reactor coupled with a membrane bioreactor for the treatment of municipal wastewater in Taiwan. *Environ. Technol. (United Kingdom)* 40, 1233–1238. <https://doi.org/10.1080/09593330.2017.1420102>
- Torà, J.A., Lafuente, J., Baeza, J.A., Carrera, J., 2011. Long-term starvation and subsequent reactivation of a high-rate partial nitrification activated sludge pilot plant. *Bioresour. Technol.* 102, 9870–9875. <https://doi.org/10.1016/j.biortech.2011.08.008>
- Tränckner, J., 2019. 12. Rostocker Abwasertagung, in: *Niederschlagswasser Auf Landwirtschaftlichen Betriebshöfen Und Biogasanlagen*. pp. 99–116.
- Tränckner, J., 2018. Workshop „Niederschlagswasser auf Biogasanlagen“. *Korrespondenz Abwasser* 65, 508–510.
- Tränckner, J., Wricke, B., Krebs, P., 2008. Estimating nitrifying biomass in drinking water filters for surface water treatment. *Water Res.* 42, 2574–2584. <https://doi.org/10.1016/j.watres.2008.01.007>
- Van Haandel, A., Van Der Lubbe, J., 2007. Handbook biological waste water treatment-design and optimisation of activated sludge systems. *Webshop Wastewater Handbook*.
- Van Haandel, A.C., Catunda, P.F.C., De Souza Araújo, L., 1998. Biological sludge

- stabilisation Part 1: Kinetics of aerobic sludge digestion. *Water SA* 24, 223–230.
- Van Loosdrecht, M.C.M., Kuba, T., Brandse, F.A., Heijnen, J.J., 1997. Occurrence of denitrifying phosphorus removing bacteria in modified UCT-type wastewater treatment plants. *Water Res.* 31, 777–786. [https://doi.org/10.1016/S0043-1354\(96\)00370-3](https://doi.org/10.1016/S0043-1354(96)00370-3)
- Van Loosdrecht, M.C.M., Lyklema, J., Norde, W., Zehnder, A.J.B., 1990. Influence of Interfaces Microbial Activity 54, 75–87.
- Vázquez-López, M., Amabilis-Sosa, L.E., Moeller-Chávez, G.E., Roé-Sosa, A., Neumann, P., Vidal, G., 2019. Evaluation of the ultrasound effect on treated municipal wastewater. *Environ. Technol. (United Kingdom)* 40, 3568–3577. <https://doi.org/10.1080/09593330.2018.1481889>
- Virdis, B., Read, S.T., Rabaey, K., Rozendal, R.A., Yuan, Z., Keller, J., 2011. Biofilm stratification during simultaneous nitrification and denitrification ( SND ) at a biocathode. *Bioresour. Technol.* 102, 334–341. <https://doi.org/10.1016/j.biortech.2010.06.155>
- Völker, J., Mohaupt, V., Emde, F.A., 2016. The Water Framework Directive - Germanys Water Bodies 2015. Fed. Environ. Agency.
- Wang, S., He, Q., Ai, H., Wang, Z., Zhang, Q., 2013. Pollutant concentrations and pollution loads in stormwater runoff from different land uses in Chongqing. *J. Environ. Sci. (China)* 25, 502–510. [https://doi.org/10.1016/S1001-0742\(11\)61032-2](https://doi.org/10.1016/S1001-0742(11)61032-2)
- Wanner, J., Kucman, K., Grau, P., 1988. Activated sludge process combined with biofilm cultivation. *Water Res.* 22, 207–215. [https://doi.org/10.1016/0043-1354\(88\)90080-2](https://doi.org/10.1016/0043-1354(88)90080-2)
- Wanner, O., Gujer, W., 1986. A Multispecies Biofilm Model. *Biotechnol. Bioeng.* 28, 314–328.
- Wanner, O., Morgenroth, E., 2004. Biofilm modeling with AQUASIM. *Water Sci. Technol.* 49, 137–144. <https://doi.org/10.2166/wst.2004.0824>
- Wheaton, F.W., Hochheimer, J.N., Kaiser, G.E., Malone, R.F., Krones, M.J., Libey, G.S., Timmons, M.B., 1994. Nitrification filter design methods. *Dev. Aquacult. fish. sci* 27, 127–171.
- White, D., 2000. Physiology and biochemistry of prokaryotes. Oxford University Press.

- Wicke, D., Cochrane, T.A., O'Sullivan, A., 2012. Build-up dynamics of heavy metals deposited on impermeable urban surfaces. *J. Environ. Manage.* 113, 347–354. <https://doi.org/10.1016/j.jenvman.2012.09.005>
- Wik, T., 2003. Trickling filters and biofilm reactor modelling. *Rev. Environ. Sci. Biotechnol.* 2, 193–212. <https://doi.org/10.1023/B:RESB.0000040470.48460.bb>
- Ye, L., Hu, S., Poussade, Y., Keller, J., Yuan, Z., 2012. Evaluating a strategy for maintaining nitrifier activity during long-term starvation in a moving bed biofilm reactor (MBBR) treating reverse osmosis concentrate. *Water Sci. Technol.* 66, 837–842. <https://doi.org/10.2166/wst.2012.252>
- Yilmaz, G., Lemaire, R., Keller, J., Ā, Z.Y., 2007. Effectiveness of an alternating aerobic , anoxic / anaerobic strategy for maintaining biomass activity of BNR sludge during long-term starvation. *Water Res.* 41, 2590–2598. <https://doi.org/10.1016/j.watres.2007.02.011>
- Zhang, J., Hua, P., Krebs, P., 2016. Chemosphere The influences of dissolved organic matter and surfactant on the desorption of Cu and Zn from road-deposited sediment. *Chemosphere* 150, 63–70. <https://doi.org/10.1016/j.chemosphere.2016.02.015>
- Zhang, J., Hua, P., Krebs, P., 2015. The build-up dynamic and chemical fractionation of Cu , Zn and Cd in road-deposited sediment. *Sci. Total Environ.* 532, 723–732. <https://doi.org/10.1016/j.scitotenv.2015.06.074>
- Zhang, J., Krebs, P., 2013. Comments on “ Characterising metal build-up on urban road surfaces ” by Egodawatta et al . ( 2013 ). *Environmental Pollution* 176 , 87 – 91. *Environ. Pollut.* 182, 500–502. <https://doi.org/10.1016/j.envpol.2013.07.009>
- Zhang, L.H., Meng, X.L., Wang, Y., Liu, L.D., 2009. Performance of biotrickling filters for hydrogen sulfide removal under starvation and shock loads conditions. *J. Zhejiang Univ. Sci. B* 10, 595–601. <https://doi.org/10.1631/jzus.B0920064>

## Curriculum vitae

### Personal

Name	Michael Cramer
Citizenship	German
Born	03.07.1985
Family	unmarried
Languages	German, English

### Education

SDU Odense	09/2014-03/2015	Chemical engineering
University of Rostock	04/2013-08/2014	Environmental engineering
University of Wismar	09/2009-04/2013	Process engineering
University of Rostock	09/2006-04/2009	Economics

### Professional work

PNC	Since 09/2019	Separation of manure into a Phosphorous, Nitrogen and Carbon fraction
ZKA HRO	Since 09/2019	Capacity consideration of the wastewater treatment plant of Rostock
ProBeNeBio	01/2017-09/2019	Prototyping of a treatment system for stormwater runoff from silo facilities
TMBR	06/2015-12/2016	Optimization of a thermophilic membrane bio reactor for wastewater treatment of a paper mil

## Scientific work

Water	2020	Development of Decay in Biofilms under Starvation Conditions — Rethinking of the Biomass Model
Environmental Technology	2019	Degradation kinetics and COD fractioning of agricultural wastewaters from biogas plants applying biofilm respirometry
Environmental Technology	2019	Kinetic of denitrification and enhanced biological phosphorous removal (EBPR) of a trickling filter operated in a sequence-batch-reactor-mode (SBR-TF)
Journal of Cleaner Production	2019	Surface contamination of impervious areas on biogas plants and conclusions for an improved stormwater
SIMBA-Anwendertreffen	2018	Anfall und Belastung von Niederschlagswasser einer Biogasanlage - Konsequenzen für den Anlagenbetrieb und die Behandlung
Ambio	2017	Multi-criterial evaluation of P-removal optimization in rural wastewater treatment plants for a sub-catchment of the Baltic Sea
IWA Conference proceeding, Athen	2016	Cost-efficient Phosphorus removal in rural WWTP Accurately Specify Subject of Paper
Journal of Water Process Engineering	2016	Optimization and fouling mechanism of a thermophile submerged MBR (TSMBR) pilot plant for wastewater treatment in a paper mill



## **In dieser Reihe bisher erschienen**

### **Band I**

10. DIALOG Abfallwirtschaft MV

– Von der Abfallwirtschaft zur Energiewirtschaft.

*Tagungsband, erschienen im Juni 2007, ISBN 987-3-86009-004-6*

### **Band II**

Ellen-Rose Trübger

Entwicklung eines Ansatzes zur Berücksichtigung der ungesättigten Zone bei der Grundwassersimulation von Feuchtgebieten.

*Dissertation, erschienen im August 2007, ISBN 978-3-86009-006-0*

### **Band III**

René Dechow

Untersuchungen verschiedener Ansätze der Wasserhaushalts- und Stofftransportmodellierung hinsichtlich ihrer Anwendbarkeit in Stickstoffhaushaltsmodellen.

*Dissertation, erschienen im September 2007, ISBN 978-3-86009-016-9*

### **Band IV**

Carolin Wloczyk

Entwicklung und Validierung einer Methodik zur Ermittlung der realen Evapotranspiration anhand von Fernerkundungsdaten in Mecklenburg-Vorpommern.

*Dissertation, erschienen im September 2007, ISBN 978-3-86009-009-1*

### **Band 5**

1. Rostocker Bioenergieforum.

Bioenergieland Mecklenburg-Vorpommern.

*Tagungsband, erschienen im Oktober 2007, ISBN 978-3-86009-013-8*

### **Band 6**

Kulturtechniktagung 2007.

Ostseeverseuchung und Flächenentwässerung.

*Tagungsband, erschienen im Januar 2008, ISBN 978-3-86009-018-3*

### **Band 7**

Enrico Frahm

Bestimmung der realen Evapotranspiration für Weide (*Salix* spp.) und Schilf (*Phragmites australis*) in einem nordostdeutschen Flusstalmoor.

*Dissertation, erschienen im Mai 2008, ISBN 978-3-86009-023-7*

## **Band 8**

Jenny Haide

Methode zur Quantifizierung der Einflüsse auf Vorgangsdauern lohnintensiver Arbeiten am Beispiel von Pflasterarbeiten.

*Dissertation, erschienen im Juni 2008, ISBN 978-3-86009-024-4*

## **Band 9**

11. DIALOG Abfallwirtschaft MV

Chancen und Risiken für die deutsche Abfallwirtschaft im Ausland.

*Tagungsband, erschienen im Juni 2008, ISBN 978-3-86009-029-9*

## **Band 10**

Stefan Cantré

Ein Beitrag zur Bemessung geotextiler Schläuche für die Entwässerung von Baggergut.

*Dissertation, erschienen im Juni 2008, ISBN 978-3-86009-032-9*

## **Band 11**

Birgit Wüstenberg

Praxis der Standortwahl von Sportboothäfen im Küstenbereich Mecklenburg-Vorpommerns und Entwicklung einer Bewertungsmethode als Planungshilfe.

*Dissertation, erschienen im Juli 2008, ISBN 978-3-86009-033-6*

## **Band 12**

André Clauß

Erhöhung der Trinkwasserversorgungssicherheit in Havarie- und Krisensituationen durch neue Handlungsalgorithmen sowie Einbeziehung bisher ungenutzter Ressourcen am Beispiel von Bergbaugrubenwasser.

*Dissertation, erschienen im September 2008, ISBN 978-3-86009-037-4*

## **Band 13**

Peter Degener

Sickerwasserkreislauf zur Behandlung von Sickerwässern der aerob-biologischen Restabfallbehandlung (Restabfallrotte).

*Dissertation, erschienen im Oktober 2008, ISBN 978-3-86009-043-5*

## **Band 14**

2. Rostocker Bioenergieforum

Innovationen für Klimaschutz und wirtschaftliche Entwicklung.

*Tagungsband, erschienen im Oktober 2008, ISBN 978-3-86009-044-2*

## **Band 15**

7. Rostocker Abwassertagung

Fortschritte auf dem Gebiet der Abwasserentsorgung.

*Tagungsband, erschienen im November 2008, ISBN 978-3-86009-045-9*

**Band 16**

Christian Noß

Strömungsstrukturen kleiner naturnaher Fließgewässer unter Berücksichtigung von Turbulenztheorie und Dispersionsmodellen.

*Dissertation, erschienen im Januar 2009, ISBN 978-3-86009-054-1*

**Band 17**

Ralf Schröder

Entwicklung von Möglichkeiten zur Messung der N<sub>2</sub>-Übersättigung sowie Methoden zur Reduzierung der Schwimmschlamm Bildung.

*Dissertation, erschienen im Februar 2009, ISBN 978-3-86009-055-8*

**Band 18**

Elmar Wisotzki

Bodenverfestigungen mit Kalk-Hüttensand-Gemischen.

*Dissertation, erschienen im April 2009, ISBN 978-3-86009-059-6*

**Band 19**

Ramez Mashkour

Untersuchungen zur Adsorption und biologischen Aktivität an Aktivkohlefilter unter den Bedingungen der Wasseraufbereitung im Wasserwerk Rostock.

*Dissertation, erschienen im April 2009, ISBN 978-3-86009-060-2*

**Band 20**

Torsten Birkholz

Handlungserfordernisse und Optimierungsansätze für kommunale Ver- und Entsorgungsunternehmen im Zusammenhang mit demografischen Veränderungen im ländlichen Raum aufgezeigt an einem Beispiel in Mecklenburg-Vorpommern.

*Dissertation, erschienen im Mai 2009, ISBN 978-3-86009-061-9*

**Band 21**

12. DIALOG Abfallwirtschaft MV

Aktuelle Entwicklungen in der Abfallwirtschaft.

*Tagungsband, erschienen im Juni 2009, ISBN 978-3-86009-062-6*

**Band 22**

Thomas Fritz

Entwicklung, Implementierung und Validierung eines praxisnahen Verfahrens zur Bestimmung von Biogas- bzw. Methanerträgen.

*Dissertation, erschienen im Oktober 2009, ISBN 978-3-86009-065-7*

**Band 23**

3. Rostocker Bioenergieforum

Bioenergie – Chance und Herausforderung für die regionale und globale Wirtschaft.

*Tagungsband, erschienen im Oktober 2009, ISBN 978-3-86009-065-8*

**Band 24**

Muhammad Mariam

Analyse von Gefahrenpotenzialen für die Trinkwasserversorgung der Stadt Rostock unter besonderer Berücksichtigung von Schadstoffausbreitungsvorgängen in der Warnow.

*Dissertation, erschienen im Februar 2010, ISBN 978-3-86009-078-7*

**Band 25**

Manja Steinke

Untersuchungen zur Behandlung von Abwässern der Fischverarbeitungsindustrie.

*Dissertation, erschienen im Juni 2010, ISBN 978-3-86009-085-5*

**Band 26**

13. DIALOG Abfallwirtschaft MV

Die Kreislauf- und Abfallwirtschaft im Wandel. Wohin gehen die rechtlichen und technischen Entwicklungen?

*Tagungsband, erschienen im Juni 2010, ISBN 978-3-86009-087-9*

**Band 27**

4. Rostocker Bioenergieforum

Zukunftstechnologien für Bioenergie

*Tagungsband, erschienen im Oktober 2010, ISBN 978-3-940364-12-8*

**Band 28**

Dirk Banemann

Einfluss der Silierung und des Verfahrensablaufs der Biomassebereitstellung auf den Methanertrag unter Berücksichtigung eines Milchsäurebakteriensilierungsmittel

*Dissertation, erschienen im Januar 2011, ISBN 978-3-86009-087-9*

**Band 29**

14. DIALOG Abfallwirtschaft MV

Abfall als Wertstoff- und Energiereserve

*Tagungsband, erschienen im Juni 2011, ISBN 978-3-940364-18-0*

**Band 30**

5. Rostocker Bioenergieforum

*Tagungsband, erschienen im November 2011, ISBN 978-3-940364-20-3*

**Band 31**

8. Rostocker Abwassertagung

Erhöhung der Effektivität von Abwasserentsorgungsanlagen

*Tagungsband, erschienen im November 2011, ISBN 978-3-86009-120-3*

**Band 32**

6. Rostocker Bioenergieforum

*Tagungsband, erschienen im Juni 2012, ISBN 978-3-940364-27-2*

**Band 33**

Ishan Machlouf

Untersuchungen zur Nitratelimination bei der Trinkwasseraufbereitung unter Berücksichtigung syrischer Verhältnisse

*Dissertation, erschienen im März 2013, ISBN 978-3-86009-204-0*

**Band 34**

Ralph Sutter

Analyse und Bewertung der Einflussgrößen auf die Optimierung der

Rohbiogasproduktion hinsichtlich der Konstanz von Biogasqualität und -menge

*Dissertation, erschienen im März 2013, ISBN 978-3-86009-202-6*

**Band 35**

Wolfgang Pfaff-Simoneit

Entwicklung eines sektoralen Ansatzes zum Aufbau von nachhaltigen Abfallwirtschaftssystemen in Entwicklungsländern vor dem Hintergrund von Klimawandel und Ressourcenverknappung

*Dissertation, erschienen im Mai 2013, ISBN 978-3-86009-203-3*

**Band 36**

7. Rostocker Bioenergieforum

*Tagungsband, erschienen im Juni 2013, ISBN 978-3-86009-207-1*

**Band 37**

Markus Helftewes

Modellierung und Simulation der Gewerbeabfallaufbereitung vor dem Hintergrund der Outputqualität, der Kosteneffizienz und der Klimabilanz

*Dissertation, erschienen im Oktober 2013, ISBN 978-3-86009-402-0*

**Band 38**

Jan Stefan Riha

Detektion und Quantifizierung von Cyanobakterien in der Ostsee mittels Satellitenfernerkundung

*Dissertation, erschienen im Oktober 2013, ISBN 978-3-86009-403-7*

**Band 39**

Peter Helmke

Optimierung der Verarbeitungs-, Gebrauchs- und Entsorgungseigenschaften eines naturfaserverstärkten Kunststoffes unter Berücksichtigung automobiler Anforderungen

*Dissertation, erschienen im November 2013, ISBN 978-3-86009-404-4*

**Band 40**

Andrea Siebert-Raths

Modifizierung von Polylactid (PLA) für technische Anwendungen  
Verfahrenstechnische Optimierung der Verarbeitungs- und Gebrauchseigenschaften  
*Dissertation, erschienen im Januar 2014 ISBN 978-3-86009-405-1*

**Band 41**

Fisiha Getachew Argaw

Agricultural Machinery Traffic Influence on Clay Soil Compaction as Measured by the Dry Bulk Density

*Dissertation, erschienen im Januar 2014 ISBN 978-3-86009-406-8*

**Band 42**

Tamene Adugna Demissie

Climate change impact on stream flow and simulated sediment yield to Gilgel Gibe 1 hydropower reservoir and the effectiveness of Best Management Practices

*Dissertation, erschienen im Februar 2014 ISBN 978-3-86009-407-5*

**Band 43**

Paul Engelke

Untersuchungen zur Modellierung des Feststofftransports in Abwasserkanälen: Validierung in SIMBA®

*Dissertation, erschienen im Februar 2014 ISBN 978-3-86009-408-2*

**Band 44**

16. DIALOG Abfallwirtschaft MV

Aktuelle Entwicklungen in der Abfall- und Ressourcenwirtschaft

*Tagungsband, erschienen im April 2014, ISBN 978-3-86009-410-5*

**Band 45**

8. Rostocker Bioenergieforum, 19.-20. Juni 2014 an der Universität Rostock

*Tagungsband, erschienen im Juni 2014, ISBN 978-3-86009-412-9*

**Band 46**

Abschlussbericht Projekt CEMUWA – Climate protection, natural resources management and soil improvement by combined Energetic and Material Utilization of lignocellulosic agricultural Wastes and residues

*Projektbericht, erschienen im September 2014, ISBN 978-3-86009-413-6*

**Band 47**

8. Rostocker Baggergutseminar, 24.-25. September 2014 in Rostock  
*Tagungsband, erschienen im September 2014, ISBN 978-3-86009-414-3*

**Band 48**

Michael Kuhn  
Mengen und Trockenrückstand von Rechengut kommunaler Kläranlagen  
*Dissertation, erschienen im Oktober 2014 ISBN 978-3-86009-415-0*

**Band 49**

8. Rostocker Abwassertagung, 10.-11. November 2014 in Rostock  
*Tagungsband, erschienen im November 2014, ISBN 978-3-86009-416-7*

**Band 50**

Mulugeta Azeze Belete  
Modeling and Analysis of Lake Tana Sub Basin Water Resources Systems,  
Ethiopia  
*Dissertation, erschienen im Dezember 2014 ISBN 978-3-86009-422-8*

**Band 51**

Daniela Dressler  
Einfluss regionaler und standortspezifischer Faktoren auf die Allgemeingültigkeit  
ökologischer und primärenergetischer Bewertungen von Biogas  
*Dissertation, erschienen im Mai 2015 ISBN 978-3-86009-424-2*

**Band 52**

9. Rostocker Bioenergieforum, 18.-19. Juni 2015 in Rostock  
*Tagungsband, erschienen im November 2014, ISBN 978-3-86009-425-9*

**Band 53**

Nils Engler  
Spurenelementkonzentrationen und biologische Aktivität in NaWaRo-Biogas-  
fermentern  
*Dissertation, erschienen im September 2015 ISBN 978-3-86009-427-3*

**Band 54**

Thomas Schmidt  
Möglichkeiten der Effizienzsteigerung bei der anaeroben Vergärung  
von Weizenschlempe  
*Dissertation, erschienen im Oktober 2015 ISBN 978-3-86009-428-0*



**Band 55**

Thomas Dorn

Principles, Opportunities and Risks associated with the transfer of environmental technology between Germany and China using the example of thermal waste disposal

*Dissertation, erschienen im Dezember 2015 ISBN 978-3-86009-429-7*

**Band 56**

Uwe Holzhammer

Biogas in einer zukünftigen Energieversorgungsstruktur mit hohen Anteilen fluktuierender Erneuerbarer Energien

*Dissertation, erschienen im Dezember 2015 ISBN 978-3-86009-430-3*

**Band 57**

17. DIALOG Abfallwirtschaft MV

Aktuelle Entwicklungen in der Abfall- und Ressourcenwirtschaft,

15. Juni 2016 in Rostock,

*Tagungsband, erschienen im Juni 2016, ISBN 978-3-86009-432-7*

**Band 58**

10. Rostocker Bioenergieforum, 16.-17. Juni 2016 in Rostock

*Tagungsband, erschienen im Juni 2016, ISBN 978-3-86009-433-4*

**Band 59**

Michael Friedrich

Adaptation of growth kinetics and degradation potential of organic material in activated sludge

*Dissertation, erschienen im Juli 2016 ISBN 978-3-86009-434-1*

**Band 60**

Nico Schulte

Entwicklung von Qualitätsprüfungen für die haushaltsnahe Abfallsammlung im Holsystem

*Dissertation, erschienen im Juli 2016 ISBN 978-3-86009-435-8*

**Band 61**

Ullrich Dettmann

Improving the determination of soil hydraulic properties of peat soils at different scales

*Dissertation, erschienen im September 2016 ISBN 978-3-86009-436-5*

**Band 62**

Anja Schreiber

Membranbasiertes Verfahren zur weitergehenden Vergärung von feststoffreichen Substraten in landwirtschaftlichen Biogasanlagen

*Dissertation, erschienen im Oktober 2016 ISBN 978-3-86009-446-4*



**Band 63**

André Körtel

Entwicklung eines selbstgängigen statischen Verfahrens zur biologischen Stabilisierung und Verwertung organikreicher Abfälle unter extrem ariden Bedingungen für Entwicklungs- und Schwellenländer, am Beispiel der Stadt Teheran  
*Dissertation, erschienen im Oktober 2016 ISBN 978-3-86009-447-1*

**Band 64**

Ayman Elnaas

Actual situation and approach for municipal solid waste treatment in the Arab region  
*Dissertation, erschienen im Oktober 2016 ISBN 978-3-86009-448-8*

**Band 65**

10. Rostocker Abwassertagung, Wege und Werkzeuge für eine zukunftsfähige Wasserwirtschaft im norddeutschen Tiefland, 8. November 2016 in Rostock  
*Tagungsband, erschienen im November 2016, ISBN 978-3-86009-449-5*

**Band 66**

Gunter Weißbach

Mikrowellen-assistierte Vorbehandlung lignocellulosehaltiger Reststoffe  
*Dissertation, erschienen im November 2016 ISBN 978-3-86009-450-1*

**Band 67**

Leandro Janke

Optimization of anaerobic digestion of sugarcane waste for biogas production in Brazil  
*Dissertation, erschienen im Mai 2017 ISBN 978-3-86009-454-9*

**Band 68**

11. Rostocker Bioenergieforum, 22.-23. Juni 2017 in Rostock  
*Tagungsband, erschienen im Juni 2017, ISBN 978-3-86009-455-6*

**Band 69**

Claudia Demmig

Einfluss des Erntezeitpunktes auf die anaerobe Abbaukinetik der Gerüstsubstanzen im Biogasprozess  
*Dissertation, erschienen im Juli 2017, ISBN 9978-3-86009-456-3*

**Band 70**

Christian Koepke

Die Ermittlung charakteristischer Bodenkennwerte der Torfe und Mudden Mecklenburg-Vorpommerns als Eingangsparameter für erdstatische Berechnungen nach Eurocode 7 / DIN 1054  
*Dissertation, erschienen im Juni 2017, ISBN 978-3-86009-457-0*

**Band 71**

Sven-Henning Schlömp

Geotechnische Untersuchung und Bewertung bautechnischer Eignung von Müllverbrennungsschlacken und deren Gemischen mit Böden

*Dissertation, erschienen im Juni 2017, ISBN 978-3-86009-458-7*

**Band 72**

Anne-Katrin Große

Baggergut im Deichbau – Ein Beitrag zur geotechnischen Charakterisierung und Erosionsbeschreibung feinkörniger, organischer Sedimente aus dem Ostseeraum zur Einschätzung der Anwendbarkeit

*Dissertation, erschienen im Juni 2017, ISBN 978-3-86009-459-4*

**Band 73**

Thomas Knauer

Steigerung der Gesamteffizienz von Biogasanlagen durch thermische Optimierung

*Dissertation, erschienen im Juli 2017, ISBN 978-3-86009-460-0*

**Band 74**

Mathhar Bdour

Electrical power generation from residual biomass by combustion in externally fired gas turbines (EFGT)

*Dissertation, erschienen im August 2017, ISBN 978-3-86009-468-6*

**Band 75**

Johannes Dahlin

Vermarktungsstrategien und Konsumentenpräferenzen für Dünger und Erden aus organischen Reststoffen der Biogasproduktion

*Dissertation, erschienen im September 2017, ISBN 978-3-86009-469-3*

**Band 76**

Sören Weinrich

Praxisnahe Modellierung von Biogasanlagen

Systematische Vereinfachung des Anaerobic Digestion Model No. 1 (ADM1)

*Dissertation, erschienen im März 2018, ISBN 978-3-86009-471-6*

**Band 77**

18. DIALOG Abfallwirtschaft MV

Aktuelle Entwicklungen in der Abfall- und Ressourcenwirtschaft

*Tagungsband, erschienen im Juni 2018, ISBN 978-3-86009-472-3*

**Band 78**

12. Rostocker Bioenergieforum

*Tagungsband, erschienen im Juni 2018, ISBN 978-3-86009-473-0*

**Band 79**

Tatyana Koegst

Screening approaches for decision support in drinking water supply

*Dissertation, erschienen im Juni 2018, ISBN 978-3-86009-474-7*

**Band 80**

Liane Müller

Optimierung des anaeroben Abbaus stickstoffhaltiger Verbindungen durch den Einsatz von Proteasen

*Dissertation, erschienen im September 2018, ISBN 978-3-86009-475-4*

**Band 81**

Projektbericht Wasserwirtschaft

KOGGE – **K**ommunale **G**ewässer **G**emeinschaftlich **E**ntwickeln

Ein Handlungskonzept für kleine urbane Gewässer am Beispiel der Hanse- und Universitätsstadt Rostock

*Projektbericht, erschienen im September 2018, ISBN 978-3-86009-476-1*

**Band 82**

Adam Feher

Untersuchungen zur Bioverfügbarkeit von Mikronährstoffen für den Biogasprozess

*Dissertation, erschienen im Oktober 2018, ISBN 978-3-86009-477-8*

**Band 83**

Constanze Uthoff

Pyrolyse von naturfaserverstärkten Kunststoffen zur Herstellung eines kohlenstoffhaltigen Füllstoffs für Thermoplasten

*Dissertation, erschienen im November 2018, ISBN 978-3-86009-478-5*

**Band 84**

Ingo Kaundinya

Prüfverfahren zur Abschätzung der Langzeitbeständigkeit von Kunststoffdichtungsbahnen aus PVC-P für den Einsatz in Dichtungssystemen von Straßentunneln

*Dissertation, erschienen im Dezember 2018, ISBN 978-3-86009-484-6*

**Band 85**

Eric Mauky

A model-based control concept for a demand-driven biogas production

*Dissertation, erschienen im Januar 2019, ISBN 978-3-86009-485-3*

**Band 86**

Michael Kröger

Thermochemical Utilization of Algae with Focus on hydrothermal Processes

*Dissertation, erschienen im Februar 2019, ISBN 978-3-86009-486-0*

**Band 87**

13. Rostocker Bioenergieforum

*Tagungsband, erschienen im Juni 2019, ISBN 978-3-86009-487-7*

**Band 88**

12. Rostocker Abwassertagung

*Tagungsband, erschienen im September 2019, ISBN 978-3-86009-488-4*

**Band 89**

Philipp Stahn

Wasser- und Nährstoffhaushalt von Böden unter Mischkulturen und Trockenstress

*Dissertation, erschienen im Juli 2019, ISBN 978-3-86009-489-1*

**Band 90**

BioBind: Luftgestützte Beseitigung von Verunreinigungen durch Öl mit biogenen Bindern

*Projektbericht, erschienen im September 2019, ISBN 978-3-86009-490-7*

**Band 91**

Jürgen Müller

Die forsthydrologische Forschung im Nordostdeutschen Tiefland: Veranlassung, Methoden, Ergebnisse und Perspektiven

*Habilitation, erschienen im Oktober 2019, ISBN 978-3-86009-491-4*

**Band 92**

Marcus Siewert

Bewertung der Ölhavarievorsorge im deutschen Seegebiet auf Grundlage limitierender Randbedingungen – Ein Beitrag zur Verbesserung des Vorsorgestatus

*Dissertation, erschienen im November 2019, ISBN 978-3-86009-492-1*

**Band 93**

Camilo Andrés Wilches Tamayo

Technical optimization of biogas plants to deliver demand oriented power

*Dissertation, erschienen im Februar 2020, ISBN 978-3-86009-493-8*

**Band 94**

Robert Kopf

Technisches Benchmarking mit Standortqualifikationsstudie biochemischer Energieanlagenprojekte (Beispiel Biogas)

*Dissertation, erschienen im Februar 2020, ISBN 978-3-86009-494-5*

**Band 95**

14. Rostocker Bioenergieforum und 19. DIALOG Abfallwirtschaft MV  
*Tagungsband, erschienen im Juni 2020, ISBN 978-3-86009-507-2*  
*DOI: [https://doi.org/10.18453/rosdok\\_id00002650](https://doi.org/10.18453/rosdok_id00002650)*

**Band 96**

Safwat Hemidat  
Feasibility Assessment of Waste Management and Treatment in Jordan  
*Dissertation, erschienen im Juli 2020, ISBN 978-3-86009-509-6*

**Band 97**

Andreas Heiko Metzing  
Verdichtung von ungebundenen Pflasterdecken und Plattenbelägen -  
Untersuchungen zur Lagerungsdichte des Fugenmaterials  
*Dissertation, erschienen im Juli 2020, ISBN 978-3-86009-510-2*  
*DOI: [https://doi.org/10.18453/rosdok\\_id00002742](https://doi.org/10.18453/rosdok_id00002742)*

**Band 98**

Ying Zhou  
Research on Utilization of Hydrochars Obtained by the Organic Components of  
Municipal Solid Waste  
*Dissertation, erschienen im November 2020, ISBN 978-3-86009-515-7*

**Band 99**

Mathias Gießler  
Ein prozessbasiertes Modell zur wirtschaftlich-technischen Abbildung von  
Abwasserunternehmen – Beispielhafte Anwendung für eine ländliche Region  
mit Bevölkerungsrückgang  
*Dissertation, erschienen im November 2020, ISBN 978-3-86009-516-4*  
*DOI: [https://doi.org/10.18453/rosdok\\_id00002790](https://doi.org/10.18453/rosdok_id00002790)*

**Band 100**

Dodieka Ika Candra  
Development of a Virtual Power Plant based on a flexible Biogas Plant and a  
Photovoltaic-System  
*Dissertation, erschienen im Dezember 2020, ISBN 978-3-86009-518-8*  
*DOI: [https://doi.org/10.18453/rosdok\\_id00002814](https://doi.org/10.18453/rosdok_id00002814)*

**Band 101**

Thomas Zeng  
Prediction and reduction of bottom ash slagging during small-scale combustion  
of biogenic residues  
*Dissertation, erschienen im Dezember 2020, ISBN 978-3-86009-519-5*

**Band 102**

Edward Antwi

Pathways to sustainable bioenergy production from cocoa and cashew residues from Ghana

*Dissertation, erschienen im Dezember 2020, ISBN 978-3-86009-520-1*

*DOI: [https://doi.org/10.18453/rosdok\\_id00002818](https://doi.org/10.18453/rosdok_id00002818)*

**Band 103**

Muhammad Waseem

Integrated Hydrological and Mass Balance Assessment in a German Lowland Catchment with a Coupled Hydrologic and Hydraulic Modelling

*Dissertation, erschienen im Januar 2021, ISBN 978-3-86009-521-8*

*DOI: [https://doi.org/10.18453/rosdok\\_id00002884](https://doi.org/10.18453/rosdok_id00002884)*

**Band 104**

Martin Rinas

Sediment Transport in Pressure Pipes

*Dissertation, erschienen im März 2021, ISBN 978-3-86009-523-2*

*DOI [https://doi.org/10.18453/rosdok\\_id00002962](https://doi.org/10.18453/rosdok_id00002962)*

**Band 105**

15. Rostocker Bioenergieforum

*Tagungsband, erschienen im Juni 2021, ISBN 978-3-86009-524-9*

*DOI [https://doi.org/10.18453/rosdok\\_id00003024](https://doi.org/10.18453/rosdok_id00003024)*

**Band 106**

Jan Sprafke

Potenziäle der biologischen Behandlung von organischen Abfällen zur Sektorenkopplung

*Dissertation, erschienen im Oktober 2021, ISBN 978-3-86009-527-0*

*DOI [https://doi.org/10.18453/rosdok\\_id00003118](https://doi.org/10.18453/rosdok_id00003118)*

**Band 107**

Mingyu Qian

The Demonstration and Adaption of the Garage - Type Dry Fermentation Technology for Municipal Solid Waste to Biogas in China

*Dissertation, erschienen im Oktober 2021, ISBN 978-3-86009-528-7*

**Band 108**

Haniyeh Jalalipour

Sustainable municipal organic waste management in Shiraz, Iran

*Dissertation, erschienen im Oktober 2021, ISBN 978-3-86009-526-3*

[https://doi.org/10.18453/rosdok\\_id00003116](https://doi.org/10.18453/rosdok_id00003116)